GIS-based predictive mapping of lode gold potential in the Lawra Belt, northwest Ghana

Forson Karikari

April, 2002

GIS-based predictive mapping of lode gold potential in the Lawra Belt, northwest Ghana

by

Forson Karikari

Thesis submitted to the International Institute for Geo-information Science and Earth Observation in partial fulfilment of the requirements for the degree in Master of Science in *Mineral Exploration And Evaluation*.

Degree Assessment Board

Thesis advisor	Dr. John Carranza
	Prof. Martin Hale
Thesis examiners	Prof. Martin Hale (**Chairman**), ITC
	Dr. H. de Boorder (**External Examiner**), I.v.A.U Utrecht
	Dr. Phil Westerhof (**Member**), ITC
	Prof. Colin Reeves (**Member**), ITC

INTERNATIONAL INSTITUTE FOR GEO-INFORMATION SCIENCE AND EARTH OBSERVATION

ENSCHEDE, THE NETHERLANDS

Disclaimer

This document describes work undertaken as part of a programme of study at the International Institute for Geo-information Science and Earth Observation (ITC). All views and opinions expressed therein remain the sole responsibility of the author, and do not necessarily represent those of the institute.

Abstract

The Lawra greenstone belt, located NW of Ghana, is known to have some loge gold mineral occurrences. The geologic features indicative of this lode gold mineralisation in the area are shear zones, hydrothermal alteration, fractures and host rock chemical sediments. The gold potential of the belt is assessed by means of two GIS-based geodata integration techniques for generating predictive maps, viz. weights of evidence and fuzzy logic.

The weights of evidence is data-driven method in which the spatial associations of the indicative geologic features with the known mineral occurrences in the area are quantified, and weights statistically assigned to the geologic features. The analysis is carried out many times with different subset of mineral occurrences to generate predictive map. The best predictive map generated by this method defines 27% of the area as having potential for gold mineralisation further exploration work and 6.2% of the area tagged highly favourable zones.

The fuzzy logic method is knowledge driven and proximity to the indicative geologic features is translated into fuzzy membership functions based upon the knowledge of spatial associations between the known mineral occurrences and geologic features. The fuzzy sets are combined using fuzzy logic as the inference engine. The best predictive map generated by the fuzzy logic method defines 15% of the Lawra greenstone belt as having potential for gold mineralisation.

The results show the usefulness of applying GIS-based integration techniques to public domain exploration datasets, to generate predictive maps to guide in mineral exploration.

Keywords

Lawra Belt, weights of evidence, data-driven, spatial association, fuzzy logic, knowledge-driven, predictive maps, gold deposits, Ghana

Acknowledgements

I would like to express my sincere gratitude to the Netherlands Fellowship Program (NFP) for providing the financial support to pursue this higher level of education in ITC and hugely improving the confidence level in my profession. My special thanks also to the Geological Survey of Ghana, for allowing me to study abroad

I am greatly indebted to Dr. John Carranza my supervisor, whose guidance, invaluable suggestions and critical reading of the manuscript have contributed to the quality of this dissertation. Particular acknowledgement is also given to my Director of Studies and Supervisor, Prof. Dr. Martin Hale for his guidance and critical reviews of the manuscript.

My sincere thanks go to Drs. Boudewijn de Smeth the students adviser for his guidance and assistance during my entire stay in the Netherland. I thank Dr. Phil Westerhof and Drs. Frank van Ruitenbeek for the discussions in their special fields. My special thanks also go Prof. Dr. Colin Reeves for his immense contribution to the interpretation of the geophysical data.

I thank my fellow students Jesus Moreira (Cuba), Gilbert Mhlanga (Zimbabwe), Emmanuel Munyikwa (Zimbabwe), Lucas Donny Setijadji (Indonesia) and Tang Yanli (China) for their companionship and assistance during the period of study.

My heartfelt gratitude goes to my sister Regina Koranteng and my parents Mr. and Mrs Karikari for looking after my family in my absence. I am most appreciative of the understanding, love, support of my wife Evelyn and son Albert Ofei. If this has been an achievement, it is for you, as you are the people who have sacrificed and suffered most.

Above all, I thank the Lord God almighty, the provider, without His will, all this would not have been possible.

Contents

Abstract i

Acknowledgements iii

List of Tables ix

List of Figures xi

1 Introduction 1
- 1.1 Background to the research . . . 1
- 1.2 Problem Definition . . . 2
- 1.3 The study area . . . 3
- 1.4 Previous work in the study area . . . 4
- 1.5 Objectives . . . 5
- 1.6 Research Questions . . . 5
- 1.7 Methodology . . . 5

2 Geological Background 7
- 2.1 Regional Geological Setting . . . 7
  - 2.1.1 Birimian Supergroup . . . 7
  - 2.1.2 The Tarkwaian System . . . 11
  - 2.1.3 Granitoid . . . 11
  - 2.1.4 Pan African mobile belt . . . 12
  - 2.1.5 Structure of the Birimian . . . 12
  - 2.1.6 Gold mineralisation and structural controls in the Birimian . . . 13
- 2.2 Geology of the study area . . . 15
  - 2.2.1 Metavolcanics . . . 15
  - 2.2.2 Detrital volcanogenic sediments . . . 17
  - 2.2.3 Chemical sediments . . . 17
  - 2.2.4 Granitoid rocks . . . 18
  - 2.2.5 Gold mineralisation in the study area . . . 18

2.3 Conclusion 20

3 Conceptual Lode Gold Model **21**
3.1 Introduction 21
3.2 The general characteristics of greenstone-hosted lode gold deposits . . 22
3.2.1 Ore mineralogy and metal association 22
3.2.2 Genesis of deposits 22
3.2.3 Size and grade of deposits 23
3.2.4 Structural Styles 24
3.2.5 Host Rocks 25
3.2.6 Wallrock alteration 25
3.3 Conceptual model of lode gold mineralisation in the Lawra belt 25
3.3.1 Proposed model for Birimian evolution 25
3.3.2 Genetic model of gold-quartz veins in the Lawra belt 28
3.4 Conclusion 30

4 Resource and Methodology **31**
4.1 Resource 31
4.1.1 Available datasets 31
4.1.2 Software 34
4.2 Methodology 34
4.2.1 Data capture 35
4.2.2 Extraction of relevant features 36
4.2.3 Data integration 36

5 Extraction Of Features Indicative of Lode Gold Mineralisation **37**
5.1 Qualitative geophysical interpretations 37
5.1.1 Qualitative interpretation of aeromagnetic map 37
5.1.2 Qualitative interpretation of radiometric maps 39
5.1.3 Qualitative interpretation of electromagnetic (EM) data 39
5.2 Extraction of favourable rocks 42
5.3 Extraction of lineaments 45
5.3.1 Lineaments extracted from geological map 45
5.3.2 Lineaments interpreted from geophysical maps 45
5.3.3 Layers of interpreted and extracted lineaments 49
5.4 Extraction of hydrothermal alterations 49
5.4.1 Alterations from airborne radiometric maps 49
5.5 Conclusion 53

6 Spatial Data Integration and Analysis **55**
6.1 Analysis using the weights of evidence method 56
6.1.1 Weights of evidence method 56
6.1.2 Application of weights of evidence analysis to the Lawra belt . 59
6.1.3 Integration of binary maps to generate predictive map 70
6.1.4 Validating of predictive maps and determining best predictive map 71
6.2 Analysis using fuzzy logic method 79
6.2.1 Fuzzy set 79
6.2.2 Application of the fuzzy logic method to the Lawra belt 81
6.3 Discussion 86

7 Conclusions and Recommendations **89**
7.1 Conclusions 89
7.2 Recommendations 90

APPENDIX **97**
.1 Other results of 18 analyses using weights of evidence method 97

List of Tables

4.1 Available spatial and non-spatial data sets 32

6.1 Results of analysis1 (Alteration zones) 60
6.2 Results of analysis1 (Favourable host rocks) 62
6.3 Results of analysis1 (Shear zones) 65
6.4 Results of analysis1 (fractures) 68
6.5 Ranking of the spatial associations between geologic features and mineral occurrences 70
6.6 Results of analysis1 (Pairwise test of CI) 70
6.7 A summary of validation of predictive maps 72
6.8 A summary of validation of predictive maps generated by the removal of fractures predictor map from analysis 75
6.9 A summary of validation of predictive maps generated by the removal of alteration binary map from analysis (supported by knowledge and conceptual model) 77
6.10 The optimum spatial association between proximity to geologic features and mineral occurrences. 81
6.11 The optimum spatial association between proximity to geologic features and mineral occurrences. 82

1 ANALYSIS 2, using weights of evidence method 98
2 ANALYSIS 3, using weights of evidence method 99
3 ANALYSIS 4, using weights of evidence method 100
4 ANALYSIS 5, using weights of evidence method 101
5 ANALYSIS 6, using weights of evidence method 102
6 ANALYSIS 7, using weights of evidence method 103
7 ANALYSIS 8 using weights of evidence method 104
8 ANALYSIS 9, using weights of evidence method 105
9 ANALYSIS 10, using weights of evidence method 106
10 ANALYSIS 11, using weights of evidence method 107

11 ANALYSIS 12, using weights of evidence method 108
12 ANALYSIS 13, using weights of evidence method 109
13 ANALYSIS 14, using weights of evidence method 110
14 ANALYSIS 15, using weights of evidence method 111
15 ANALYSIS 16, using weights of evidence method 112
16 ANALYSIS 17, using weights of evidence method 113
17 ANALYSIS 18, using weights of evidence method 114
18 ANALYSIS 19, using weights of evidence method 115

List of Figures

1.1 Location of study area 4

2.1 Generalised distribution of Birimian supracrustal belts in West Africa (after Wright et al.,1985) 8
2.2 Geological map of Ghana showing the major Gold belts (modified after Kesse, 1985) 9
2.3 Schematic and simplified diagram of facies relationships in the Birimian of Ghana, (after Leube et al.,1990) 11
2.4 Au and Mn occurrences in Central and Western. Ghana 14
2.5 Geological map of the Lawra belt 16
2.6 Location of the poura mine 19

3.1 Model for the evolution of the Birimian 27
3.2 Genetic model of gold-quartz veins. Migration of elements from Chemical sediments rocks into quartz veins is shown schematically after (Melcher and Stumpfl, 1994). 29
3.3 photographs illustrating the style of alteration related to lode gold mineralisation 29
3.4 Lode gold vein sets enveloped by alteration 29

4.1 Flow Chart of the methodology 35

5.1 Geological boundaries overlaid on total intensity map, CC shows the high analytical signal portion of the CapeCoast granitoid, and a NE-SW trending dyke mapped from total intensity map 38
5.2 Geological boundaries overlaid on radiometric K map, MTV, with the metavolcanics showing as low K analytical signal 40
5.3 Geological boundaries overlaid on EM map, the Dixcove granites, DxGr, are shown as rounded structures with moderate electrical conductivity 41
5.4 Edited geological map from the qualitative interpretation 43

5.5 Map showing favourable host rocks, the chemical sediments (an indicative geologic features) extracted from geological map 44
5.6 Lineaments obtained from geological map 46
5.7 Lineaments obtained from magnetics map 47
5.8 Lineaments obtained from EM geophysical map 48
5.9 Fractures layer (an indicative geologic features), obtained by reclassifying the extracted lineaments 50
5.10 Shear zones (an indicative geologic features) in the study area obtained by reclassifying lineaments obtained from EM geophysical map 51
5.11 Alteration zones (an indicative geologic feature) mapped from K radiometric map 52

6.1 Variation of spatial association (sigC) with cummulative distances from alteration zones 60
6.2 Binary predictor pattern of alteration zones and mineral occurrences . 61
6.3 Variation of spatial association (sigC) with cumulative distances away from favourable rocks 63
6.4 Binary predictor pattern of host rocks and mineral occurrences 64
6.5 Variation of spatial association (sigC) with cumulative distances away from Shear zones 66
6.6 Binary predictor pattern of shear zones and mineral occurrences . . . 67
6.7 Variation of spatial association (sigC) with cumulative distances away from fractures 68
6.8 Binary predictor pattern of fractures and mineral occurrences (proximity distance of 1500m) 69
6.9 Best predictive map out of 19 analyses using all the evidence maps (WALT, WFHR, WSHEA, WFRAC) 73
6.10 Analysis 5, predictive map using only WFHR, WALT and WSHE evidence maps 76
6.11 Best predictive map of gold in the Lawra belt using weights of evidence method 78
6.12 Schematic inference network for generating predictive map of lode gold in the Lawra belt 83
6.13 Inference network for generating the best predictive map of lode gold in the Lawra belt 84
6.14 Fuzzy logic predictive map of gold in the Lawra belt 85

Chapter 1

Introduction

1.1 Background to the research

Before its independence from Britain in 1957, Ghana was called Gold Coast. The country's mineral endowment potential is well known internationally and the bulk of its gold comes from Early Proterozoic greenstone Birimian rocks. The history of gold mining activities in the country dates back to the 17th century (Amedufo, 1995). In spite of this long history of gold mining activities, gold took over from cocoa as the major foreign exchange earner for the country only after the government lunched the Economic Recovery Programme (ERP) and reviewed the mining laws and regulations in 1983 to attract investors. The result of this generous investment incentives was a gold boom in the 1990s.

The mining sector's contribution to the national export earnings of less than 20% in the mid-1980s increased as much as 40% of Ghana's total merchandise export earnings in 1992 (Aryee, 2001). The mineral industry has since became Ghana's single largest foreign exchange earner from that year.

The gold boom in the country, however, has declined slightly in recent times, as reserves are exhausted and mines closed down. There is therefore a need to search for new deposits in less known areas using better exploration techniques than the conventional exploration methods to sustain exploration and mining activities.

Area selection in mineral exploration is based on the presence or absence of specific geologic features, or alternatively, geophysical or geochemical features that reflect geological features (Westerhof, 1999). Mineral potential mapping is the process of area selection to distinguish prospective areas from less or non-prospective areas. In recent years the use of Geographic Information System (GIS) in mineral exploration

has provided a way by which multivariate spatial information, such as conventional geological maps and sections, satellite imagery, geophysical map and geochemical data are stored, manipulated and analysed. GIS-based mineral potential mapping techniques, involves integration and interpretation of the different kinds of exploration data sets, to assess the mineral potential of an area, and is a much more effective approach rather than assessing individually, each of the exploration data sets.

There are two types of GIS-based mineral potential mapping methods, empirical methods and conceptual methods. Empirical methods are data-driven and involve the examination and analysis of the locations of known deposit with respect to the surrounding geology (Bonham-Carter et al., 1989). The conceptual methods on the other hand are model-driven or knowledge-driven and involves the realization that a mineral occurrence or deposit is only a minor part of a regional scale mineralisation which comprises the heat source, metal source, transport pathways and host rocks (Knox-Robinson and Groves, 1997).

The conceptual GIS-based exploration method is particularly well suited to lode-gold deposits in greenstone belts for a number of reasons. 1) in regional scale, the majority of the deposits are now considered to belong to a single deposit group in which the deposits are epigenetic and formed from structurally focussed hydrothermal fluids (Eilu et al., 1998). 2) The deposits are considered to form as a result of the conjunction of a number of interacting factors, and hence precise definition of controls is complex Phillip et al.(1987). 3) Structure is the single most important factor controlling the distribution of gold deposits and the form of gold ore shoots. 4) The majority of deposits can be shown to be very late in the evolution of their host terranes, as summarised by Groves (1991) and Boyle (1991).

1.2 Problem Definition

The Lawra belt is one of six Early Proterozoic greenstone belts in Ghana. It trends northwards for about 150 km from Wa to the border with Burkina Faso, from where it continues for about 400 km into neighbouring Burkina Faso. The belt is located in NW of Ghana, is far from Accra and difficult to access.

Unlike the other gold belts in the country, especially the Ashanti and Sefwi belts in the southern Ghana, the Lawra belt is less explored and studied. Notwithstanding the small-scale mines of some gold occurrences and a major gold mine at Poura, in the Burkina Faso portion of the belt, the gold potential of this belt is not fully assessed. This has led to an apparent exploration inactivity as there is lack of an up-

to-date gold potential map of the belt to show prospective and non-prospective areas of the belt. The lack of gold potential map is also a major contributing factor that holds back investment and development for gold exploration and mining in the belt. There is therefore a need to generate mineral potential map of the belt by identifying the prospective zones to stimulate exploration activities in the area.

1.3 The study area

The study area (the Lawra greenstone belt) situated in northwest Ghana in West African, Fig 1.1. The area lies between latitude 10^o 00'N and 11^o 00'N, and longitude 2^o 30'W and 3^o 00'W and covers an area of about 8,800 km^2. The northern and western parts of the Lawra belt form the boundary Ghana shares with Burkina Faso.

The climate in the study area is humid with two clearly defined seasons - rainy and dry. The average annual temperature is about 29^{o}C. Annual precipitation averages 1,200 mm. The rainy season starts from May and attains its peak in August-September. The rains are normally in the form of tropical rainstorms. The dry season starts from November and attains a peak in January. Humidity is reduced by a dry and dusty south westerly wind, which blows from the Sahara during the period.

The area has a dense drainage system.The main river in the area is the Black Volta River which flows from north to south along the border with Burkina Faso. Most rivers and streams are tributaries of the Black Volta and there is dendritic pattern.

Vegetation in the area is savanna grassland type with thick grass and relatively few trees, mainly different species of Accacia, Baobab and Shea butter trees.

The population of the area is concentrated in settlements usually located along highways and valleys of large rivers. The fairly populated towns are Wa, Lawra and Nandom.

Farming is the major occupation of the population. Yams, sorghum and groundnuts are the main crops grown; cattle, goats and poultry are also reared. Some of the population, especially that in the towns, is engaged in handicrafts and trade.

The study area is linked to other parts of the country mainly by means of motor transport along the feeder road network. Most of the feeder roads are motorable only in the dry season.

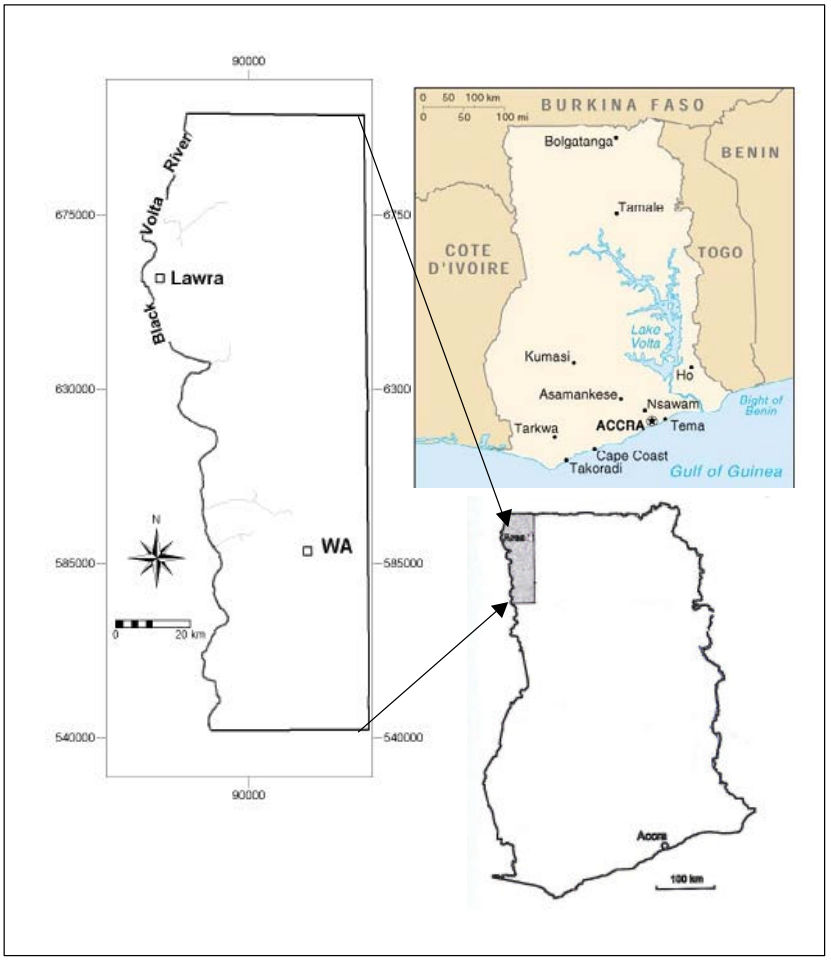

Figure 1.1: Location of study area

1.4 Previous work in the study area

In general, geological investigations and prospecting in the study area have been carried out to a lesser extent as compared to the other belts in the heavily populated south of the country where the bulk of Ghana's gold comes from. Nevertheless, some idea of the lode gold potential of the study area is however given in the reports of pioneer geologists who mapped some parts of the study area.

Kitson (1928) and Junner (1935) reported of auriferous quartz reefs near Duri and in the area 13 km southeast of lawra town. Roudakov (1965) and Pobedash (1965), mapped and prospected the north and south of the study area respectively by geochemical sampling, trenching and drilling. They discovered a number of gold occurrences including the Dorimon and Billaw mineral occurences. Melcher and Stumpfl (1994), presented perhaps the most comprehensive report on the geology and gold

mineralisation of the Lawra and Nangodi belts both in the north of Ghana. They reported about the spatial relationship of gold-bearing quartz veins and chemical sediments occurring in narrow transition zones between volcanic belt and pyroclastic/sedimentary basin of the belt. Amoako et al (1998), used various airborne geophysical methods to survey and assess the mineral potential of the area and reported an electrical conducting horizons in the belt, prospective for massive sulphide deposits near Billaw. They also reported of dot-like magnetic anomalies and probable deformation zones.

1.5 Objectives

The research objectives are as follows.

- To define spatial controls on the formation and localisation of lode-gold deposits at occurrence-scale to terrane-scale.
- To test at which scale, or scales, of digital maps these spatial controls can best be defined.
- To generate a lode gold potential model of the Lawra belt based on the defined spatial controls using GIS.

1.6 Research Questions

The research will attempt to answer the following questions.

- Are the gold occurrences of the area controlled by the same or similar geologic factors?
- Are the available datasets adequate for producing a gold potential map?
- Is the conceptual predictive model used valid?

1.7 Methodology

The objectives of the research will be achieved through the following steps:

- Collect relevant spatial exploration data (aeromagnetic, gamma-ray spectrometry, electromagnetics, structural and geological maps) and associated non-spatial data.
- Create a digital database of exploration data sets.

- Study lode gold deposits and identify the spatial controls on their localisation.
- From the digital database create binary predictor patterns of features having spatial association with lode gold deposits.
- Use GIS based integration techniques to integrate the various binary predictor patterns of lode gold deposits to generate a gold potential map.

Chapter 2

Geological Background

2.1 Regional Geological Setting

Rocks of early Proterozoic rocks form a substantial part of the Man shield which occupies the southernmost third of the West Africa craton. The craton is bounded to the east and southwest by Pan-African belts and has remained stable since 1.7 Ga (Wright et al., 1985). The Man shield on the other hand comprises a western domain consisting essentially of Archean rocks of Liberian age (3.0-2.5 Ga) and an eastern domain consisting of Birimian rocks of early Proterozoic age which have been folded, metamorphosed, and invaded by granitoids during the Eburnean event at 2.1 Ga (Leube et al., 1990).

The early Proterozoic Birimian rocks, crop out extensively in Ghana, Ivory Coast, Burkina Faso and Mali (Fig 2.1). Ghana contains the eastern portion of the West African Birimian terrane.

The geology of Ghana can be divided into three main geologic provinces (Hasting, 1982): 1) an early Proterozoic Birimian Supergroup and Tarkwaian group of the Man shield occupying the west and northern parts of the country; 2) a Pan African province covering the Dahomeyan, Togo and Buem formations in the southeast and eastern parts of the country; and 3) Infracambrian/Palaeozoic sedimentary basin situated in the central and eastern parts of the country (Fig 2.2).

2.1.1 Birimian Supergroup

The Birimian Supergroup in Ghana has long been divided into two series: (1) a lower series of mainly sedimentary origin, and (2) an upper series of the greenstones, mainly metamorphosed basic and intermediate lavas and pyroclastic rocks (Junner, 1935). The lower Birimian rocks comprise an assemblage of fine-grained rocks with

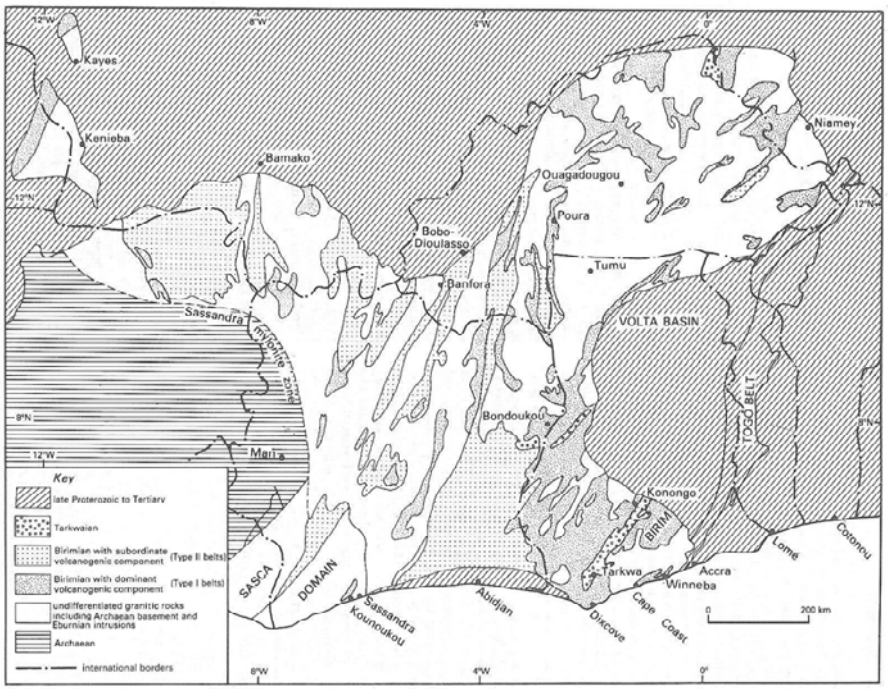

Figure 2.1: Generalised distribution of Birimian supracrustal belts in West Africa (after Wright et al.,1985)

a large volcanoclastic component. Typical lithologies include tuffaceous shale, phyllite, siltstone, greywacke and some chemical (Mn-rich) sediment. The upper Birimian rocks comprise mostly basalts with some interflow sediments (Eisenlohr and Hirdes, 1992).

Recent studies, however, shows that the lavas of the greenstone belts in Ghana and the sediments of the sedimentary sequence in the basins were deposited contemporaneously as lateral facies equivalents (Leube et al., 1990; Loh and Hirdes, 1999). The greenstone belts consist mainly of low grade metamorphic, tholeitic lavas (MORB chemistry) and are separated by sedimentary sequences in the basins, which are isoclinally folded. In the transition zone between belt volcanics and basin sediments a chemical facies occurs. This is defined by chert, manganiferous and carbon-rich sediments.

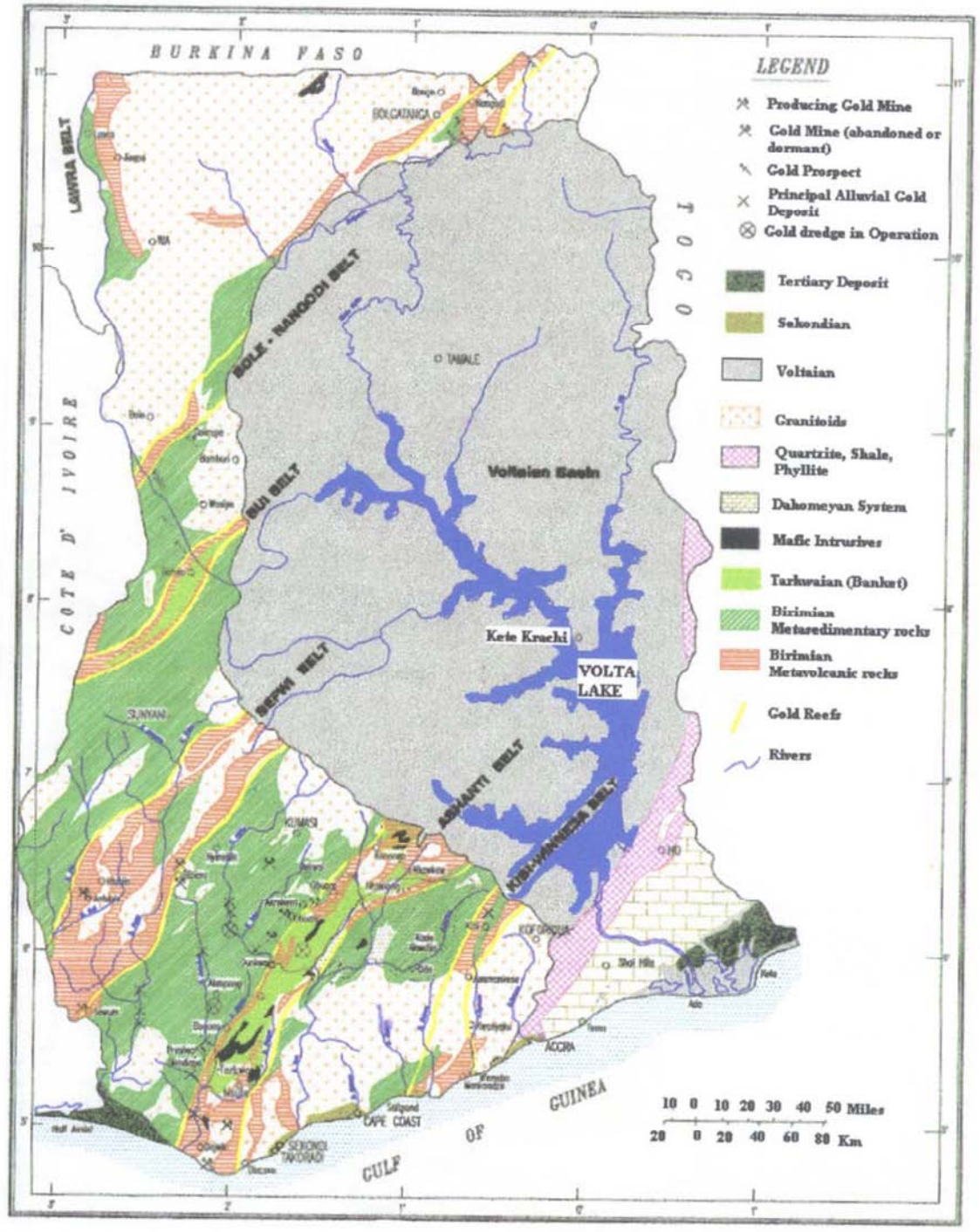

Figure 2.2: Geological map of Ghana showing the major Gold belts (modified after Kesse, 1985)

Birimian Metavolcanics

There are six volcanic belts in the Birimian, namely the Kibi-Winneba, Ashanti, Sefwi, Bui, Bole-Navrongo and Lawra belts. The belts have a slight keel-shaped outline that is perhaps produced by the associated diapiric, intrusive plutons. The width of the belts are 15-40 km and they are separated from each other by the intervening sedimentary basins.

The belts consist mainly of metamorphosed basaltic and andesitic lavas, now hornblende-actinolite-schists, calcareous chlorite-schists and amphibolites (the greenstones). Minor intrusions of mafic rocks cut the volcanics. Volcaniclastic sediments occur interbedded within the basaltic flows of all volcanic belts. The proportion of metalavas to metapyroclastics varies between belts. The highest pyroclastics/lava ratios are encountered in the Ashanti belt, the lowest in the Sefwi belt (Leube et al., 1990).

Metamorphism in most volcanic rocks is confined to the chlorite zone of the greenschist facies. Amphibolite-facies assemblages occur sporadically but especially along the margins of granitoid bodies.

Birimian Metasediments

Birimian metasedimentary rocks of Ghana are divided into: (1) volcaniclastic rocks; (2) turbidite-related wackes; (3) argillitic rocks; and (4) chemical sediments (Fig 2.3). Boundaries between these subdivisions are gradational (Leube et al., 1990).

The volcaniclastic sediments comprise chiefly sand-to silt-sized, partly reworked pyroclastics that is shown by the presence of quartz, idiomorphic plagioclase crystals, chloritised glass fragments, and the absence of heavy minerals.

The turbidite-related wackes consist of chert (partly graphitic), graphitic schist, quartz and, to a lesser degree, lava.

Argillitic sedimentary rocks of the Birimian occur as two types: phyllites and carbonaceous schists. Argillites in transition zones between belt volcanics and basin sediments seem to be especially rich in carbonaceous matter. This might be spatially related to exhalation of volcanic gases as increase in CO_2 supply favours the growth of plant-like organisms.

The following facies types may occur from the volcanic belts towards the centre of the sedimentary basins: $volcanic - volcaniclastic facies \rightarrow wacke(turbidite)$

$facies \rightarrow volcaniclastic - argillite facies \rightarrow argillite - volcaniclastic facies.$

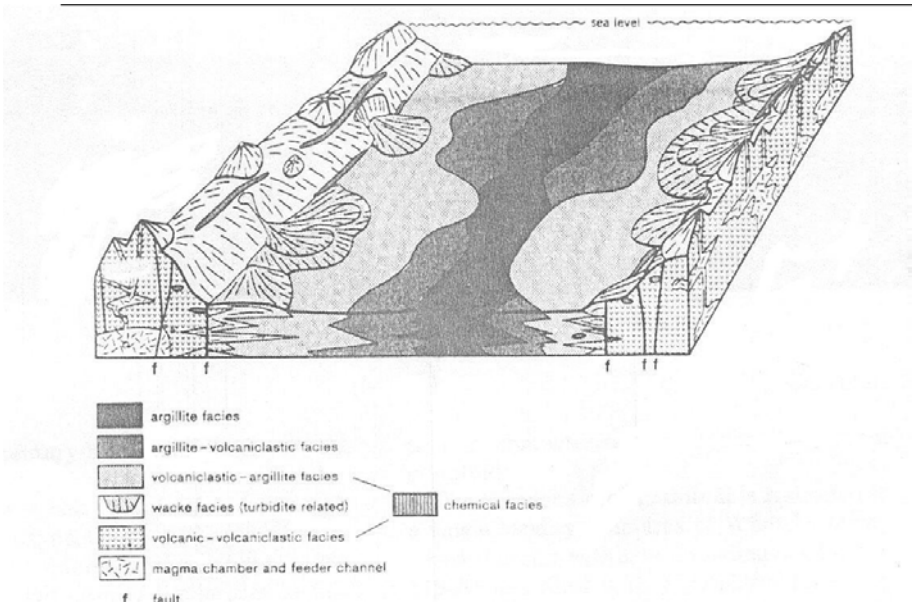

Figure 2.3: Schematic and simplified diagram of facies relationships in the Birimian of Ghana, (after Leube et al.,1990)

2.1.2 The Tarkwaian System

The Tarkwaian, is a Proterozoic supracrustal system overlying the Birimian. It consists mainly of shallow water sediments and is present in all the Birimian volcanic belts,(Junner, 1935).It consists of coarse clastic sedimentary rocks that include conglomerates, arkoses, sandstones and minor amounts of shale. The Tarkwaian is usually regarded as the detritus of Birimian rocks that were uplifted and eroded following the Eburnean tecto-thermal event ((Eisenlohr and Hirdes, 1992)).

Economically, the most important unit of the Takwaian is the Banket series which contains economic concentrations of gold in several areas.

2.1.3 Granitoid

The Eburnean tectono-thermal event, which stabilized most of the West African craton, affected the Birimian sediments and lavas, causing folding and intrusion of various types of granitoids. Two major types of Eburnean granitoid intrusions into the Birimian are: 1) basin granitoid (Cape Coast type 2070-2115 Ma), which is syn-to late tectonic, foliated, biotite-bearing peraluminous and also generally granodioritic in composition batholiths chiefly in the central portions of Birimian basin; 2) belt

granitoids (Dixcove type 2170-2180 Ma) mostly form late-orogenic unfoliated intrusions in volcanic belts. They possess a metaluminous character and commonly are of tonalitic composition.

2.1.4 Pan African mobile belt

The Pan African thermotectonic event is represented in Ghana by the southeastern rock units, which comprises the Dahomeyan, the Togo and the Buem formations. The Dahomeyan rocks consist of gneisses, schists and migmatites. Intrusives into the Dahomeyan consists of porphyry dikes, aplites and dolerites with occasional granite and syenite. The Togo formation comprises arenaceous and argillaceous sediments. The Buem series on the other hand consist of argillaceous and calcareous shales, sandstones, conglomerates, quartzites, limestones, basaltic and trachytic lavas.

2.1.5 Structure of the Birimian

The Birimian greenstone belts in Ghana, like any other greenstone belt else where in the world, are faulted synform with fold axes and major faults paralleling the synformal axes.

The structure of the rocks is characterised by isoclinal folds with near vertical axial planes ($65 - 90^o$). Open symmetrical folds with slight vergence to the southeast occur locally in the volcanic belt owing to competency differences between massive lava and volcaniclastic, argillitic strata. An axial plane cleavage (S_1) is developed parallel to bedding through out the steeply inclined sediments. A weak second cleavage striking oblique or perpendicular to (S_1) is only locally well developed, (Leube et al., 1990).

On a regional scale, two deformation types, low strain and high strain, are recognized. In the low strain domain, rocks contain a northeast-trending subvertical foliation (S_1) that is subparallel or at a small angle to bedding and a subhorizontal foliation/bedding intersection lineation (L_1). Rocks belonging to the high strain domain occur predominantly along the northwest margin of the volcanic belts and are characterized by the presence of a penetrative northeast trending foliation (S_2) and a southwest plunging stretching lineation (L_2) that is present in both Birimian and Tarkwaian rocks (Eisenlohr and Hirdes, 1992).

2.1.6 Gold mineralisation and structural controls in the Birimian

On a regional scale, the vast majority of the Birimian gold deposits occur aligned along the flanks of the volcanic belts, Fig 2.4. To a considerably lesser extent, gold deposits are present within volcanic belts where they sometimes show a spatial association with belt-type granitoid intrusions (Dixcove granite).

A spatial relationship between manganese and gold occurrences on a regional scale was first described by Junner(1935). Manganese is predominantly located on the flanks of volcanic belt, i.e the transitional facies between belt volcanics and basin sediments, as are zones or 'corridors' formed by individual gold deposits. On a local scale, however, manganese and gold do not coincide with each other, i.e., no gold mining occurs directly within Mn-rich strata (Leube et al., 1990).

In addition to manganese and gold occurrences, the transition zones along the flanks of the volcanic belts are characterised by the presence of other chemical sediments, namely sulphides, cherts, Fe-Ca-Mg carbonates and rocks rich in carbon (Ntiamoah-Agyakwa, 1979). The chemical facies probably constitutes the most important favourable regional exploration guide for gold deposits in the Birimian of Ghana. The chemical sediments occur intermittently and are superimposed on and are intercalated with metavolcanics as well as metavolcaniclastics and minor phyllites.

On a regional scale structural elements only carry gold mineralisation if they are developed within the zone of the auriferous chemical sediments; those outside tend to be barren. Structure seems to be of importance as as a local ore control (i.e. on mine scale), whereas lithofacies (chemical sediments) controls gold regionally and to a lesser degree locally (Leube et al., 1990).

There are two major types of lode gold in the Birimian: the disseminated-sulphide type (DST) and the quartz-vein type (QVT). The QVT is always structure controlled. The DST occurs as two types: (1) lithofacies controlled, i.e. bound to chemical sediments; (2) structure controlled, i.e. bound to the selvages of quartz veins.

In general, QVT gold ores carry better grades than those of the DST (Leube et al., 1990). Major differences between DST ores and QVT ores with respect to their ore mineralogy are: QVT ores contain visible 'free gold', whereas DST ores carry gold largely as submicroscopic inclusions in sulphide. According to Leube et al.(1990), sericite- and pyrite/arsenopyrite-rich selvages frequently carry higher gold contents than the quartz itself in the structure controlled deposit types.

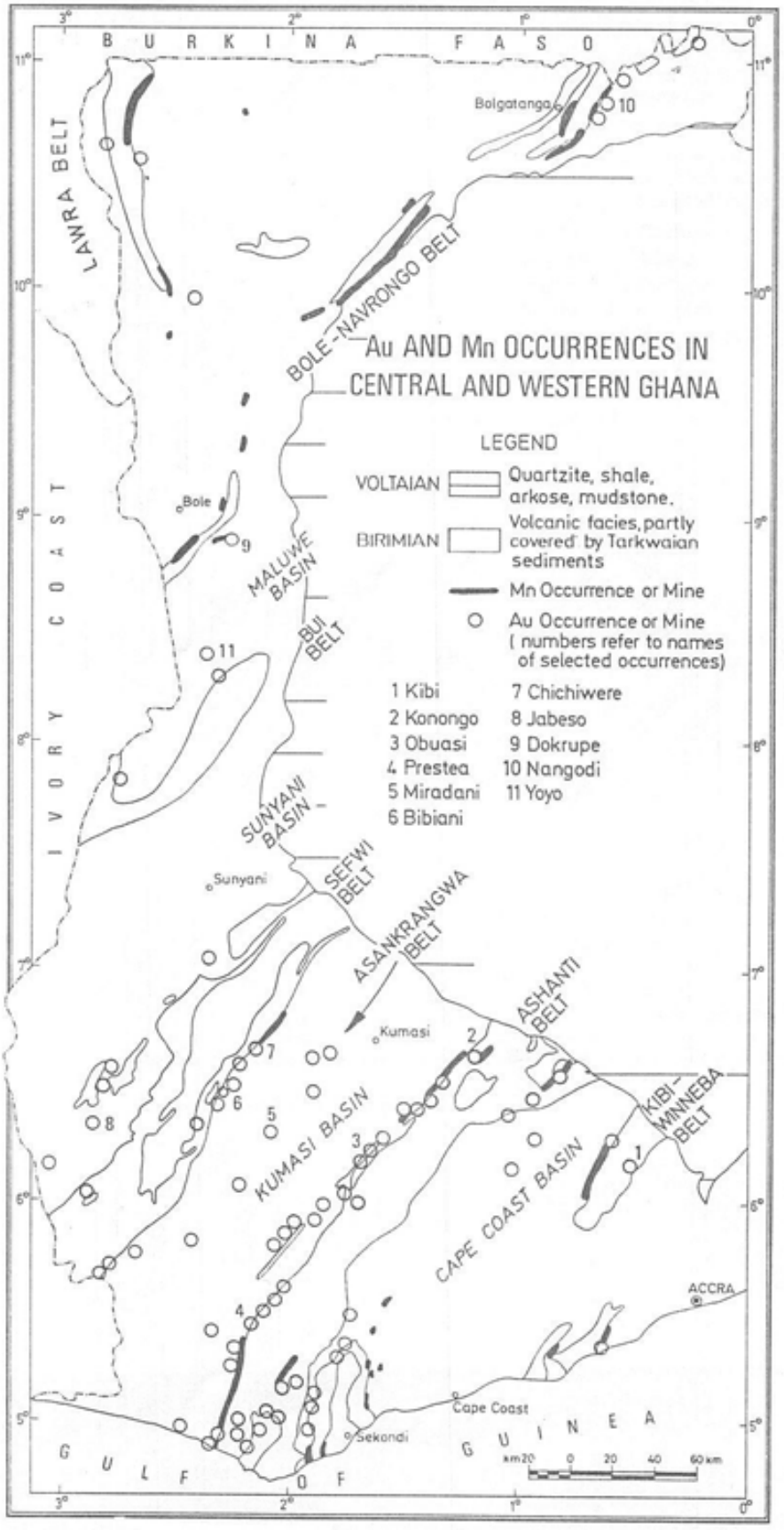

Figure 2.4: Au and Mn occurrences in Central and Western. Ghana

2.2 Geology of the study area

The Lawra belt consists of a volcanic belt made up of tholeitic greenstones, and a sedimentary basin intruded by granitoids (Fig 2.5). The N-S striking belt, like other greenstone-granitoid terraine else where in the world is granitoid-dominated and the transition zone between belt and basin is usually marked by the development of extensive chemical facies. There is also a component of detrital volcanogenic sediments in the transition zone.

The main structural elements in the area according to Roudakov (1965) and Pobedash (1965) are the Dorimon synclinorium and the Sawla-Wa anticlinorium (Fig 2.4). The synclinorium consists of a combination of simple, major lineal folds and extremely complex minor ones. In cross section it appears to be a large synclinal structure with relatively gentle east limb and a steep west limbs.

2.2.1 Metavolcanics

In the Lawra belt, tholeitic subalkaline metabasalts (now upper greenschist /lower amphibolites facies metamorphic greenstones) dominate over porphyritic, calc-alkaline meta-andesites and meta-rhyodacites now mainly hornblende-actinolite-schists. Pyroxene- and uralitized porphyrites are subordinate.

The amphibole schists are dark green and dark grey tinted green, reveal well-foliated structure and nematoblastic texture. They consist of hornblende or actinolite, plagioclase, quartz, epidote, sphene and ore minerals.

The amphibolites are dark grey tinted green or dark green rocks which exhibit massive, hardly foliated structure. The main rock constituents according to Roudakov (1965) are hornblende and plagioclase.

The pyroxene- and uratilised porphyrites are black, more rarely greenish-grey rocks which shows massive structure with granoblastic texture of the groundmass composed of plagioclase and actinolite.

The metavolcanics are overlain and sometimes interlayered with chemical sediments (manganese-rich rocks, cherts) and pyroclastic-volcanosedimentary rocks.

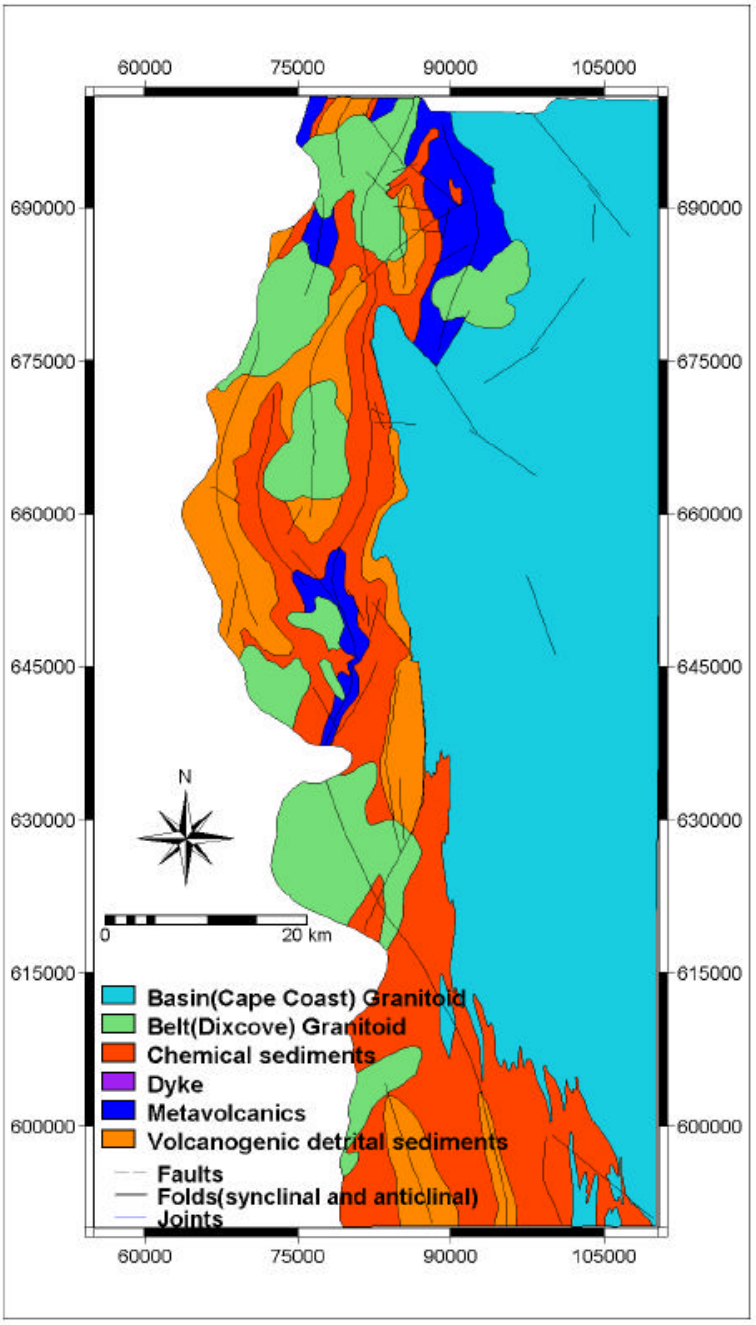

Figure 2.5: Geological map of the Lawra belt

2.2.2 Detrital volcanogenic sediments

These are mainly volcaniclastics, volcaniclastic wackes and argillites which have been metamorphosed to schists, phyllites, greywackes and tuffs. These pyroclastic and epiclastic rocks are isoclinally folded and inter-finger the greenstone units at some places.It also occurs in the transition zones

A chemical facies consisting of manganese-bearing rocks, cherts, suphide-bearing rocks, carbonate-bearing rocks and carbonaceous rocks is frequently present in transition between metasediments and metavolcanics.

2.2.3 Chemical sediments

The zones between volcanic belts and sedimentary basins are composed of various types of chemical sediments, pyroclastic-volcaniclastic rocks and volcanic rocks. Chemical sediments also occur in the top parts of the basaltic volcanic sequence. The chemical sediments include manganese-rich rocks (gondites), cherts, ferruginous cherts, and rocks variably enriched in sulphides, cabonates, barium, and carbon.

The manganese-bearing rocks and cherts often form lenticular bodies several 100m along strike. The manganese-bearing rocks are the most common type of chemical sediments in the Lawra belt.

According to Melcher and Stumpfl (1994), four types of Mn-bearing rocks can be distinguished mineralogically and geochemically. 1) Manganese oxide-rich rocks composed mainly of manganese oxides or hydroxides (pyrolusites, manganomelane minerals) which can be divided into maganiferous phyllites and altered/weathered gondites. 2) Pure gondites, which are metamorphosed non-calcareous, manganiferous, arenaceous and argillaceous sediments with sperssartine and quartz (Roy, 1965). 3) Gondites containing a manganese silicate and oxide assemblage. 4) Manganese-poor chlorite schists.

Cherts are widespread in the chemical sediments of the belt. They form layers and lenses up to several metres thick. They occur as dark or multi-coloured, fine-grained rocks consisting of quartz and accessory silicate, carbonate and sulphide phases (Melcher and Stumpfl, 1993).

The structure of the transition zone rocks is sometimes complicated by extreme deformation. Due to competency differences between basaltic and pyroclastic rocks, transition zones often host shear zones.

2.2.4 Granitoid rocks

There are two major types of Eburnean granitoid intrusions in the Lawra belt. The CapeCoast and Dixcove granitoids. The Capecoast granitoid occupies about 60% of the study area. According to Roudakov (1965), the magmatic rocks of the Capecoast granitoids were emplaced in four stages. 1) Uratilised gabbros and gabbro-pyroxenites phase. 2) Coarse and medium-grained biotite and less common hornblende-biotite granodiorites. 3) Medium-grained gneissic plagiogranites, granodiorites and granites. 4) Biotite, leucocratic pegmatoid granites.

The Dixcove granitoid is less widespread than the Capecoast. It often occurs as quartz diorites, plagiogranites and granodiorites according to Roudakov (1965).

2.2.5 Gold mineralisation in the study area

Quartz veins occur in almost all the lithologic units of the area. However, gold-bearing quartz veins have a distinct maximum in rocks of the chemical facies in transition zones between volcanic belts and sedimentary basins. The gold-bearing veins are observed in association with:

- shear zones paralleling belt/basin boundaries, especially dextral shear zones in chemical sediments, which are parallel to the contact; and
- discordant strike-slip faults cutting transition zone rocks.

The chemical sediments are of particular interest as a source of gold. According to Melcher and Stumpfl (1993), and the widespread manganiferous phyllites of the chemical sediments carry high background gold contents in the 11 to 64 ppb range. The gondites (spessartine-quartz rocks) in the greenstone succession carry 53 ppb Au, whereas those in the sedimentary succession carry 3 to 5 ppb Au.

The wall rocks of the transition zone of the belt are altered pyroclastic rocks and manganiferous phyllites and are characterised by more ”hydrous” minerals (e.g., chlorite) than the metamorphic assemblages in the volcanic belts, which are dominated by amphibole. The gold quartz veins reveal a secondary mineral assemblage characteristic of hydrothermal alteration i.e., chlorite, carbonate, muscovite, graphite, epidote and sulphides.

A number of gold occurrences are known in the belts. However, only a few of them are even mined at small-scale. A major mining (open pit and underground) operation is however carried out at the Poura mine in the Burkina Faso portion of the belt, which

is well studied and is generally believed to have a similar mineralisation style as the lode gold occurrences in the Ghana portion of the Lawra belt.

Poura mine

The Poura mine is located in the Mouhoun Province of southwestern Burkina Faso (Fig 2.6). It is centered over 11^o 35' North Latitude and 2^o 45' West Longitude and situated on the portion of Lawra greenstone belt in the Burkina Faso (also called Boromo-Goren greenstone belt in that country).

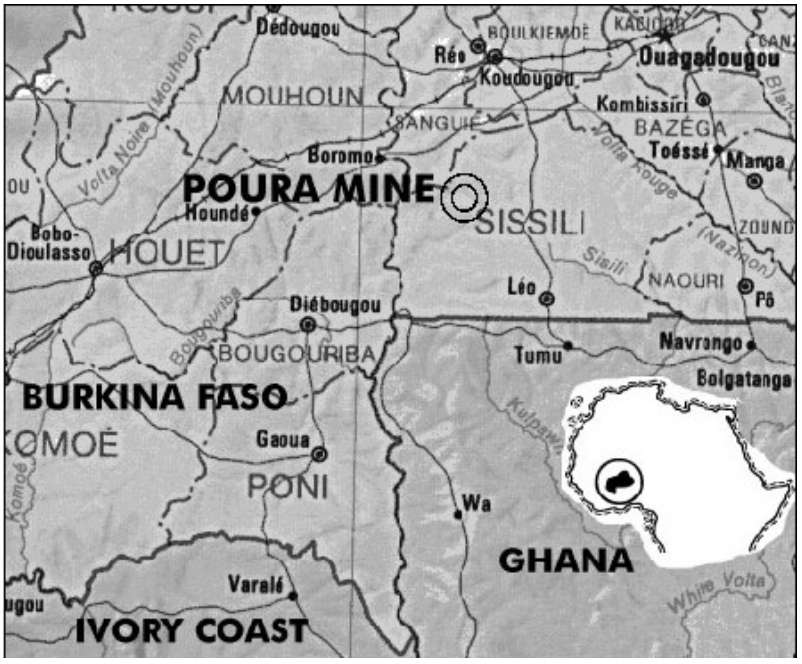

Figure 2.6: Location of the poura mine

Laterite covers the bedrock with a thickness that ranges from 0.5 metres to about twenty metres. Numerous mining excavations and drill holes provide a view of the bedrock geology. The footwall consists of dark green volcaniclastic rocks that are greater than 200m thick. They consist of welded tuffs, lapillis, pyroclastic breccias, and doleritic basalts with veinlets of quartz and rose carbonate. Younger detrital sedimentary formations, 20-200 metres thick, form the hanging wall. The ore is often fully surrounded by them. They consist of conglomerates, greywackes, sandstones, chert, and pelites. The base consists of conglomerates, sandstones, and greywackes with periodic intercalations of chert. The top consists of banded siltstone-mudstone with typical turbiditic structures.Volcanic formations, greater than two hundred metres thick, overlie the detrital formations. They consist of massive andesite flows, ash tuffs, lapilli tuffs, pyroclastic breccias, agglomerates, and volcanic dikes that cut the agglomerates.

The ore is vein quartz with silver-bearing (11 % average silver content) native gold and a minor percentage (about 2 %) of polymetallic sulphides. The deposit is oxidised (weathered) down to one hundred metres depth by supergene alteration that also produced locally high gold grades. The ore is made up of several different types. There is low-grade milky, massive white quartz. There is also grey vein quartz within the massive white quartz vein that is rich in pyrite-associated gold. A third type is heterogeneous milky white quartz that is present in the sinistral fractures. That type is barren of gold. The final type is boxwork quartz in the upper one hundred metres of the deposit where the gold was leached and concentrated. The boxwork quartz has the highest grades of all the ore types. Reconnaissance work in 1974 revealed 1.6 million tonnes of ore with an average grade of 13.5 g/tonne (Roy, 2000).

2.3 Conclusion

In conclusion, there is a close spatial relationship between gold bearing quartz veins in the study area and the metamorphosed chemical sediments now occurring as phyllites and schists in the transition zones on regional scale. On a local or occurrence scale and to a lesser extent regional scale, ductile shear zones in these rocks have a spatial relationship with gold bearing quartz veins. Auriferous orebodies in the shear zones marked by the chemical sediments are generally localised in narrow quartz veins and lenses enveloped by restricted alteration zones. The orebodies in the parallel shear zones of the chemical sediments are also localised in dilatant zones especially where dragging or mashing of the schist or phyllite has occurred.

Chapter 3

Conceptual Lode Gold Model

3.1 Introduction

The conceptual or knowledge-driven method of GIS-based mineral potential mapping involves the application of conceptual mineral deposit models to appropriate spatial digital data stored in GIS database to generate a mineral potential map. This method can be applied both to mature mineral fields and to areas that are barren of, or contain only few known deposits or mineral occurrences. The conceptual method is therefore much more suitable to the study area since few lode gold occurrences are known.

A mineral deposit model is a conceptual model that describes the typical characteristics of a group of deposits. It provides the frame work in data selection, in deciding which features to enhance and extract as evidence, and in deciding how to weigh the relative importance evidence in estimating mineral potential (Bonham-Carter, 1994).

The understanding and the usage of conceptual mineral deposit models in GIS-based deposit predicting modelling of mineral potential is based on the realisation that each deposit or mineral occurrence is only a minor part of a regional-scale mineralisation which comprises the following components: 1) mineral source, 2) heat source, 3) transport pathways (structures), 4) host rocks.

From the knowledge of the geology and the type of mineralisation in the study area, lode gold deposit model will be adopted.

3.2 The general characteristics of greenstone-hosted lode gold deposits

A lode deposit consists of a zone of veins, veinlets, disseminations, or planar breccias, (Bates and Jackson, 1985). Lode gold deposits are a characteristic feature of greenstone-sedimentary terranes. They have accounted for a high percentage of world gold production in the past, and contain a high proportion of known gold resources. The widespread distribution of greenstone lode gold mineralization is reflected by its high contribution to the total world gold production. The Superior Province of the Canadian Shield, for example, has produce more than 5000t of gold (Colvine et al., 1988), and Western Australia more than 3000t of Gold (Groves and Foster, 1991). Lode gold accounts for approximately a quarter of Canada's output (Ash and Alldrick, 1996). Thus, the greenstone lode gold deposits described above are extremely important group of deposits.

3.2.1 Ore mineralogy and metal association

Greenstone lode gold deposits are commonly termed 'gold-only' deposits because of the extreme enrichment of Au relative to other metallic elements (e.g. Cu, Pb, Zn, Ag) that commonly accompany Au in other deposits-types (e.g. porphyry Cu-Au, epithermal deposits, Au-rich VMS deposits).

The lode gold deposits, generally have simple mineralogy. Free gold and/or gold are sited in pyrite, pyrrhotite and arsenopyrite, with a heterogeneous distribution of accessory scheelite, tellurides, stibnite, galena, sphalerite, chalcopyrite, magnetite, hematite and anhydrite: all may be locally abundant in specific ore shoots (Groves and Foster, 1991).

3.2.2 Genesis of deposits

Lode gold deposits are now widely considered to be epigenetic to the environments in which they are found and also closely related to the tectonic setting which occurred during evolution of the greenstone-sedimentary terraine in which they occur.

The genesis of greenstone-sedimentary lode gold deposits worldwide is a subject of considerable controversy. Whereas epigenetic models are currently in vogue there are major controversies concerning the source of ore fluids and ore components, with metamorphic, magmatic (granitic, felsic porphyry or lamprophyle intrusions) and mantle sources all being invoked (Groves and Foster, 1991). A unifying model of

the models (Colvine, 1989; Groves et at., 1992) suggests gold mineralisation to be related to a single crustal scale process that involves deep-seated tectono-metamorphic event incorporating melting of mantle, magmatism and metamorphic fluids at upper crustal levels.

Gold is precipitated from highly focused auriferous fluids along ductile transcraton shear zones with transient fluid flow into adjacent brittle-ductile structures. The nature of ore fluid, ore-element association, high gold:base-metal ratios, and commonly intimate association of gold with Fe-sulphides all suggest that gold was transported as reduced sulphur complexes (Phillips and Groves, 1983).

In many of the larger deposits, where the bulk of the gold is intimately associated with Fe-sulphides in host rocks with high Fe/(Fe+Mg) ratios, it is likely that wallrock sulphidation reactions induced instability of the reduced sulphur complexes and caused gold precipitation (Philips and Groves, 1984). Such mechanisms are, however, not universal because some rock types with low Fe/(Fe+Mg) ratio are mineralised, and it is likely that other fluid-wallrock reactions induced changes in pH and fO_2 that initiated gold deposition (Groves and Foster, 1991). Fluid-wallrock reaction are thus the probably most important in producing large average-grade gold deposits as fluid permeates through the fractures and shear zones.

3.2.3 Size and grade of deposits

A majority of greenstone lode gold deposits has an average production of only about 1 t Au; however, in any terrane there are commonly several large deposits in a highly mineralized greenstone belt, often with one or more giant gold districts or camps, (Groves and Foster, 1991). For example, in the superior province of Canada, there are 25 deposits that contain more than 45 t Au and the Timmins (Porcupine) ditrict has contributed more than 1530 t Au (Colvine et al., 1988). Similarly, in the Yilgarn district of Western Australia, 14 deposits have produced more than 20 t of gold. Golden Mile at Kargoorlie have produced about 1150t Au with further reserves of more than 120 t Au . The Ashanti Belt in Ghana, has also produced the bulk of West Africa's greenstone lode gold, where the Obuasi mine of Ashanti Goldfields produces 16,000 kg Au per year since 1990 (DzigbodiAdjimah, 1993).

The ore grade of greenstone lode deposits, as mined, varies widely between operating mines or group of mines (Groves and Foster, 1991). For example, greenstone lode gold deposits in the Yilgarn Block has fallen from excess of 40 g/t Au in 1890s to

less than 5 in 1988 (Ho and Groves, 1987). Recent technology has allowed open-pit mining of weathered ore zones with grades typically below 5 g/t (cut-off grades below 0.5 g/t), in the Yilgarn Block of Western Australia and in the Birimian of West Africa.

3.2.4 Structural Styles

Structure is the single most important factor controlling the distribution of gold deposits and the form of gold ore shoots.

On the regional scale, major gold deposits are commonly sited adjacent to transcraton shear zones and on the district scale they are usually sited in shorter strike-length, geometrically related, smaller scale structures. These structures hosting the gold deposits appear to largely reflect the movement on the transcraton shear zones, with different structural styles of mineralization resulting from variations in the orientation of the regional stress field and the strength of the host rocks (Groves and Foster, 1991).

At the goldfield to deposit scale, the major control on the location of the lode-gold deposits is structure, with most deposits in second- or third-order structures, most commonly near regional-scale (typically transcrustal) deformational zones.

Variety of structural styles can develop, even in small area. Important hosting structures include; (1) brittle faults to ductile shear zones with low-angle to high-angle reverse,strike-slip or oblique-slip movements, (2) fracture arrays, stockwork network or breccia zones in competent rocks, (3) foliated zones with pressure solution cleavage, or (4) fold hinges and associated reverse faults in ”locked-up” folds modified after (Eilu et al., 1998). Most of the shear-zones form at major structural discontinuities near the contact between major sedimentary and volcanic rock sequences is sub parallel to stratigraphy, continuous, or anastomising over distances of greater than 30 km, and are as much as 2km wide (Klein and Day, 1994).

Steep reverse shear zones may be particularly important ore-controlling structures (Colvine et al., 1988). In many cases, the ore shoots have a marked plunge sub parallel to mineral-elongation lineations in the host rocks, suggesting a fundamental structural link between stretching and development of conduits which focused fluid-flow (Groves and Foster, 1991). For example in Ghana, and in the Birimian greenstone, major primary gold lodes are associated with persistent and deep-seated shear zones (Wright et al., 1985).

3.2.5 Host Rocks

On a world and regional scale all lithologies in greenstone belts can be mineralized, and at the mine scale several different rock-types may host economic gold mineralization (Groves and Foster, 1991). Greenstone lode deposits can occur in virtually all rock types within the hosting volcanic-sedimentary rock sequences (Eilu et al., 1998). The favourable host rocks are commonly basalts, andesites, latites, and trachytes and rhyolites. Many deposits also occur in tuffs, agglomerates and sediments interbedded with volcanic flows (Boyle, 1979). A typical example of mineralisation in sediments, is the Birimian of West Africa.

3.2.6 Wallrock alteration

Wallrock alteration, associated with greenstone lode gold deposits normally involves massive introduction of CO_2, K_2O, S and H_2O, with either introduction or redistribution of SiO_2 and more localized introduction of Na_2O; Rb, Li and Ba are also commonly enriched.

Wallrock alteration shows much stronger lateral variation around gold-bearing veins than vertical variation in the plane of the ore bodies. Mineral assemblage and width of the zones vary with wallrock type and crustal level of hydrothermal alteration. However, most alteration zones show evidence for additions of significant amounts of CO_2, S, K, H_2O. In general, the shape of the alteration envelope is similar to the form of the gold mineralization (Eilu et al., 1998).

3.3 Conceptual model of lode gold mineralisation in the Lawra belt

Lode gold mineralisation in the Lawra belt is considered to be epigenetic and also closely related to the tectonic setting which occurred during the evolution of the Birimian rocks.

3.3.1 Proposed model for Birimian evolution

(Leube et al., 1990), described an intra continental rift setting of the Birimian Supergroup. They proposed the following model for the evolution of the Birimian greenstone sedimentary rocks, as presented in (Fig 3.1). The events occurring during each stage of the evolution are described as follows:

Stage I. Beginning of attenuation and fracturing of a sialic crust by a small-scale convective system in an upper mantle. Development of a parallel, evenly-spaced fracture pattern.

Stage II. Progressive attenuation to near-complete destruction of sialic crust. Rifting at sites of the previously formed fracture pattern. Beginning of the rise of tholeitic lava in rifts.

Stage III. Accumulation of large volumes of volcanics. Formation of volcanic ridges. Growth of volcanoes above sea-level; deposition of volcanic-derived sediments in slowly derived sediments subsiding basins.

Stage IV. Termination of volcanic activity. Exertion of lateral compression by two counteracting sialic blocks. Crustal shortening by folding. Emplacement of synorogenic G1 granitoids into basin sediments. Emplacement of late-orogenic G2 granitoids into belt volcanics.

Stage V. Reactivation of rifting. Formation of intramontane basins in volcanic belts. Infilling of clastic sediments derived from Birimian rocks eroded nearby. Gravity deformation of Tarkwaian sediments. Emplacement of mafic sills and post-Eburnean K-rich granitoid (G3).

Tectonic setting

Boyle, (1991) suggested that the compressional tectonic forces that acted during the sinking of greenstone rift basins operated in the following time sequence: 1) initiation of folding of the volcanics and interbedded sediments; 2) structural failure (shearing) along incompetent structural features such as volcanic/sedimentary contacts, resulting in the formation of parallel shear zones; and 3) continued sinking of the greenstone pile initiated thrust faulting (transecting the shear zones).

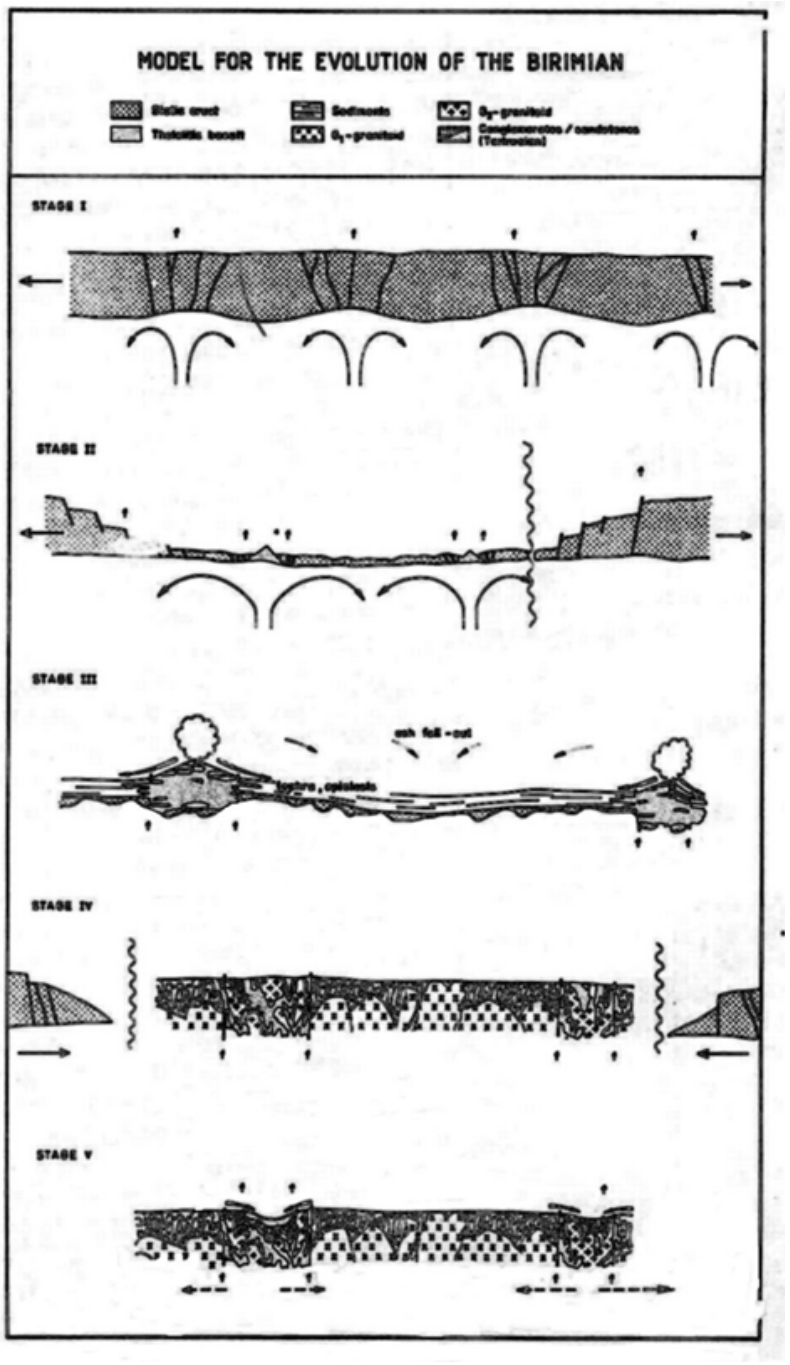

Figure 3.1: Model for the evolution of the Birimian

3.3.2 Genetic model of gold-quartz veins in the Lawra belt

In the Lawra greenstone-sedimentary belt situation, the deep-seated parallel shearing acted as a conduit for convective gold- and base metal- bearing hydrothermal fluids to be exhaled during stage III, resulting in the precipitation of chemical sediments along the volcanic/sedimentary boundary. This is evidenced by elevated background contents of gold in the chemical sediments (mean 20-30 ppb) (Melcher and Stumpfl, 1994). The continued folding and emplacement of belt-granitoid caused the rise of geotherm and the subsequent mobilisation of gold from the chemical sediment into structurally favourable sites. The conceptual Lode gold model used in this study to explain Lode gold occurrences in the narrow transition zones of the Lawra belt is illustrated in (Fig 3.1), and is after (Melcher and Stumpfl, 1994).

Metal source Submarine exhalation of base metal- and gold-bearing fluids during Birimian volcanic activity in stage III produced chemical sediments with elevated background content of gold (mean 20-30 ppb); During this stage Au is transported in chloride complexes and precipitated together with sulphides or hydroxides.

Heat source Hydrothermal metamorphogenic fluids mobilized gold from the chemical sediments and deposited it in structurally favourable zones.

Transport pathways (Structures) Transport of the remobilised gold fluid occur in the form of reduced sulphur complexes and deposited into dilatant sites within; 1) the parallel belt/basin shear zones and 2) discordant strike-slip faults cutting transition zone rocks. Precipitation of gold occurred with arsenopyrite and later as native gold in quartz veins.

Favourable host rocks

Host rocks On a regional scale all lithologies in greenstone belts can be mineralized, and at the mine scale several different rock-types may host economic gold mineralization (Groves and Foster, 1991). The case of the Lawra belt is different, the chemical sediments now occurring as manganiferous phyllites, schists, cherts are the main host rocks. To a very lesser extend the volcanogenic detrital sediments and metavolcanics are favourable host rocks.

Alteration Wall rocks of the quartz veins show secondary minerals such as chlorite, muscovite, graphite, carbonate, quartz and sulphides, (Fig 3.3). Altered rocks in the transition zone are characterised by more hydrous minerals (e.g., chlorite).

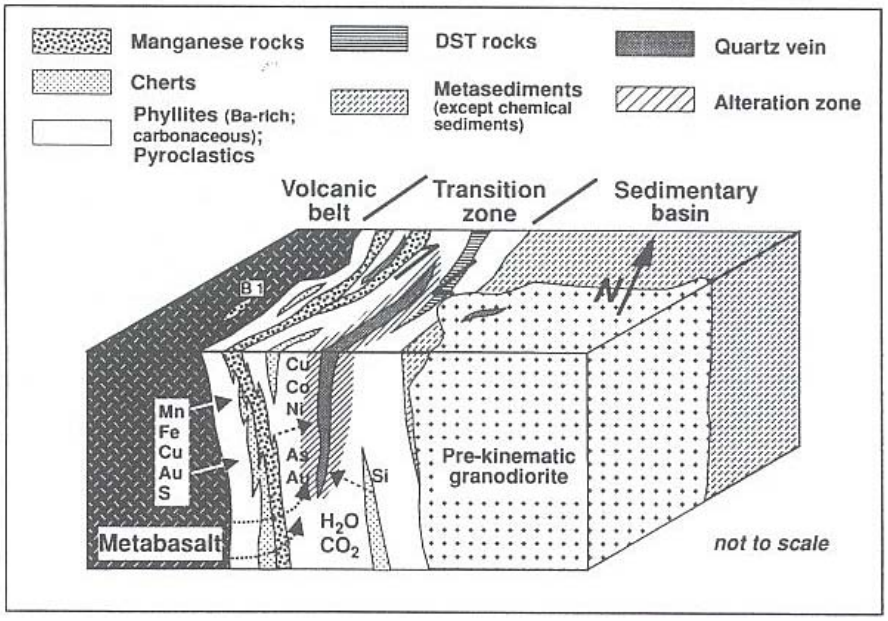

Figure 3.2: Genetic model of gold-quartz veins. Migration of elements from Chemical sediments rocks into quartz veins is shown schematically after (Melcher and Stumpfl, 1994).

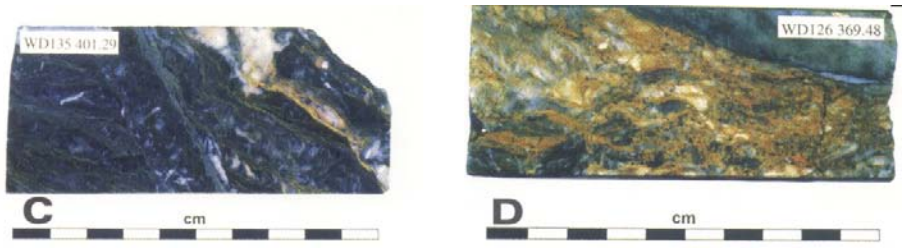

Figure 3.3: photographs illustrating the style of alteration related to lode gold mineralisation

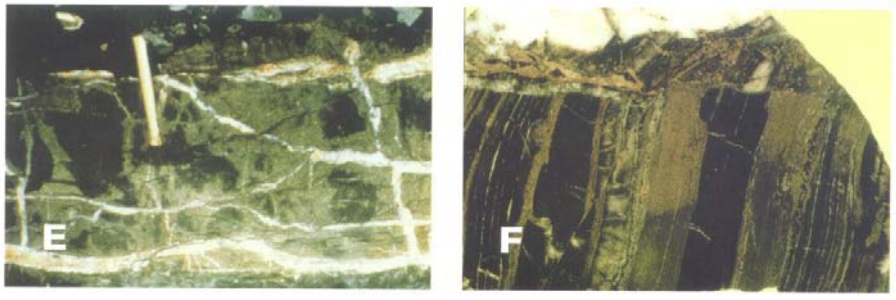

Figure 3.4: Lode gold vein sets enveloped by alteration

3.4 Conclusion

Gold is concentrated in the Lawra belt by volcanic related syngenetic processes (stage III), principally chemical precipitation in exhalative sediments. The gold and associated minerals are remobilized from these chemical sediments by post depositional processes, which include compaction and diagenesis of auriferous sediments, deformation and metamorphism and the deformation-metamorphic processes associated with the emplacement of belt-granitoids. The auriferous fluid is then transported and deposited in structurally favourable sites

The four most important spatial features or exploration guides to greenstone hosted lode gold mineralisation in the Lawra belt as seen in the genetic model are structures, host rocks, metal source and wall rock alterations. The following parameters serve as guides from exploration point of view.

- At occurrence scale the important hosting structures may be; 1) brittle faults to ductile shear zones with high-angle reverse, strike-slip movements, 2) fold hinges and associated reverse faults in ”locked-up” folds. At regional scale, important structures are the major parallel shear zones in the chemical sediments.

- Wallrock alteration patterns are also important for exploration, because they are in most cases, easily detected in outcrops, and because the alteration halos are more extensive than the gold ore itself. Alteration halo mapping helps in defining target areas for further exploration. Further study and mapping of the sequence of alteration zones can also be used to define a rough vector towards the potential gold mineralisation.

  In the Lawra belt, extensive alteration halos are characterised by clay minerals and swamps which are due to weathering of the alteration minerals.

- Gold-bearing quartz veins occur preferentially in chemical sediments at the belt/basin boundaries.

  Chemical sediments, earlier produced by submarine exhalation of base metal- and gold-bearing fluids during volcanic activity served as the metal source. This concept of the chemical sediments as the primary source is supported by the elevated background values of Au in the chemical sediments and occurrence of Cu deposits in the Burkina Faso portion of the belt.

Chapter 4

Resource and Methodology

4.1 Resource

The first step of any GIS-based approach is to provide a spatial database. Much of the success of a GIS project depends on the quality and nature of the data that is entered into the system. Thus the nature and provenance of datasets for this study as well as the software used are discussed here.

In addition, spatial datasets in GIS, such as geological maps, satellite imagery, geophysical maps, etc. can be classified into two broad categories: objective and subjective. Satellites imagery and geophysical datasets are objective in nature, in that the maps show the distribution of a measurable quantity (e.g. reflectance for Landsat imagery). Conventional geological maps, on the other hand, contain a high degree of interpretation and are therefore considered to be a more subjective dataset. Objective and subjective datasets can further be divided as being spatially consistent or spatially inconsistent. Satellite data are a good example of spatially consistent dataset in that an entire area is captured uniformly to the same level of detail (e.g. 30m pixel size). Geological maps tend to be less spatially consistent. Areas that are difficult to access are normally mapped with lower detail than areas that are easily accessible.

4.1.1 Available datasets

The next step after examining the geology and lode gold mineralisation of the study area, and defining the spatial controls on the formation and localisation of lode-gold deposits at occurrence-scale to terrane-scale, is to determine which data sets are available and useful for enhancing and extracting such spatial control features.

Table 4.1: Available spatial and non-spatial data sets

Data	*Description*
1.Geological Maps (hard copy)	1. Geological map of the northern part of study area (1:250,000) 2. Geological map of the southern part of study area (1:250,000)
2. Mineral occurrence map (hard copy)	gold occurrence in a thematic map
3 Structural Map from geological mapping	Structural map to be prepared from geological maps, scale (1:250,000)
4. Air borne Magnetics (digital)	Total magnetic field map, in mapinfo format (pixel size 110m)
5. Airborne Electromagnetics	1) High frequency in phase imaginary (HFI) component map (pixel size 100m) 2) High frequency in phase real (HFR) component map 3) Low freqency in phase imaginary (LFI) component map 4) Low frequency in phase real (LFI) component map
6. Airborne Radiometric data	1) Uranium ground content map (pixel size 100m) 2) Thorium ground content map 3) Potassium ground content map
8. Structural map interpreted from Geophysical dataset	Structural map from processing and interpreting magnetics, electromagnetics and radiometrics geophysical data sets
9. Airborne Geophysical report	Final report of processing and interpretation of data from Airborne geophysical survey concerning certain areas of Ghana by both Geological surveys of Sweden and Ghana.
10. Geological reports	Geological reports of the study area in the Geological survey

The relevant spatial and non-spatial data available for this study are listed in (Table 4.1). The intention is to prefer datasets that are objective and spatially consistent and less subjective datasets for the extraction of features, representing spatial controls of gold occurrence in the study area.

Geological Map

Two geological maps, each at 1:250,000 scale covering the southern and the northern parts of the study area, were obtained from reports of Roudakov (1965) and Pobedash (1965) respectively. The Geological Survey of Ghana prepared the map in 1965 based on field surveying and prospecting with the aid of a base map at a scale of 1:125,000 and 1:250,000. According to Roudakov (1965) some portions of the area were however detail mapped to make it possible to construct geological maps to scale of 1:50,000, 1:10,000 and 1:5,000 . There is therefore a degree of subjectivity in this data as the mapping scale varies. Fortunately, as the purpose of this study is a regional-scale predictive modelling, the above problem is significantly reduced by the degree of generalisation required to produce such a regional geological map from the field maps. There is therefore spatial consistency in the resulting geological map.

Mineral Occurrence Map

The gold occurrence map of the study area is obtained from a thematic map (hard-copy) prepared by the Geological Survey of Ghana. This include 19 occurrence sites.

Geophysical Data

The geophysical data comprises processed airborne magnetics, electromagnetics and radiometrics in digital formats. The data were obtained from Geological Survey of Ghana and cover an area bounded by latitude 9^o 30'N and 11^o 00'N, and longitude 2^o 23'W and 3^o 00'W. The processing and interpretation were done by a geophysical team from Geological Surveys of Sweden and Ghana. The project was part of a World Bank Project Mining Sector Development and Environment Project, (this particular sub-project, which was financed by the Nordic Development Fund was to carry out the processing and interpretation of airborne geophysical surveys in certain areas of Ghana.The specific processing of airborne data by the team were as follows:

Magnetic data

- Manual removal of remaining spikes caused by hydraulic pump in the aircraft.
- International Geomagnetic Reference Field (IGRF)-reduction

- Low pass filtering of survey and tie lines, cut off wavelength 12km.
- Statistical levelling of tie lines.
- Standard Oasis tie line levelling.
- Fine levelling using levelling lines extracted from grid or tie line levelled data. The tie levelling was again made applying the Oasis tie line levelling procedure after low pass filtering of the survey lines.

Electromagnetic data

- Non linear filtering of data to remove thunder storm spikes and high frequent noise.
- Low pass filtering of survey and tie lines, cut off wavelength 12km.
- Statistical levelling of tie lines.
- Standard Oasis tie line levelling

The geophysical maps received were stored in Mapinfo format in both Ghana national (meter) grid and Ghana national (Lat-Long) coordinate systems.

4.1.2 Software

The softwares used in this research are as follows.

ILWIS 3.0 The Integrated Land and Water Information System is a GIS software package by ITC and was used for; 1) digitising and editing of geological map. 2) extraction and analysis of spatial features. 3) modelling (data integration)

Mapinfo 4.5 To access the geophysical data and import into ILWIS.

4.2 Methodology

The freedom to select an empirical (data-driven) method rests solely on the number of known deposits or occurrences in the study area. Since the method is a statistical method, it is therefore appropriate to use a significant number of mineral occurrences. Notwithstanding the constraint by the number of known mineral occurrences in the Lawra belt, both knowledge and data driven methods are used in generating predictive model of the area.

The different steps in capturing spatial data, extraction of spatial features and integrating spatial features to generate a predictive model by the above methods are summarised in the flow chart (Fig 4.1).

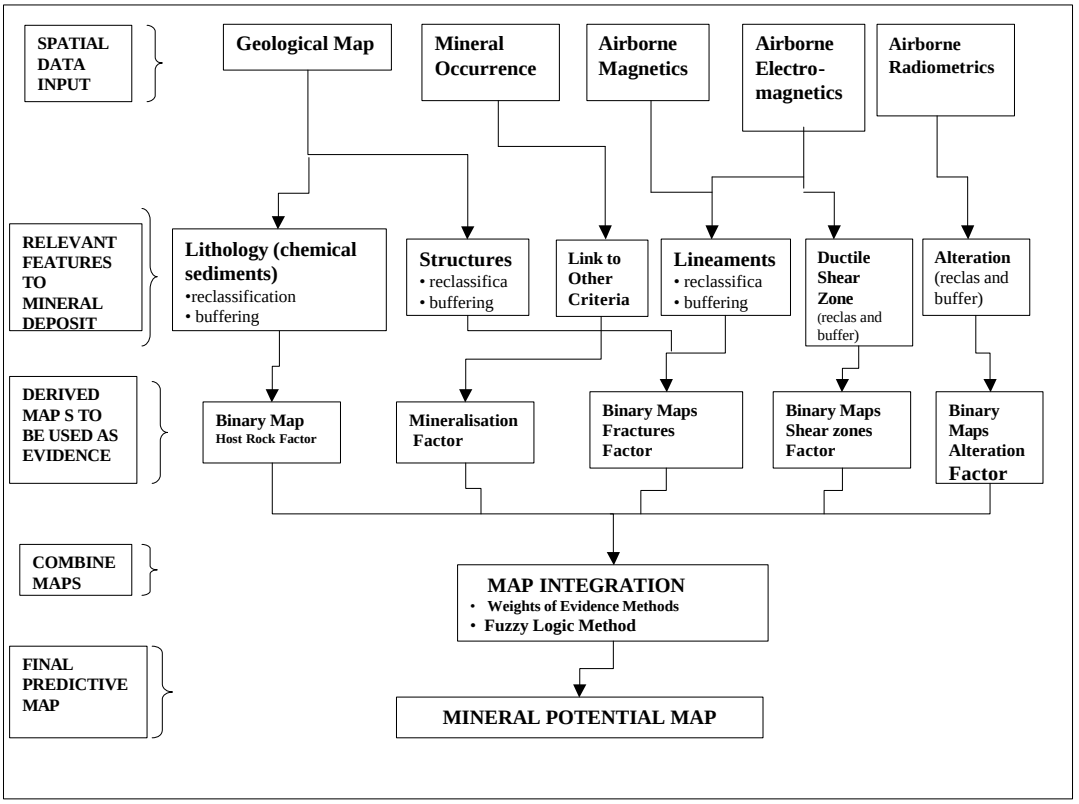

Figure 4.1: Flow Chart of the methodology

4.2.1 Data capture

In order to capture digital formats of datasets which were available in hardcopy, the datasets were first scanned and the rows and columns of the resulting scanned raster formats related to the real world coordinates by georeferencing using 'tiepoints'.

Geological and Structural data

Data from the hardcopy geological and structural maps were captured by digitising the lithological contacts and structures as segment maps. Since there were two different geological maps, these maps were digitised separately and then later merged as one segment map. The geological segment map was then polygonised to produce a polygon map of the geology of the study area.

Mineral occurrences data

The mineral occurrences map was also captured from hardcopy map by digitising as a point map in ILWIS.

4.2.2 Extraction of relevant features

The next step of this study methodology is to extract the identified spatial features relevant to the conceptual mineral deposit model described in chapter 3. The spatial feature or features extracted from each input dataset and the importance of such dataset in providing the relevant features are described in the chapter5. The various techniques used in extracting those features from the input datasets are also described. The favourable host rocks i.e. the chemical sediments will be extracted from the Geological map. Fractures which are conduits for mineral fluids will be extracted as lineaments from both magnetics and EM geophysical maps.

4.2.3 Data integration

After extracting the spatial control features, which are the evidence critical to the prediction of lode gold from the available datasets, the next step is to quantify these spatial relationships to a map illustrating how the spatial feature behaves in the study area. These maps are binary predictor maps comprising two states (prospective and unprospective). The binary predictor pattern maps are then integrated into a predictive model using two different GIS-based integration methods: the Index overlay (knowledge driven) method; and the Bayesian (data-driven) method. The two integration methods used to generate the predictive models are discussed in chapter six.

Chapter 5

Extraction Of Features Indicative of Lode Gold Mineralisation

From the conceptual model of lode gold mineralisation described in chapter 3, the four most important indicative spatial features or exploration guides are shear zones, favourable host rocks, hydrothermal alterations and fractures. This chapter involves mapping of these features and the use of various GIS-based techniques to extract them from the available datasets.

5.1 Qualitative geophysical interpretations

The available geological map which was prepared in 1965 comprises five different domains of rock units, namely the Cape Coast granitoid, the Basin metasediments, the Dixcove granitoid, the metavolcanics and the chemical sediments. To improve the available geological map and also to reduce the level of its subjectivity, a qualitative interpretation of the bedrocks from some of the geophysical datasets is done. This process involves overlaying the existing geological map and interpreting geological boundaries to the geophysical maps.

5.1.1 Qualitative interpretation of aeromagnetic map

An airborne magnetic survey is a helpful geophysical method in mapping subsurface bedrock geology due to variations in magnetic susceptibility of rocks.

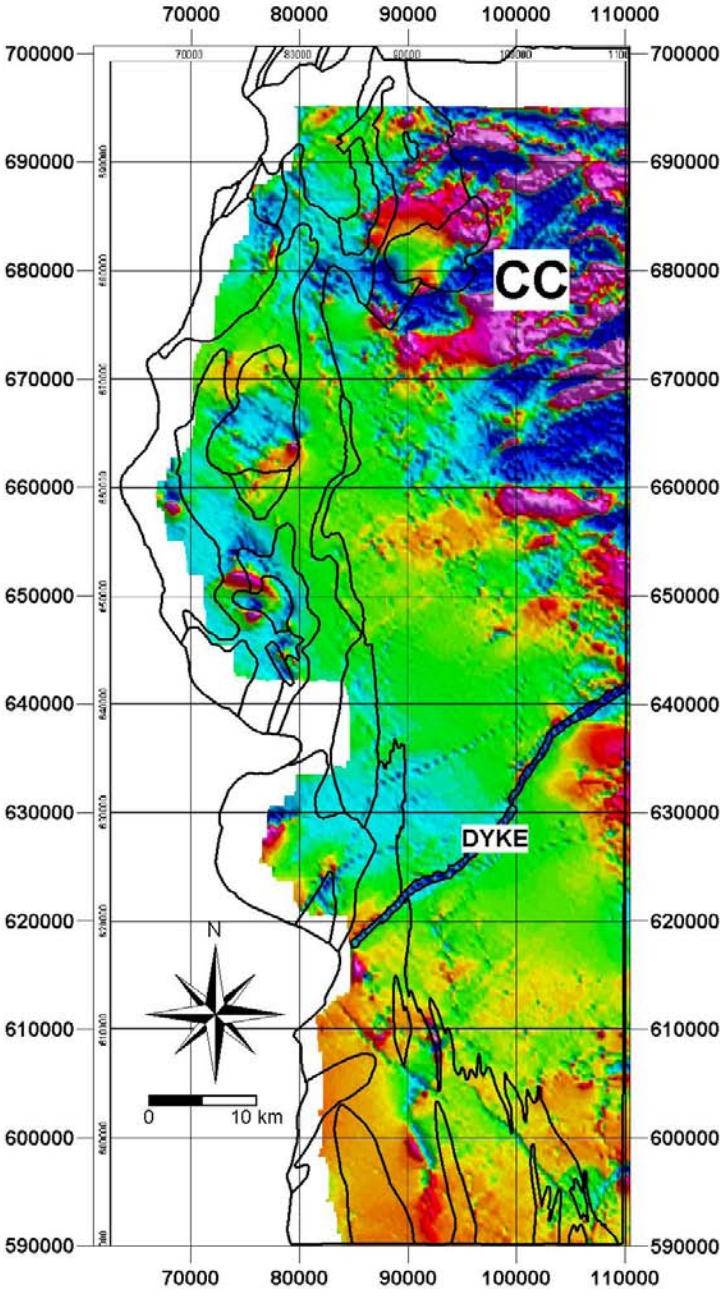

Figure 5.1: Geological boundaries overlaid on total intensity map, CC shows the high analytical signal portion of the CapeCoast granitoid, and a NE-SW trending dyke mapped from total intensity map

According to Reeves (2000), where the bedrock geology cannot be mapped due to thick jungle, swamp, deep weathering or sand cover, aeromagnetics can give information on the hidden geology using methods of inference that are similar to those used in photogeological interpretation. Asadi and Hale (1999), for a example used the analytical signal of total magnetic intensities to delineate intermediate composition magmatic rocks in the Takab area of Iran. In the study area, the high analytical signals of total magnetic intensities can be attributed to the Cape Coast granitoids (Fig 5.1). The volcanogenic detrital sediments and chemical sediments of the study area generally have low to moderate analytical signal. In the study area a dyke that trends SW-NE which is not indicated in the geological map is interpreted from the aeromagnetic map.

5.1.2 Qualitative interpretation of radiometric maps

Radiometric geophysical data indicates the variation in the chemical abundances of radioactive elements uranium, thorium and potassium. Potassium occurs in rock-forming minerals such as feldspar, mica and amphibole. These minerals are common in most rocks but not in sedimentary precipitates and evaporites such as the chemical sediments in the study area. Potassium abundances are higher in acid and alkali feldspar granitoids and lower to nil in mafic rocks (Gunn et al., 1997). Uranium and thorium on the other hand can be abundant in igneous and clastic sedimentary rocks that contain minerals such as zircon, sphene and apatite as minor accessory minerals (Woods, 1987). According to Reeves (1990), changes in the concentration of the three radio elements could therefore be used as a tool for geologic mapping in many areas. The metavolcanics of the study area are mapped out by their low analytical signals from the potassium map (Fig 5.2). The signature of the chemical sediments in the K, U and Th maps however varies and a systematic signature for delineation is therefore difficult to observe.

5.1.3 Qualitative interpretation of electromagnetic (EM) data

The Dixcove granites are recognised in the EM geophysical maps as rounded structures with moderate electrical conductivity, though some of them show patchy areas with increased conductivity (Fig 5.3). The Birimian, rocks namely the chemical sediments, the metavolcanics and the volcanogenic sediments, appear as banded anomaly complexes around the Dixcove granites (rounded structures) with more or less parallel bands of moderate and high conductivity.

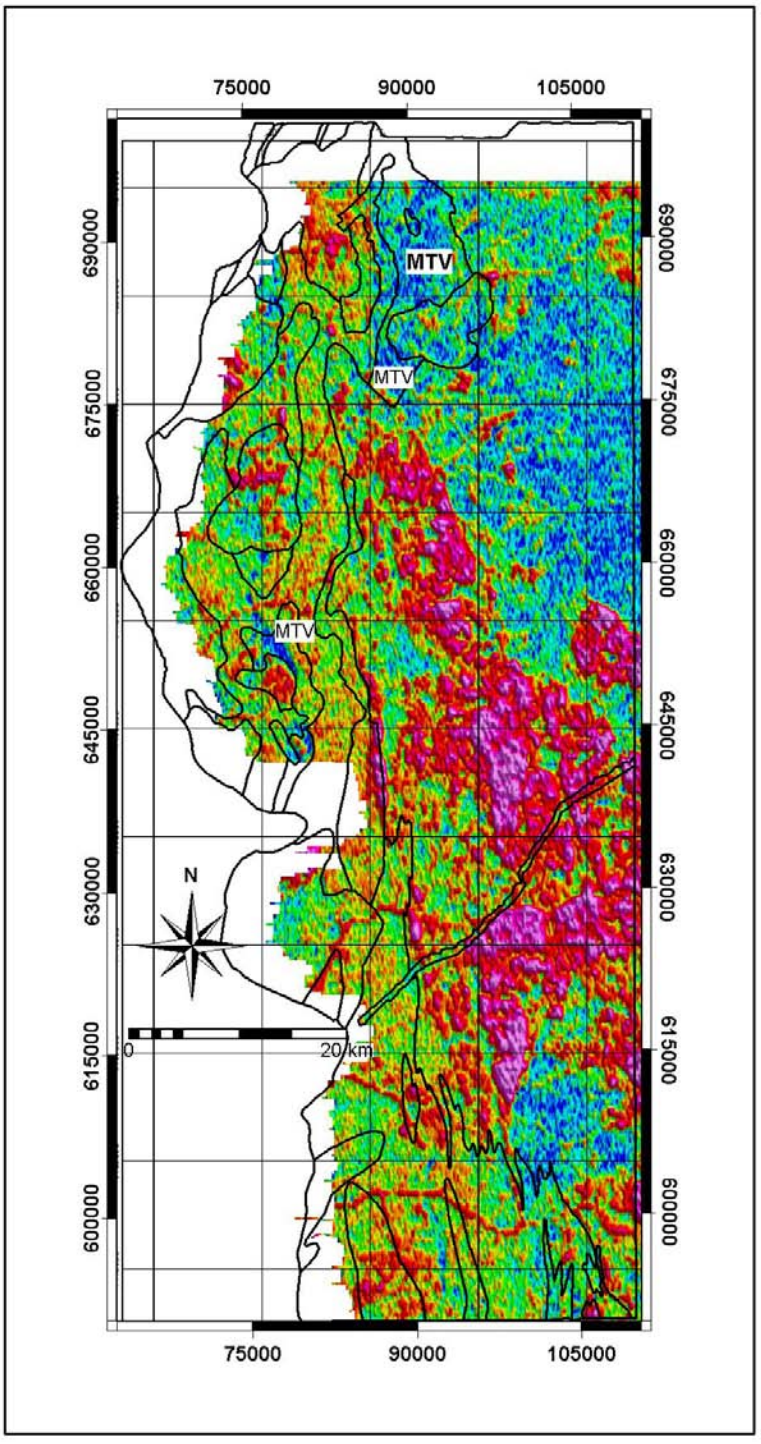

Figure 5.2: Geological boundaries overlaid on radiometric K map, MTV, with the metavolcanics showing as low K analytical signal

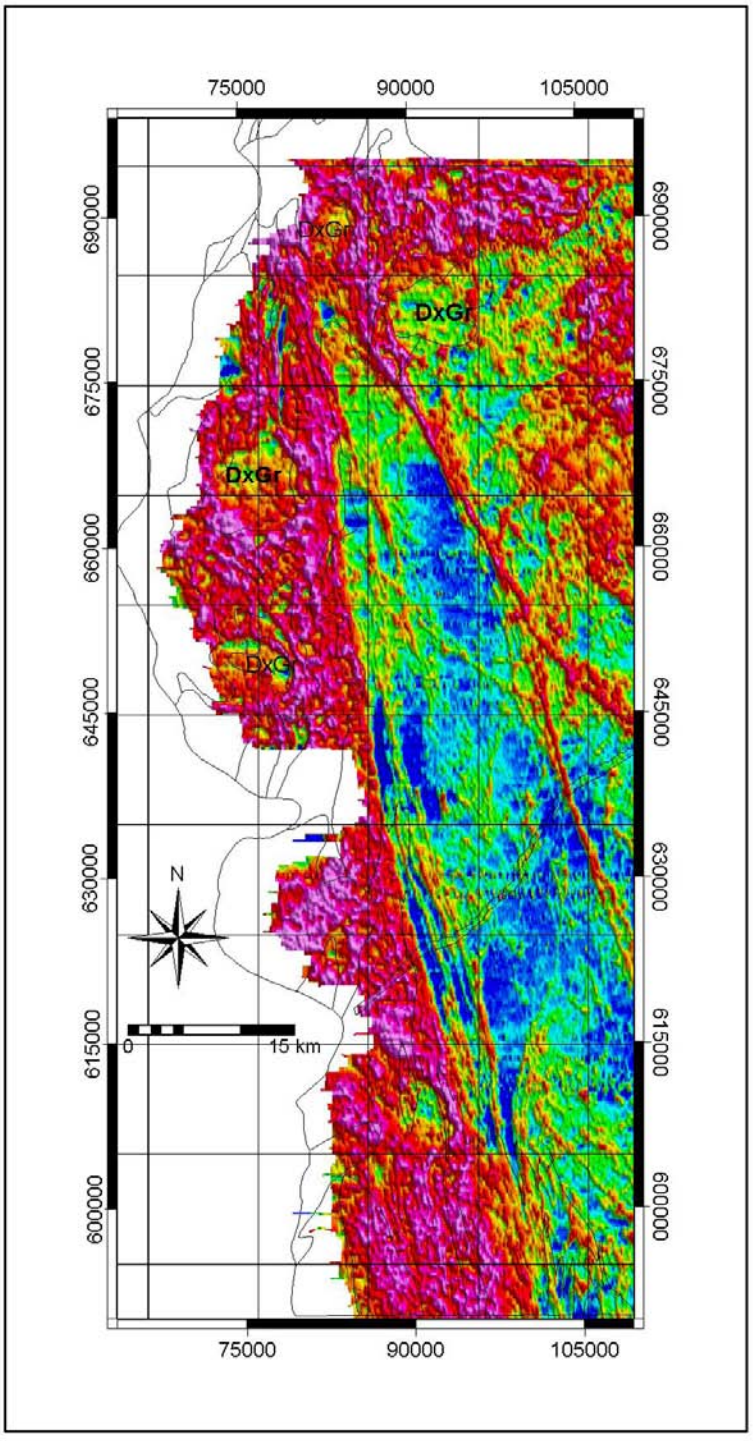

Figure 5.3: Geological boundaries overlaid on EM map, the Dixcove granites, DxGr, are shown as rounded structures with moderate electrical conductivity

5.2 Extraction of favourable rocks

With the exception of an interpreted dyke not much modification to the old geological map was done from the geophysical interpretations, nevertheless the exercise has given much confidence in the old geological map as the geophysical responses of the various units could be interpreted. The resulting edited geological map is shown in Fig 5.4

The extraction of favourable host rocks of the chemical sediments, from the edited geological map involves reclassification using map calculations in ILWIS. The polygon geological map is first rasterised and a map calculation is used to extract the relevant features. The result of the extraction of the favourable host rocks is shown in Fig 5.5.

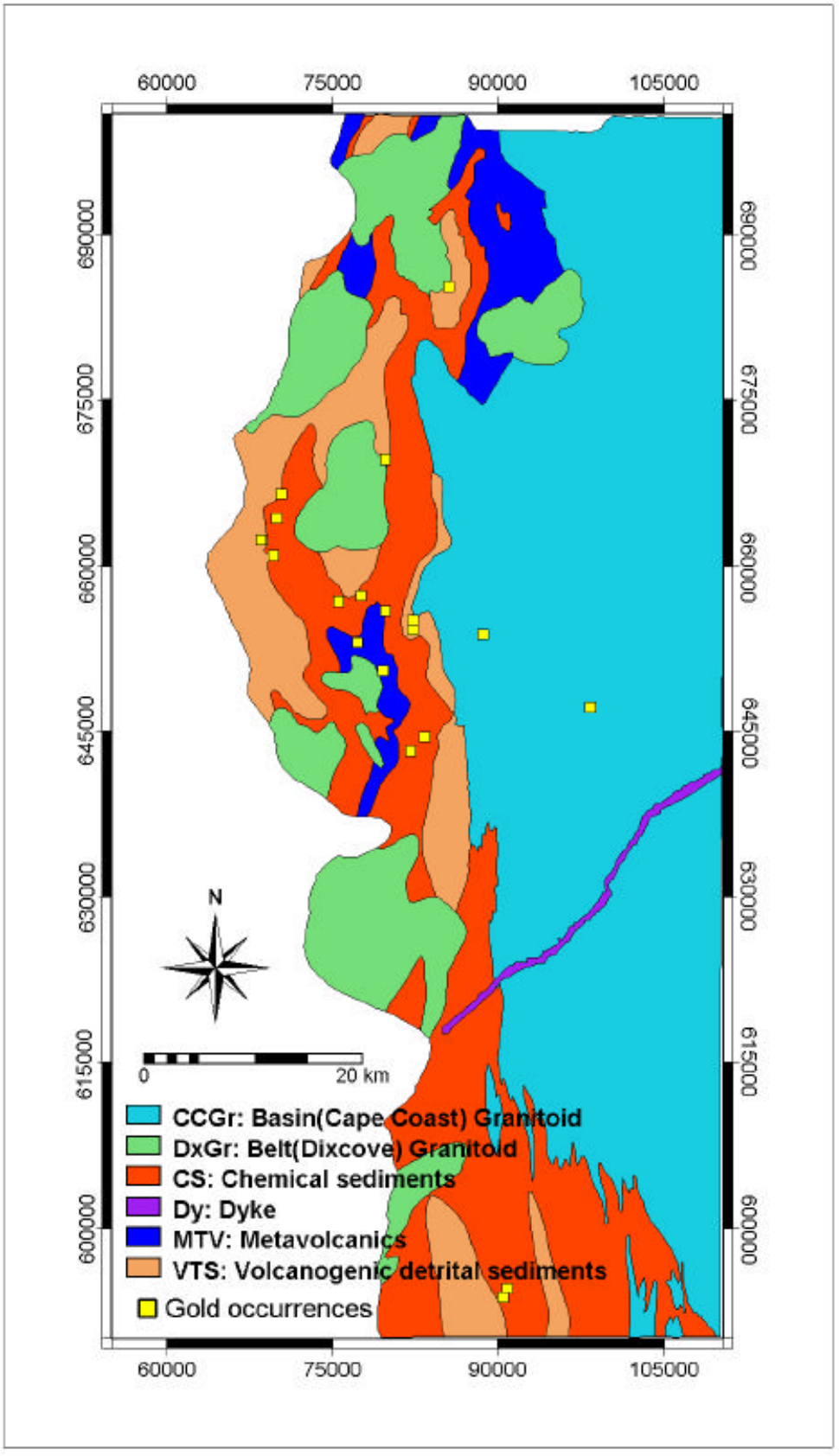

Figure 5.4: Edited geological map from the qualitative interpretation

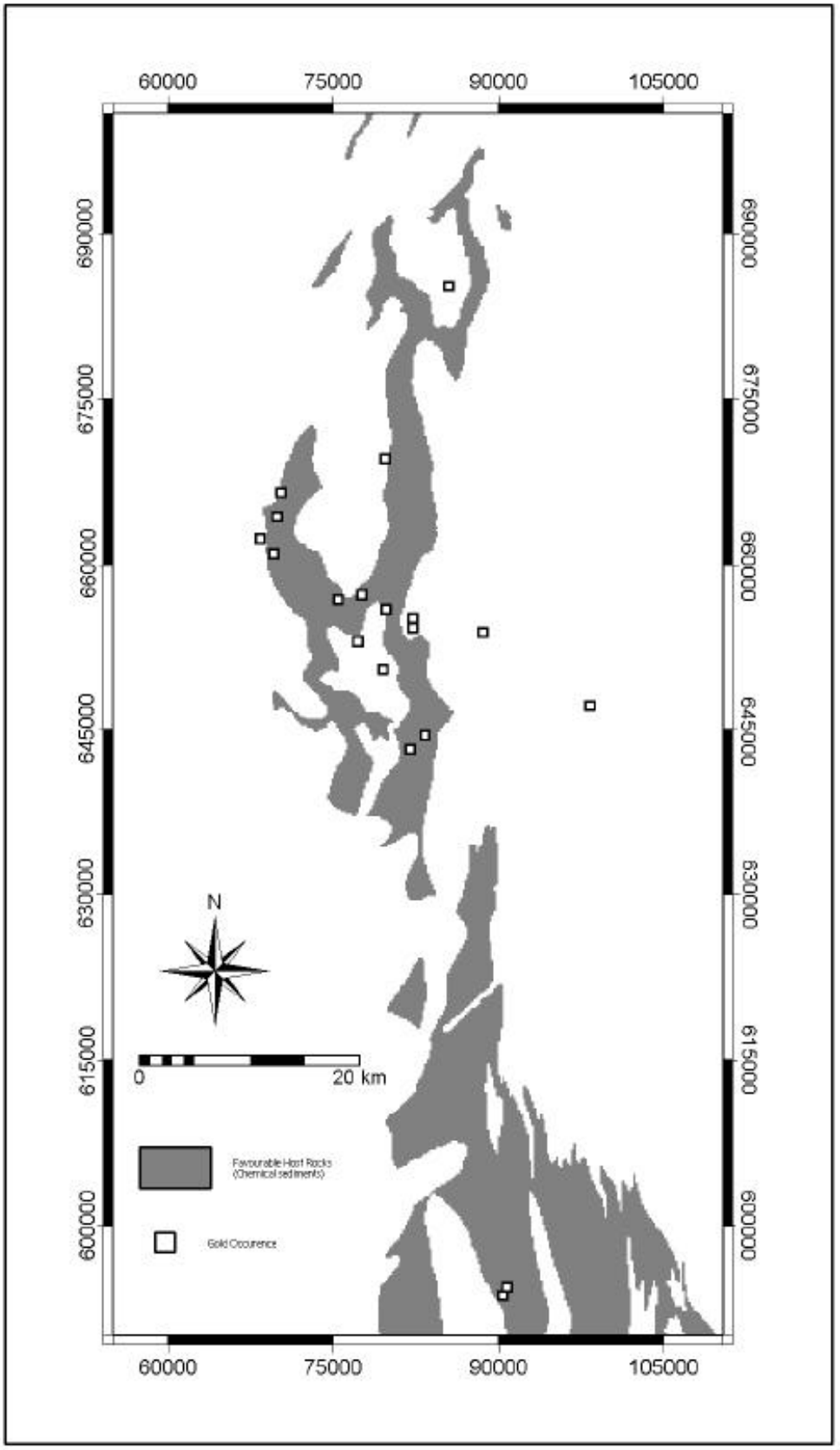

Figure 5.5: Map showing favourable host rocks, the chemical sediments (an indicative geologic features) extracted from geological map

5.3 Extraction of lineaments

A lineament is a mappable, simple or composite linear feature of a surface, whose parts are aligned in a rectilinear or slightly curvilinear relationship which differs distinctly from the patterns of adjacent features and presumably reflects a subsurface. phenomenon (Oleary et al., 1976). Lineaments are believed to be the expressions of ancient, deep-crustal or trans-lithospheric structures, which periodically have been reactivated as planes of weakness during subsequent tectonic events. These planes of weakness, and in particular their intersections, may provide high-permeability channels for ascent of deeply derived mineralisation fluids (Richards, 2000).

In the conceptual model of chapter 3, structures (lineaments) were considered as conduits and trap zones for mineralisation fluids. The important structures that played these roles are parallel shear zones and fractures due to discordant strike-slip faults ,foliations, and folds. These lineaments are therefore extracted from the available geological and interpreted geophysical maps. The extracted structural map obtained from surface geological mapping provides surface lineaments information, whereas lineaments extracted from geophysical maps provide subsurface information.

5.3.1 Lineaments extracted from geological map

Lineaments digitised from geological maps as segment maps are shown in Fig 5.6.

5.3.2 Lineaments interpreted from geophysical maps

Total intensity airborne magnetic data are important in mapping lineaments in mineral exploration. As lineaments (structures) are one of the spatial controls on lode gold mineralisation in the study area, important subsurface structures are mapped from the processed magnetic map by digitising lineaments and converting to a raster map (Fig 5.7).

Airborne electromagnetic data are also important for subsurface mapping of structures. A digital structural map is obtained by interpreting lineaments from the processed electromagnetic map. Ductile shear zones mainly in the greenstones in the study area are obtained from the EM component maps (Fig 5.8).

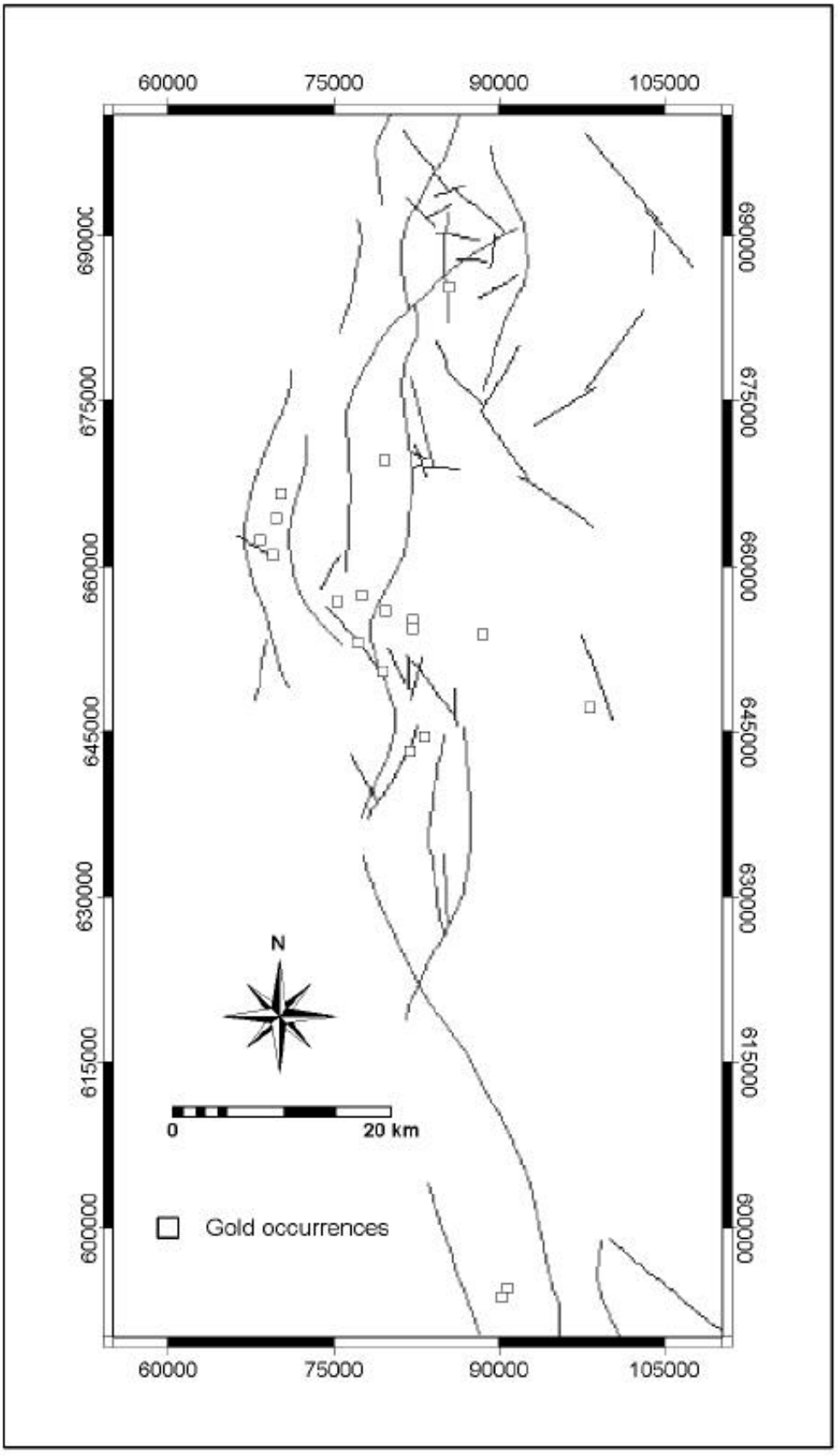

Figure 5.6: Lineaments obtained from geological map

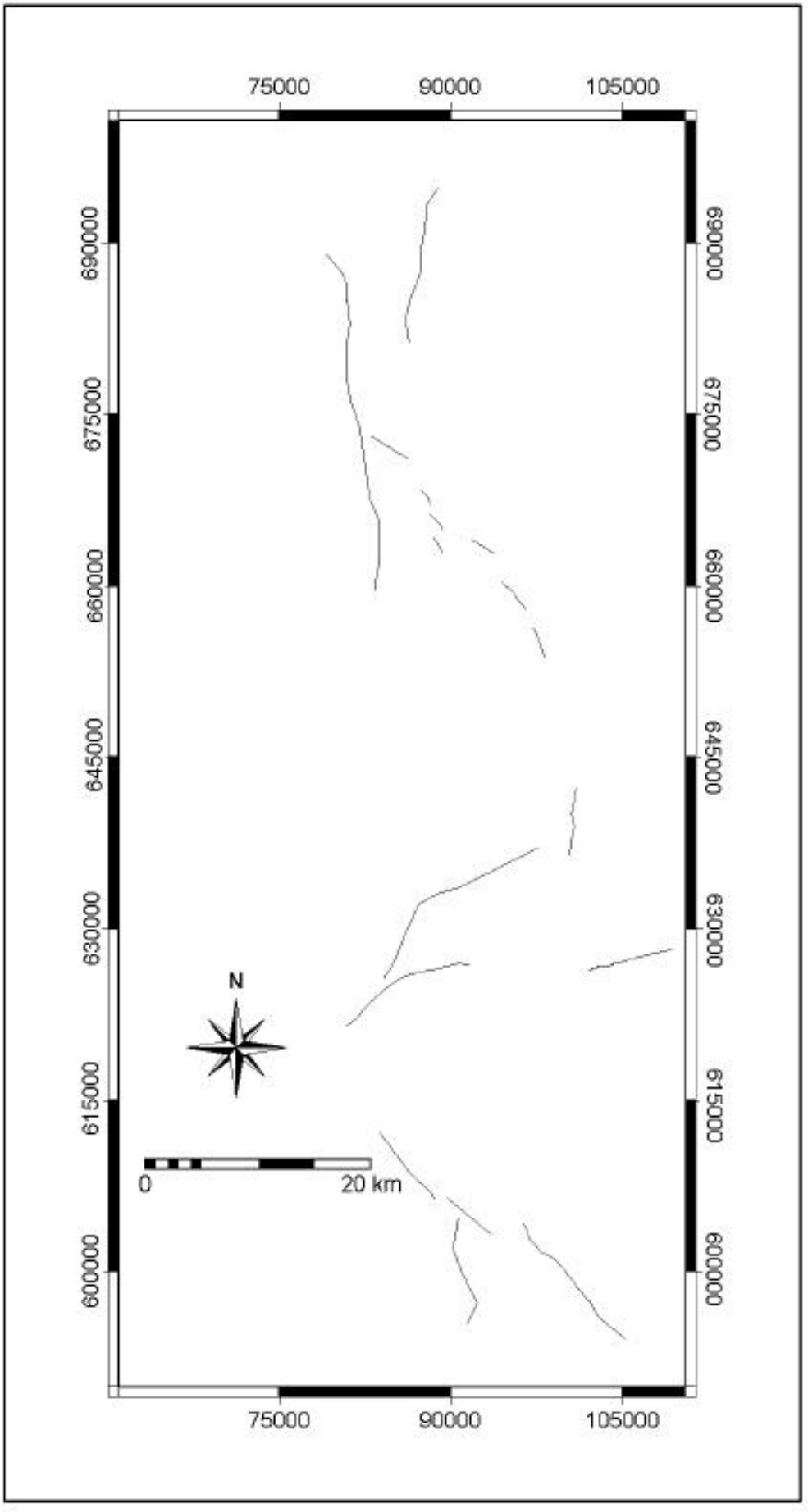

Figure 5.7: Lineaments obtained from magnetics map

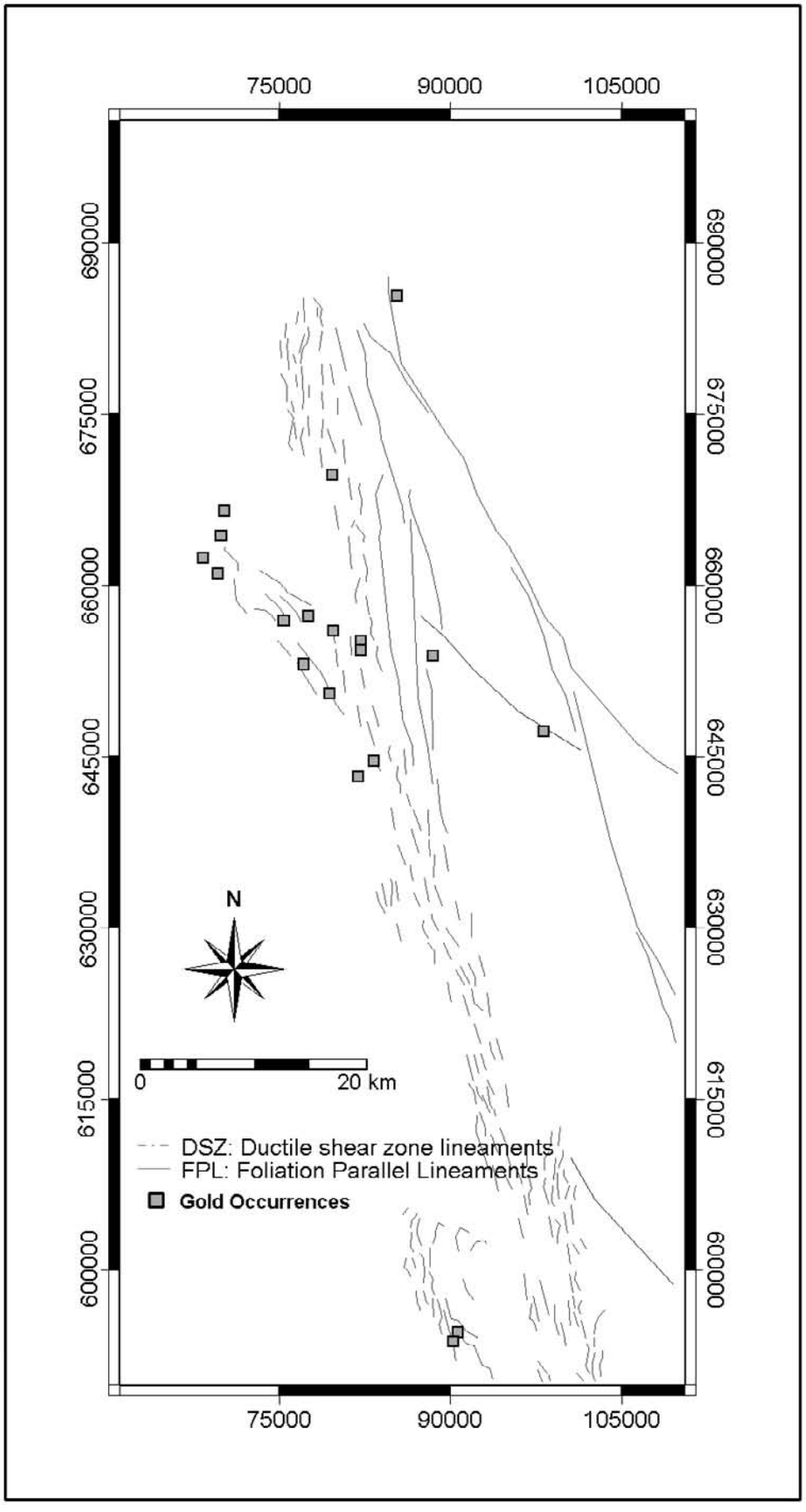

Figure 5.8: Lineaments obtained from EM geophysical map

5.3.3 Layers of interpreted and extracted lineaments

Extracted lineaments were classified into two layers, one for shear zones (Fig 5.10) and the other for fractures (Fig 5.9). The shear zones are important to gold mineralisation on the regional scale while the fractures are important on the local scale. They therefore carry different weights to the lineament factor to the conceptual model.

5.4 Extraction of hydrothermal alterations

5.4.1 Alterations from airborne radiometric maps

As previously mentioned, potassium occurs in rock-forming minerals such as feldspar, mica and amphibole. These minerals are common in most rocks but not in sedimentary precipitates and evaporites such as the chemical sediments and metavolcanics in the study area. These potassium minerals are however formed during hydrothermal alteration of these rocks and when they weather, the K is released. As a result, occurrences of high K concentrations (anomalies) in chemical sediments and in the metavolcanics can be attributed to the weathering of secondary alteration minerals. It is important therefore during alteration mapping to distinguish in situ K, which replace the geochemical signature of the upper levels of the parent bedrock, from transported K, which involves the mobilisation of the products of bedrock weathering.

With in situ weathering, the host minerals of K are destroyed. The weathering results in K depletion through leaching. However, the potassium is adsorbed by any clay minerals formed during weathering. As a result the clay minerals (alteration minerals) have elevated potassium values. Transported weathered materials are distinguished as drainage patterns with high K values, while in situ K products, which are due to alterations, are mapped out from the potassium map by identifying the provenance of the transported material (i.e., high K values with drainage pattern features in the chemical sediments and metavolcanics). Since topography is a principal control on transport of weathered materials it's influence is a factor when identifying provenance of the transported weathered product. The extracted alteration polygon map is shown in Fig 5.11.

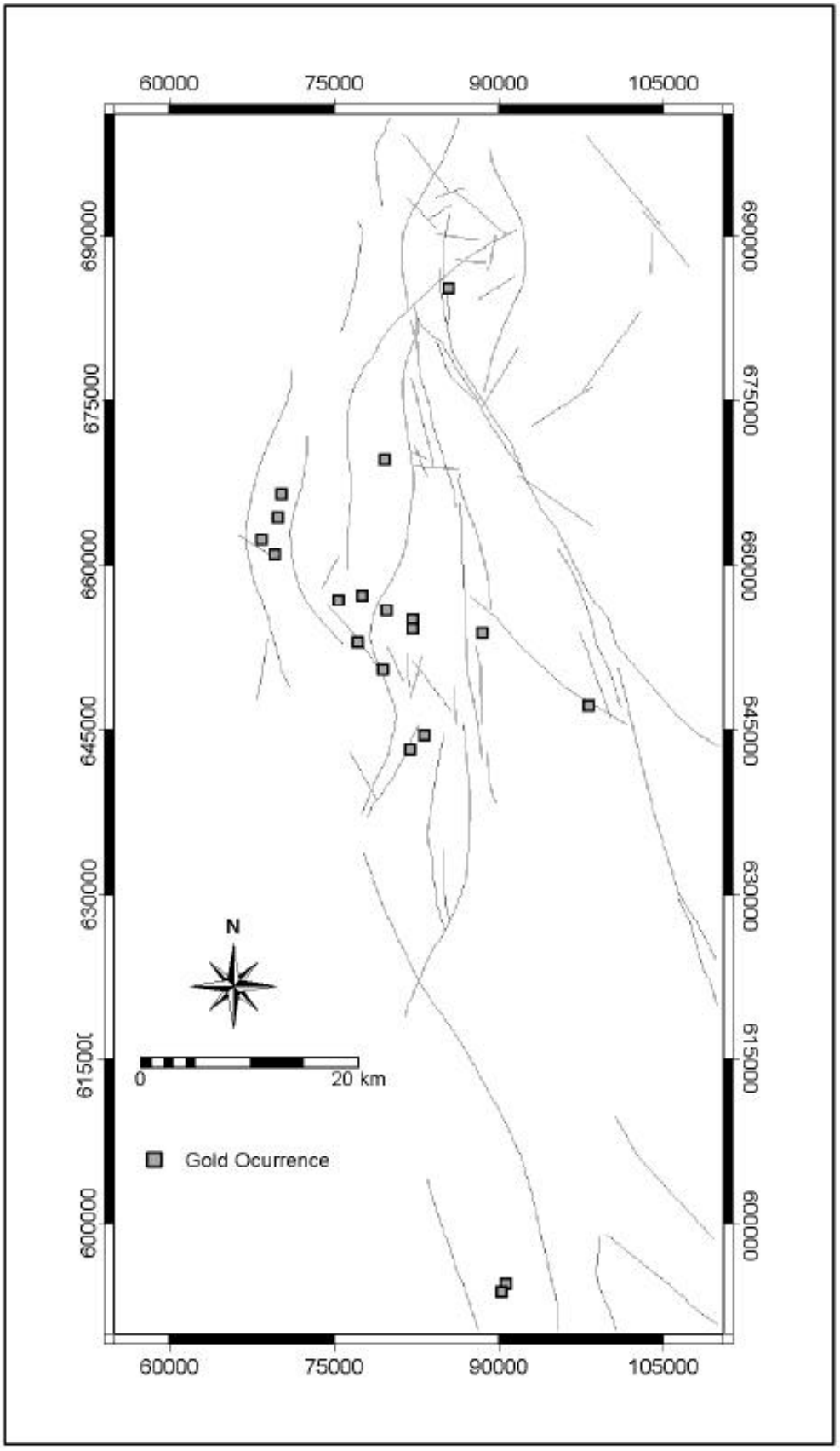

50 Figure 5.9: Fractures layer (an indicative geologic features), obtained by reclassifying the extracted lineaments

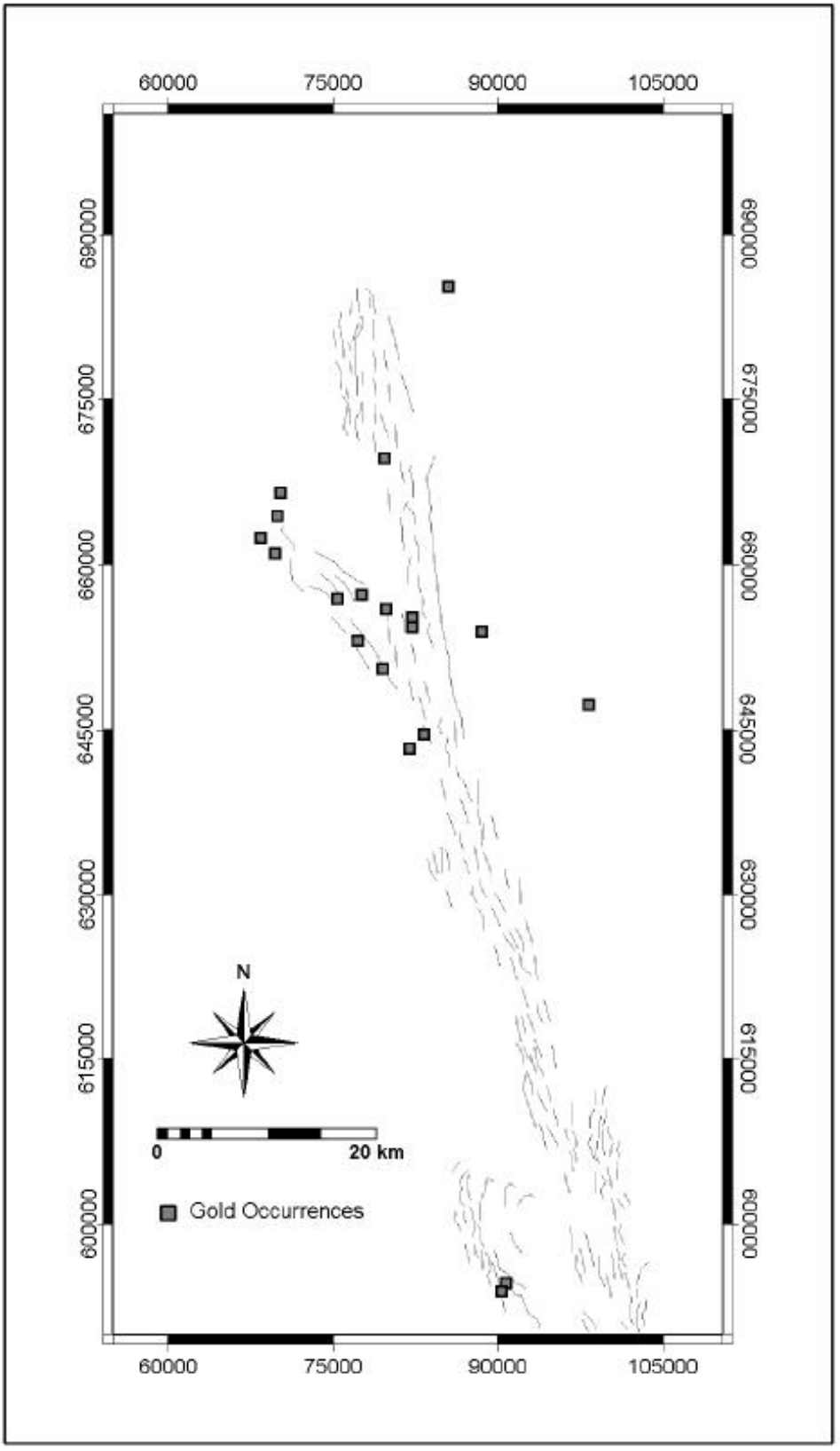

Figure 5.10: Shear zones (an indicative geologic features) in the study area obtained by reclassifying lineaments obtained from EM geophysical map

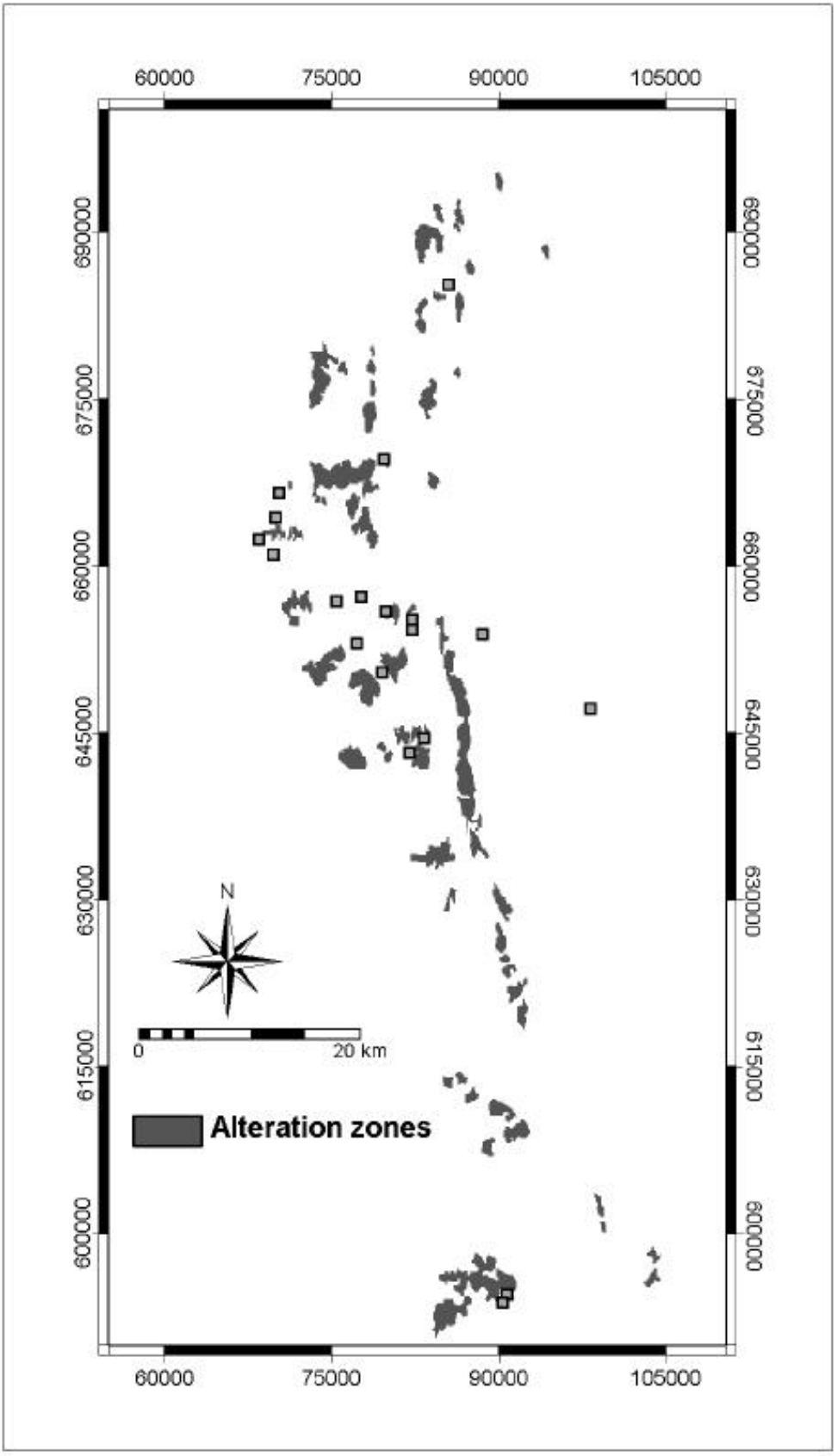

52 Figure 5.11: Alteration zones (an indicative geologic feature) mapped from K radiometric map

5.5 Conclusion

The qualitative interpretation of the various airborne geophysical surveys have proved the old geological map to be of high quality since most of the geophysical responses of the various rock units could be interpreted. The favourable host rocks, which are mainly the chemical sediments of the transition zones together with the detrital volcanogenic sediment components, are reflected in the EM data as banded anomaly complexes with moderate and high conductivity.

Structural information, especially about shear zones in the study area which are not indicated on the available geological map is easily obtained from EM component maps.

On the basis of the release of K due to weathering of alteration minerals in the chemical sediments and metavolcanics, and adsorption of K by formed clay minerals, alterations are mapped.

The extracted spatial control features indicative of gold mineralisation are next integrated into a single mineral potential map using both knowledge-driven and data-driven GIS-based integration methods.

Chapter 6

Spatial Data Integration and Analysis

Data analysis is the extraction of significant information embodied in a dataset. Spatial data analysis is the process of seeking out patterns and association on maps that help to characterise, understand and predict spatial phenomena (Bonham-Carter, 1994). Modelling is part of an analytical process of predicting a spatial phenomenon, and is the symbolic representation of the relationship between spatial objects.

This chapter describes the generation of predictive models of lode gold from the extracted spatial geologic features indicative of lode gold mineralisation in the Lawra belt using two GIS-based integration methods the weights of evidence (data-driven) method and the fuzzy logic (knowledge-driven) method. The spatial association between the geologic features and the mineral occurrences are first quantified before the use of either of the above integration methods. This spatial relationship could either be proximity relationship, where most mineral occurrences occur within a distance to a geologic feature (e.g. proximity to structures) or association relationship, in which the mineral occurrences mostly occur within polygon-type geologic feature (e.g. favourable host rocks). The quantified spatial association illustrates the behaviour of each geologic feature with the mineral occurrences in the study area. In the weights of evidence method, the spatial relationship of a geologic feature is represented as binary map with two domains, the presence of the feature (prospective area) and the absence of the feature (unprospective areas). In the fuzzy logic method the spatial association is represented as a multi-class map with varying degrees for indicating association with lode gold mineralisation.

The spatial association of a geologic feature is quantified by first buffering the indicative geologic feature by an appropriate distance and reclassifying. In this study,

all spatial analyses for creating predictive models were done in raster mode and a pixel size of 100m by 100m was used. The decision to use this pixel size is based on a consideration of the sizes of the known mineral occurrences and the scale of this study.

The integration of the evidence maps, which quantify the spatial association of the geologic features with the mineral occurrences, into a single predictive map by the weights of evidence method and the fuzzy logic method is discussed below.

6.1 Analysis using the weights of evidence method

6.1.1 Weights of evidence method

The weights of evidence method uses the Bayesian approach of combining datasets, which is based on a probability framework. The method developed by the Geological Survey of Canada has been in use since the late 1980s (Bonham-Carter et al., 1989). Bonham-Carter (1994) applied the method to gold prospectivity in Nova Scotia. Carranza and Hale (1999) also used the method to predict favourable areas for gold deposits in the Baguio district of the Philippines.

The spatial association of each geologic feature with the mineral occurrences is represented as a binary map with two domains, the presence and absence of the feature (i.e., a predictor pattern).

The favourability of finding a mineral occurrence given the presence of a predictor pattern is given by

$$P\{D/B\} = \frac{P\{D \cap B\}}{P\{B\}} = P\{D\}\frac{P\{B/D\}}{P\{B\}} \tag{6.1}$$

where $P\{D/B\}$ is the conditional or posterior probability of a mineral occurrence given the presence of the predictor pattern, $P\{D/B\}$ is the conditional probability of being in the predictor pattern B, given the presence of a mineral occurrence D, P{B} is the prior probability of being in the predictor pattern.

The favourability of finding a mineral occurrence given the absence of a predictor pattern is expressed by

$$P\{D/\overline{B}\} = \frac{P\{D \cap \overline{B}\}}{P\{\overline{B}\}} = P\{D\}\frac{P\{\overline{B}/D\}}{P\{\overline{B}\}} \tag{6.2}$$

where $P\{D/\overline{B}\}$ is the conditional probability of a mineral occurrence given the absence of a predictor pattern, $P\{\overline{B}/D\}$ is the conditional probability of the absence of a predictor B given the presence of a mineral occurrence. $P\{\overline{B}\}$ is the probability of being in the absence of a predictor pattern.

The same model can be expressed in an odds formulation, where odds, O, are defined as O$= P/\left(1-p\right)$, the above equations are respectively expressed as

$$O\{D/B\} = O\{D\}\frac{P\left(B/D\right)}{P\left(B/\overline{D}\right)} \tag{6.3}$$

$$O\{D/\overline{B}\} = O\{D\}\frac{P\left(\overline{B}/D\right)}{P\left(\overline{B}/\overline{D}\right)} \tag{6.4}$$

The weights of evidence for the binary map relationships are defined as

$$W^{+} = \ln\left[\frac{P\left(B/D\right)}{P\left(B/\overline{D}\right)}\right] \tag{6.5}$$

and

$$W^{-} = \ln\left[\frac{P\left(\overline{B}/D\right)}{P\left(\overline{B}/\overline{D}\right)}\right] \tag{6.6}$$

where W^{+} and W^{-} are the weights of evidence when a binary is present and absent respectively.

The variances of the weights can be calculated by the following expressions,

$$s^{2}\left(W\right) = \frac{1}{N\{B \cap D\}} + \frac{1}{N\{B \cap \overline{D}\}} \tag{6.7}$$

$$s^{2}\left(W\right) = \frac{1}{N\{\overline{B} \cap D\}} + \frac{1}{N\{\overline{B} \cap \overline{D}\}} \tag{6.8}$$

The contrast C, defined as

$$C = W^{+} - W^{-} \tag{6.9}$$

provides a useful measure of the spatial association between a binary predictor pattern and the mineral occurrence points. For a positive spatial association, C is positive and for a negative association C is negative. The standard deviation of C is calculated as

$$s\left(C\right) = \sqrt{s^2\left(W^+\right) + s^2\left(W^-\right)} \tag{6.10}$$

The studentised C, defined as

$$sigC = c/stdc \tag{6.11}$$

serves as a guide in selecting the optimum proximity distance to a geologic feature according to Boham-Carter (1994) and shows the statistical significance of such a spatial association.

Using the log-odds formulation of Bayes's rule, two or more binary predictor patterns can be combined to generate a predictor map using the expression

$$lnO\{D/B_1^k \cap B_2^k \cap B_3^k ....B_n^k\} = \sum_{j=1}^{n} W_j^k + lnO\{D\} \tag{6.12}$$

where the superscript k is positive (+) or negative (-) if the binary predictor pattern is present or absent, respectively.

One requirement of the Bayes's rule is that all input maps should be conditionally independent of one another with respect to the mineral occurrences. If this rule is not obeyed then the resultant map (predictive map) will be biased and under- or overestimate the favourable areas.

The following relationship is satisfied if two binary maps are conditionally independent.

$$N\{B_1 \cap B_2 \cap D\} = \frac{N\{B_1 \cap D\} N\{B_2 \cap D\}}{N\{D\}} \tag{6.13}$$

The left hand side of the equation is the observed number of occurrences in the overlap zone of B_1 and B_2. The right-hand side is the predicted number of deposits in this overlap zone. A contingency calculation table is used to test the conditional independence of the two binary maps. The chi-square test is then calculated to test the hypothesis by the expression

$$\chi^2 = \sum_{i=1}^{4} \frac{\left(observed_i - predicted_i\right)^2}{predicted_i} \tag{6.14}$$

An overall test of conditional independence can also be applied after combining the binary predictor patterns. The predicted number of occurrences $N\{D\}_{pred}$ can be calculated as the sum of the products of the number of pixels, N{A}, and their posterior

probabilities, P, for all pixels on the map, thus

$$N\{D\}_{pred} = \sum_{k=1}^{m} P_k * N\{A\}_k \tag{6.15}$$

6.1.2 Application of weights of evidence analysis to the Lawra belt

The weights of evidence method is applied to the 19 known mineral occurrences in the Lawra belt to generate a predictive model. Analysis to generate a predictive map is done 19 times, each time modelling with 18 mineral occurrences and validating the resulting maps with the remaining occurrence. This procedure is followed because the known number of mineral occurrences in the Lawra belt is not large enough to divide them into two sets, one to generate the model and the other to validate the model. In addition, weights of evidence is a statistical method and therefore significant number of mineral occurrences is needed for modelling. The predictive model of the generated models which best passes a number of validation tests is then determined.

The extracted geologic features whose spatial association with the mineral occurrences are first quantified are the favourable rocks, fractures, shear zones and alteration zones. The procedure and results of the first of the 19 analyses to generate a predictive model are described below.

Calculating the weights of evidence of alteration zones

A binary map of cumulative distances 0, 500, 1000, 1500, 2000, 2500, 3000, 4000, 6000, 8000, 10000 and 27000m from the alteration zones is first created. The map is then crossed with the mineral occurrence map (of 18 occurrences) to estimate the weights of evidence using the formulae above (i.e. equations 6.5 to 6.11). The result of the analysis is shown in Table 6.1 (npixb and npixd are the number of pixels in the cumulative buffer zones and number of pixels in the cumulative buffer zone with mineral occurrences respectively). The variation in the quantified spatial association of proximity distances to the alteration zones and the mineral occurrences in the belt is shown in Fig 6.1. The optimum proximity distance to the alteration zones, which is 1000m for this analysis is determined by the distance class with the highest studentised C value. The binary predictor map of the optimum distance to alteration zones is then created using the values of $\mathbf{W^+}$**(1.3538)** and $\mathbf{W^-}$**(-0.7727)** as the domains, (Fig 6.2)

Table 6.1: Results of analysis1 (Alteration zones)

dist(m)	**npixb**	**npixd**	**W^+**	**stdW$^+$**	**W^-**	**stdW$^-$**	**C**	**stdC**	**sigC**
0	15209	2	1.0766	0.7072	-0.0792	0.2500	1.1558	0.750	1.5409
500	38411	6	1.2488	0.4083	-0.3050	0.2887	1.5538	0.500	3.1072
1000	**63403**	**11**	**1.3538**	**0.3015**	**-0.7727**	**0.3780**	**2.1265**	**0.484**	**4.3980**
1500	88794	13	1.1840	0.2774	-1.0311	0.4472	2.2151	0.526	4.2092
2000	112307	14	1.0232	0.2673	-1.1762	0.5000	2.1994	0.567	3.8793
3000	152083	16	0.8535	0.2500	-1.7214	0.7071	2.5749	0.750	3.4332
4000	186493	17	0.7101	0.2425	-2.2662	1.0000	2.9763	1.02	2.8925
6000	238106	17	0.4658	0.2425	-1.9920	1.0000	2.4578	1.02	2.3886
8000	271546	17	0.3344	0.2425	-1.7633	1.0000	2.0977	1.02	2.0386
1000	297688	17	0.2424	0.2425	-1.5390	1.0000	1.7814	1.02	1.7312
27000	401673	18	0.0000	0.2357	?	?	?	?	?

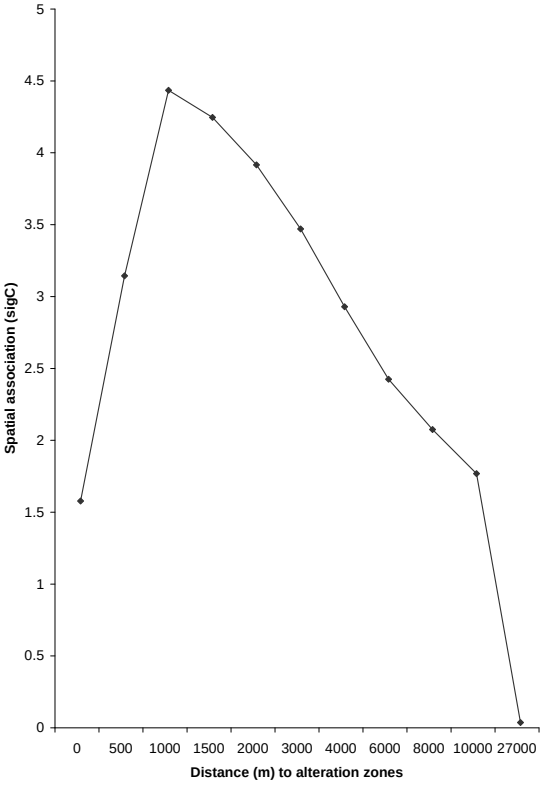

Figure 6.1: Variation of spatial association (sigC) with cummulative distances from alteration zones

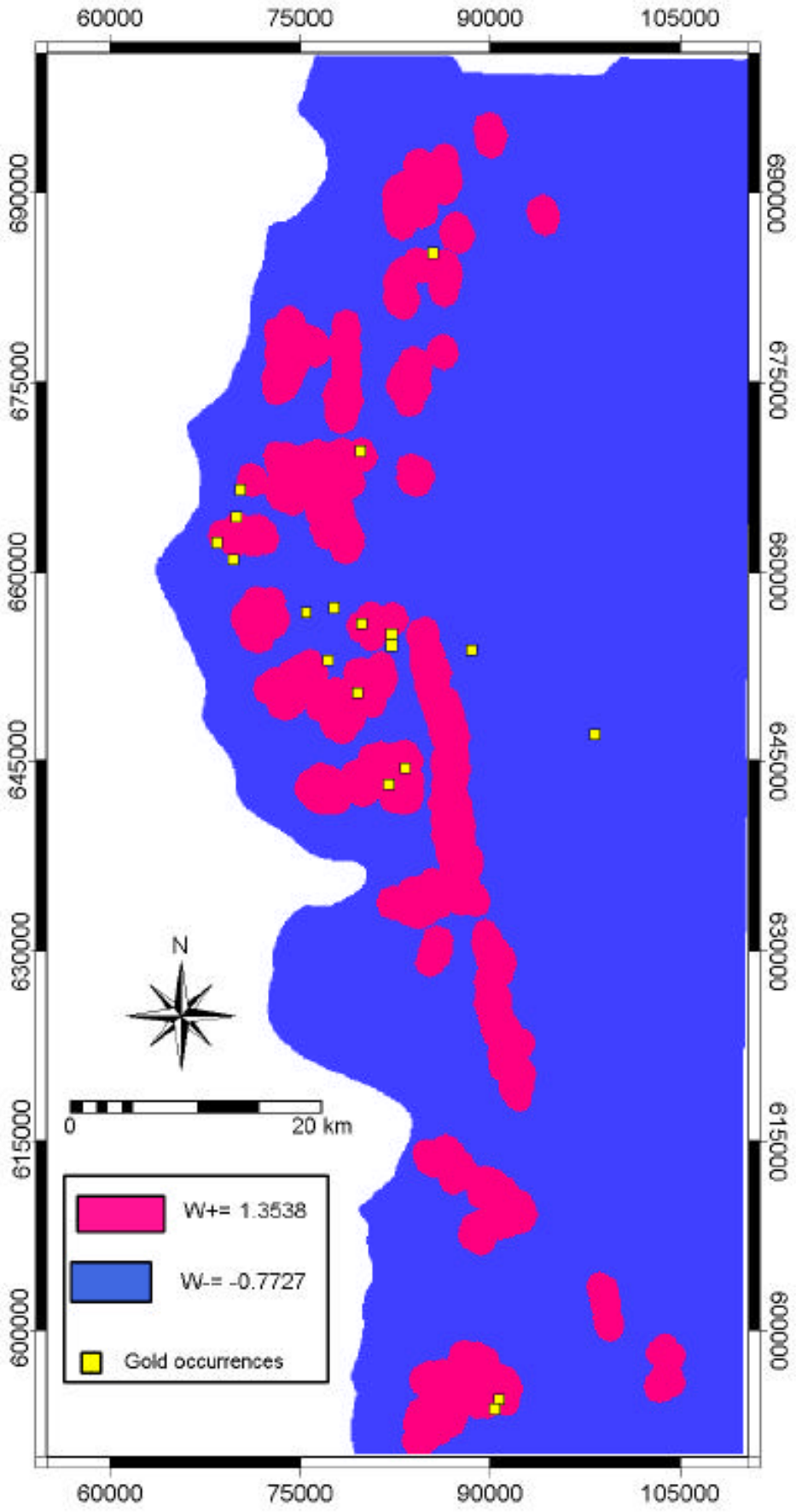

Figure 6.2: Binary predictor pattern of alteration zones and mineral occurrences

Calculating the weights of evidence of favourable rocks

The following cumulative distances of 0, 500,1000, 1500, 2000, 4000, 6000, 8000, 12000, 28000m from the favourable rocks (chemical sediments) are considered, and the optimum proximity distance to the favourable rocks was calculated. The distance class having the highest spatial association (studentised C) with the mineral occurrences is then determined. The results are shown in Table 6.2 with the optimum distance being 1000m, (npixb and npixd are the number of pixels in the cumulative buffer zones and number of pixels in the cumulative buffer zone with mineral occurrences respectively). The variation in the spatial association of cumulative distance to this geologic feature and the mineral occurrences in the Lawra belt is shown in Fig 6.3. From the graph, the optimum distance is 1000m. The resulting binary predictor map of the optimum distance is shown in Fig 6.4 with two domains, the presence of the predictor pattern assigned a weight value of **0.8462** and the absence of the pattern assigned **-1.0980**

Table 6.2: Results of analysis1 (Favourable host rocks)

dist(m)	**npixb**	**npixd**	**W^+**	**stdW$^+$**	**Wn^-**	**stdWn$^-$**	**C**	**stdC**	**sigC**
0	81967	10	1.0016	0.3162	-0.5827	0.3536	1.5843	0.474	3.3399
500	109400	11	0.8082	0.3015	-0.6265	0.3780	1.4347	0.484	2.9672
1000	**134050**	**14**	**0.8462**	**0.2673**	**-1.0980**	**0.5000**	**1.9442**	**0.567**	**3.4291**
1500	155456	16	0.8316	0.2500	-1.7078	0.7071	2.5394	0.750	3.3859
2000	172732	16	0.7262	0.2500	-1.6351	0.7071	2.3612	0.7500	3.1483
4000	219506	16	0.4865	0.2500	-1.4065	0.7071	1.8930	0.7500	2.5240
6000	248263	17	0.4240	0.2425	-1.9279	1.0000	2.3519	1.029	2.2857
8000	271783	17	0.3335	0.2425	-1.7615	1.000	2.0950	1.029	2.0360
12000	311267	17	0.1978	0.2425	-1.3991	1.0000	1.5969	1.029	1.5519
28000	401673	18	0.0000	0.2357	?	?	?	?	?

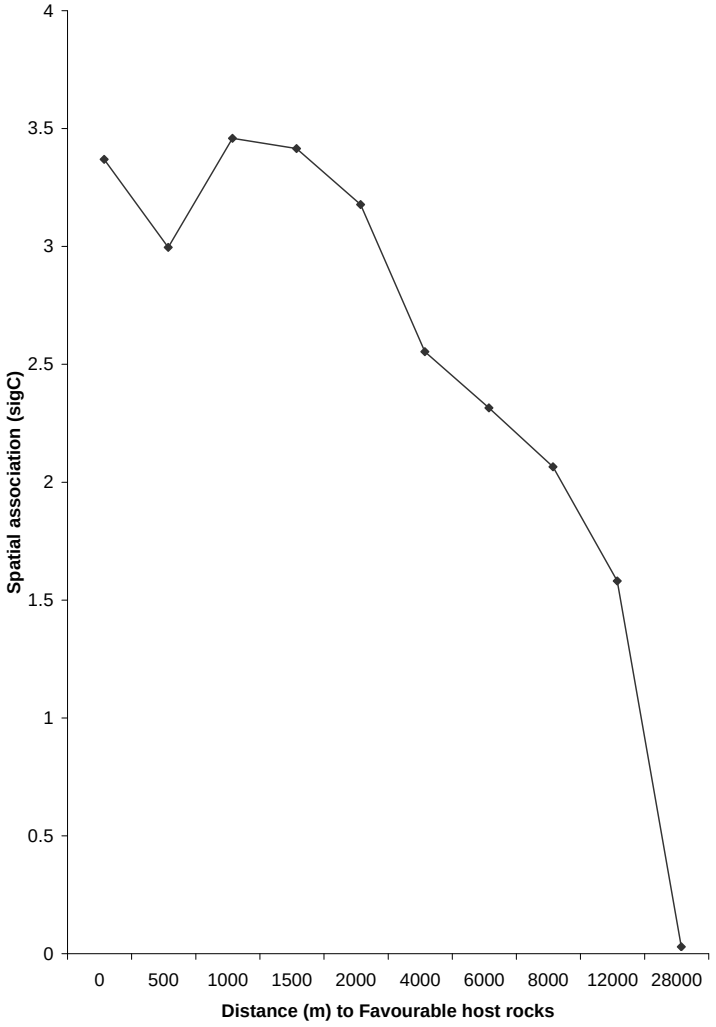

Figure 6.3: Variation of spatial association (sigC) with cumulative distances away from favourable rocks

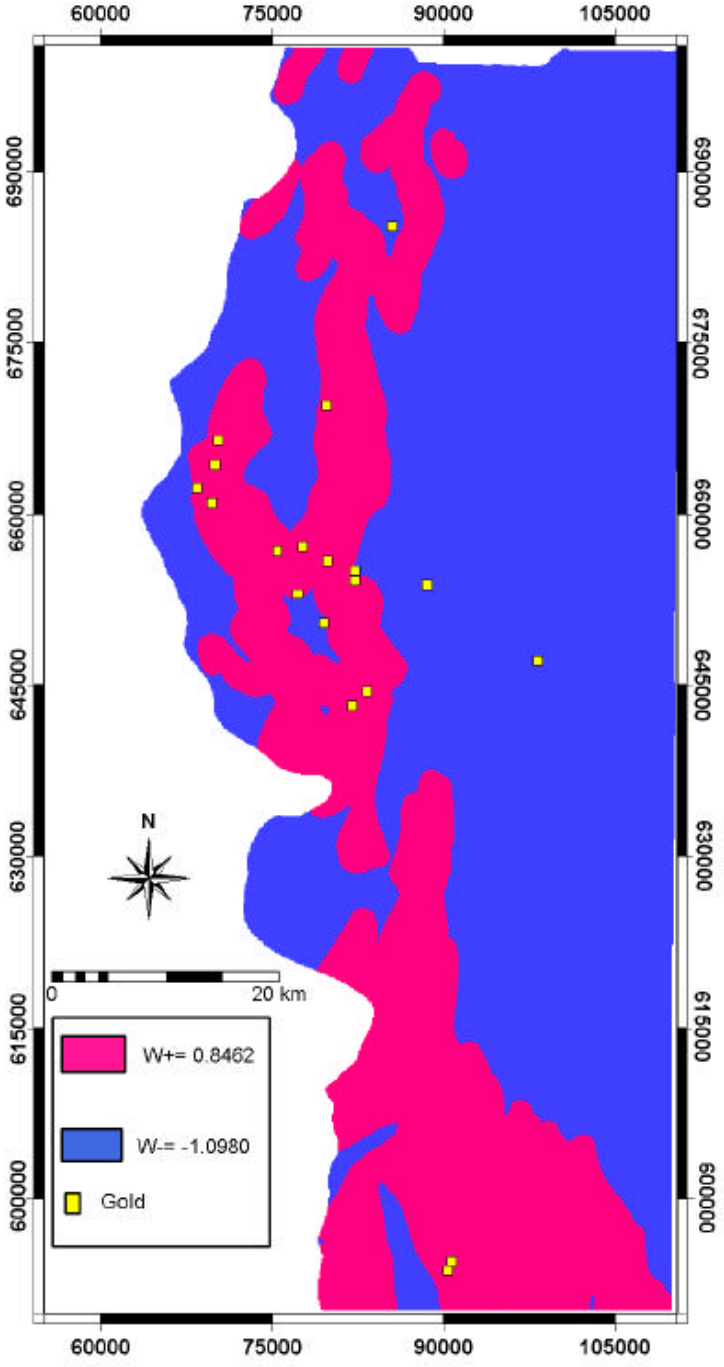

Figure 6.4: Binary predictor pattern of host rocks and mineral occurrences

Calculating the weights of evidence of shear zones

The spatial association of shear zones with the mineral occurrences in the Lawra belt is also quantified by buffering and reclassifying the extracted shear zones using cumulative distances of 500, 1000, 1500, 2000, 3000, 4000,6000, 8000, 10000, 37000m which is then crossed with the mineral occurrence map. The result of the first analysis to obtain the optimum spatial association is shown in Table 6.3. (Fig 6.5), shows the variation in the spatial association of the proximity to the shear zones with the mineral occurrences. The optimum proximity distance, 1000m, is again determined by the highest studentised C. (Fig 6.6) is the binary map of the optimum distance with W^+(**1.2016**) and W^-(**-0.7414**) values as the domains.

Table 6.3: Results of analysis1 (Shear zones)

dist(m)	**npixb**	**npixd**	**W$^+$**	**stdW$^+$**	**Wn$^-$**	**stdWn$^-$**	**C**	**stdC**	**sigC**
500	45924	7	1.2243	0.3780	-0.3711	0.3015	1.5954	0.484	3.2996
1000	**73825**	**11**	**1.2016**	**0.3015**	**-0.7414**	**0.3780**	**1.9430**	**0.484**	**4.0186**
1500	92610	12	1.0619	0.2887	-0.8365	0.4083	1.8984	0.500	3.7964
2000	107904	14	1.0632	0.2673	-1.1913	0.5000	2.2545	0.567	3.9764
3000	134304	16	0.9778	0.2500	-1.7903	0.7071	2.7680	0.75	3.8583
4000	159399	17	0.8671	0.2425	-2.3848	1.0000	3.252	1.029	3.1605
6000	202687	17	0.6269	0.2425	-2.1880	1.0000	2.814	1.029	2.7357
8000	237951	17	0.4664	0.2425	-1.9929	1.0000	2.459	1.029	2.3902
10000	265655	17	0.3563	0.2425	-1.8076	1.0000	2.163	1.029	2.1030
37000	401673	18	0.0000	0.2357	?	?	?	?	?

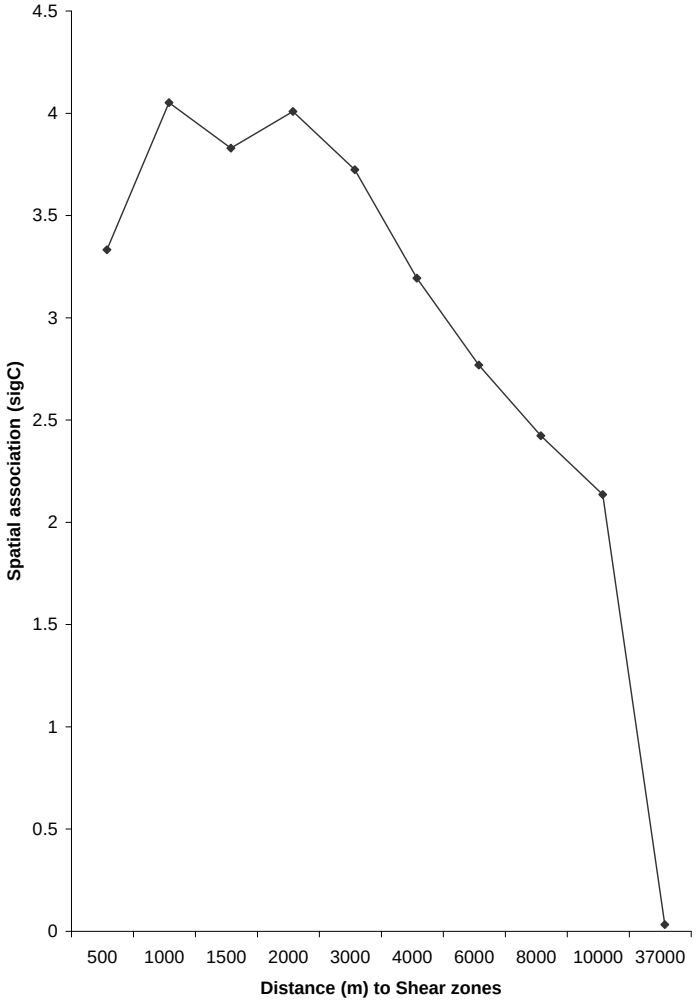

Figure 6.5: Variation of spatial association (sigC) with cumulative distances away from Shear zones

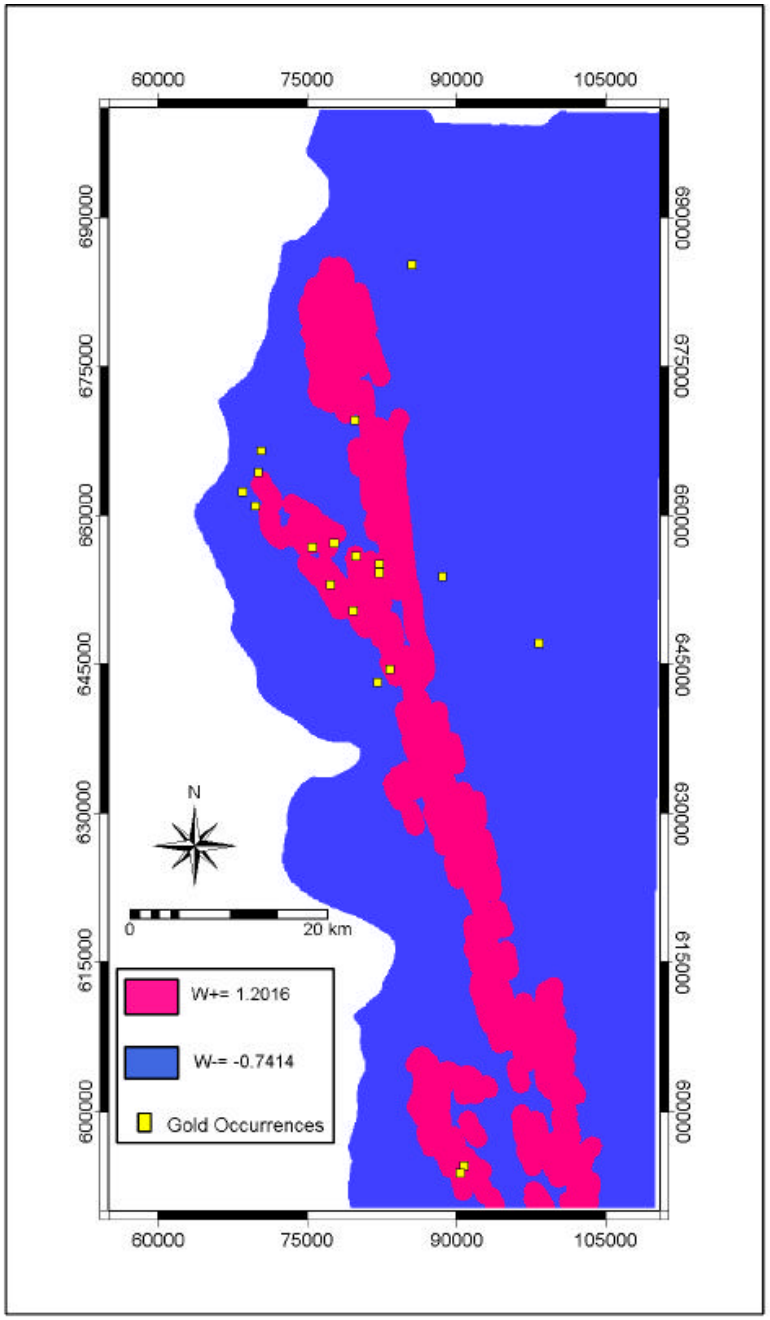

Figure 6.6: Binary predictor pattern of shear zones and mineral occurrences

Calculating the weights of evidence of fractures

The spatial association of fractures with the mineral occurrences are also quantified by the weights of evidence method. The results of the first analysis to obtain the optimum proximity distance with the 18 mineral occurrences are shown in Table 6.4 and the variation of the spatial association (sigC) with cummulative distance away from the fractures is shown in Fig 6.7. The resulting binary map of the optimum spatial association to fractures is shown in (Fig 6.8) with W^+(**0.8335**) and W^-(**-0.1489**) as the weight values for the two domains.

Table 6.4: Results of analysis1 (fractures)

dist(m)	**npixb**	**npixd**	**W$^+$**	**stdW$^+$**	**Wn$^-$**	**stdWn$^-$**	**C**	**stdC**	**sigC**
500	71557	5	0.4442	0.4472	-0.1292	0.277	0.5735	0.526	1.0898
1000	128565	8	0.3283	0.3536	0.2020	0.316	0.5303	0.474	1.1179
1500	**177826**	**12**	**0.4094**	**0.2887**	**-0.5140**	**0.408**	**0.9233**	**0.500**	**1.8466**
2000	216934	13	0.2906	0.2774	-0.5043	0.447	0.7949	0.526	1.5105
2500	248378	15	0.2984	0.2582	-0.8285	0.447	1.1269	0.633	1.7817
14000	401673	18	0.000	0.2357	?	?	?	?	?

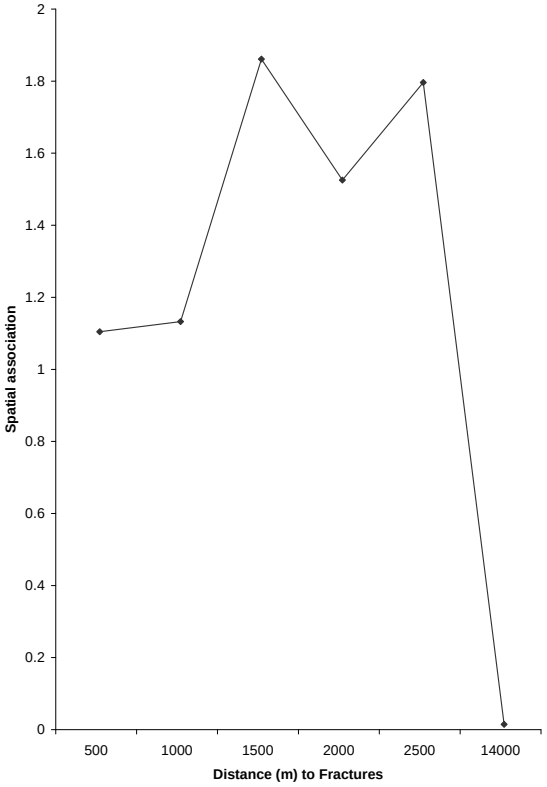

Figure 6.7: Variation of spatial association (sigC) with cumulative distances away from fractures

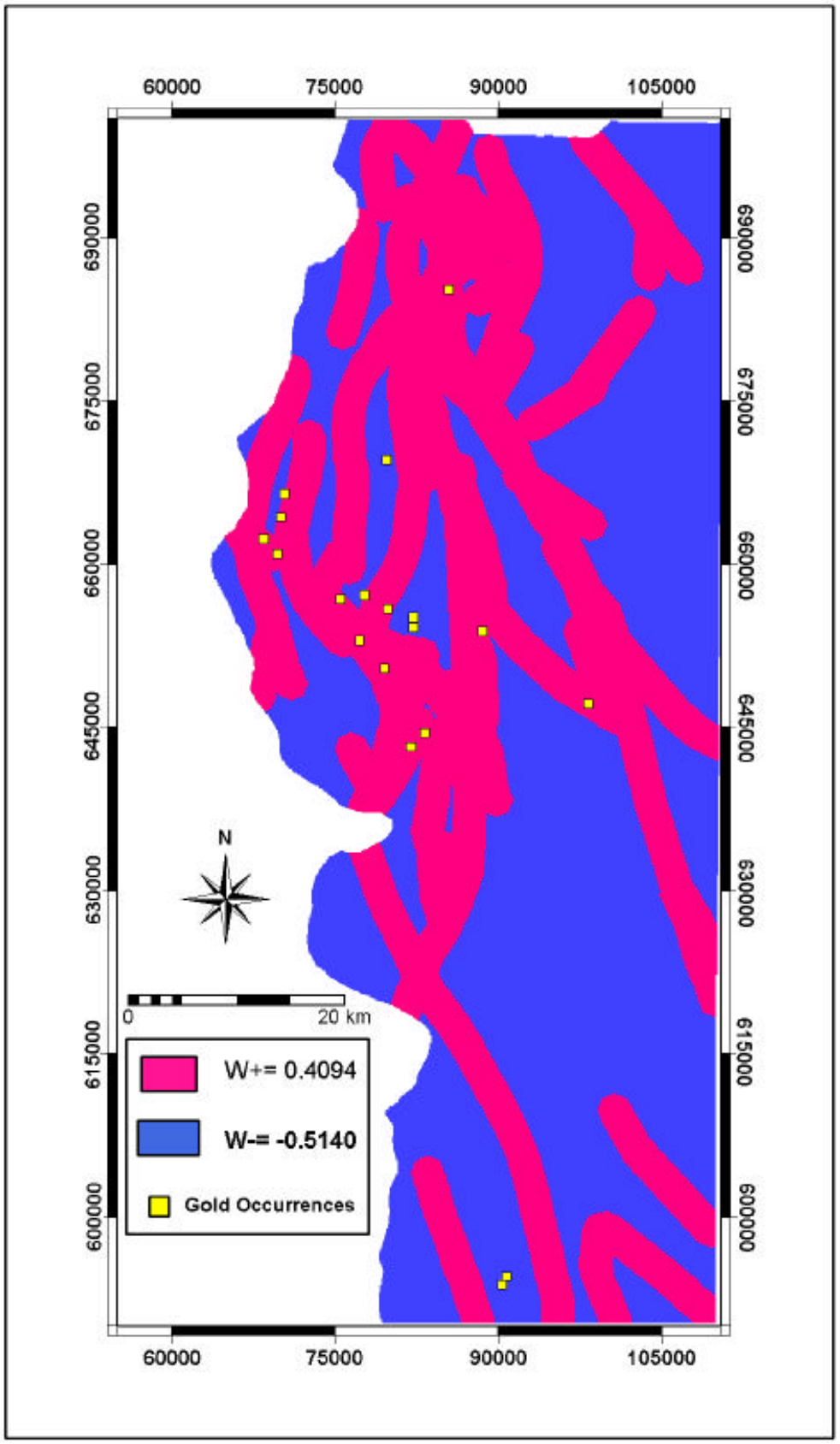

Figure 6.8: Binary predictor pattern of fractures and mineral occurrences (proximity distance of 1500m)

Ranking of evidence maps based on studentised C (sigC)

The generated evidence maps which quantify the spatial association of each of the geologic features with the known mineral occurrences are ranked based on the value of the studentised C. This gives a useful information about which of the geologic features has the strongest and weakest spatial association with Gold occurrences in the Lawra belt. The results of the ranking is shown below in table 6.5.

Table 6.5: Ranking of the spatial associations between geologic features and mineral occurrences

Evidence Maps	W^+	W^-	sigC
1.Hydrothermal altera.	1.3538	-0.3015	4.3980
2. Shear zones	1.2016	-0.7414	4.0186
3. Fav. host rocks	0.8462	-1.0980	3.4291
4. Fractures	0.4094	-0.5140	1.8466

6.1.3 Integration of binary maps to generate predictive map

As previously mentioned one requirement of Baye's rule is that all input maps should be conditionally independent of one another with respect to the mineral occurrences. A pairwise conditional independence test of all possible pairings of the binary predictor maps is therefore done using the chi-square test (equations 6.13 and 6.14). With 1 degree of freedom and confidence level of 95% the critical χ^2 value is 3.84. The conditional independence hypothesis is therefore to be rejected at this level of probability when χ^2 is greater than 3.84. The results of the pairwise tests are in table 6.6.

Table 6.6: Results of analysis1 (Pairwise test of CI)

	Host rocks	Shear zones	Alteration zones
Fractures	0.16	1.87	0.12
Host rocks		0.27	0.27
Shear zones			0.08

From the table, the calculated values for χ^2 are smaller than the 3.84, thus the hypothesis for conditional independence is obeyed or accepted at this probability level.

The binary predictor maps are integrated to generate a predictive map using equation 6.12, which based on Bonham-Carter (1994) can also be written as

$$\text{Pred. map} = exp(-10 + \text{WHR} + \text{WSZ} + \text{WALT} + \text{WFr}/(1 + exp(-10 + \text{WHR} + \text{WSZ} + \text{WALT} + \text{WFr})) \tag{6.16}$$

where the value -10 is the $log_e O\{D\}$ and O{D} is the prior odds of mineral occurrences of 0.000045. WHR is the binary predictor map of host rocks, WSZ the binary predictor map of shear zones, WALT the binary predictor map of alteration zones and WFR the binary predictor map of fractures.

The above analysis is repeated 19 times to generate posterior or predictive map, each time using different set of 18 mineral occurrences. The table of results of the other 18 analyses are shown in appendix A.

6.1.4 Validating of predictive maps and determining best predictive map

Three different approaches or methods were used to validate the 19 generated predictive maps and also to determine the best predictive map. The following are the validating methods used.

- Performing an overall test of conditional independence, according to equation 6.15, to determine which of the generated predictive maps least violates the conditional independence rule by comparing the predicted numbers to the observed number of 18 mineral occurrences. Maps which are biased and are (under- or over-estimating the observed mineral occurrences) are then be rejected.
- Determining the percentage area covered by the favourable target zones i.e. areas with probabilities greater than the prior probability of 0.000045. Since in nature, potentially mineralised zones are rare, a smaller percentage area of favourable zones is much more appropriate to recommend for further exploration work than a large percentage area.
- Determine whether the generated predictive maps are able to predict each remaining mineral occurrence. Thus, Yes or No as to whether a predictive map is able to predict the one remaining mineral occurrence and what is the predictive value for the occurrence.

A summary of the analyses to validate the generated predictive maps using all the four binary predictor pattern is shown in Table 6.6. From the table, the predictive map resulting from the analysis 5 (Fig 6.9) is considered to be the best predictive

map, since of all the 19 generated maps, analysis 5 least violates the overall conditional independence rule (i.e. comparing the predicted number of 35 as against observed number of 18 mineral occurrences) than the others. In addition, its able to predict the remaining mineral occurrence used in the validation, and the percentage area covered by the favourable zones (i.e. areas with probability >0.000045, the prior probability) zones is 22% of the study area and therefore appropriate for further exploration. Most of the other predictive maps are on the other hand are over predicting the target areas.

Table 6.7: A summary of validation of predictive maps

Sets of analysis	Predicted No. of mineral occu.	% area of favou. zones	predicts mineral occu.? (Yes/No)	Value of post. prob.
1	38	21	Yes	0.000075
2	42	23	Yes	0.000089
3	41	23	No	<0.000045
4	43	27	Yes	0.00006
5	**35**	**22**	**Yes**	**0.00005**
6	39	23.7	No	<0.000045
7	41	25	No	<0.000045
8	42	26	Yes	0.00006
9	40	26	Yes	0.002
10	38	23	No	<0.000045
11	38	27	No	<0.000045
12	38	23	Yes	0.000052
13	36	27	No	<0.000045
14	43	22	No	<0.000045
15	43	21	Yes	0.002
16	40	21	No	<0.000045
17	38	21	No	<0.000045
18	41	28	Yes	0.001
19	41	28	Yes	0.001

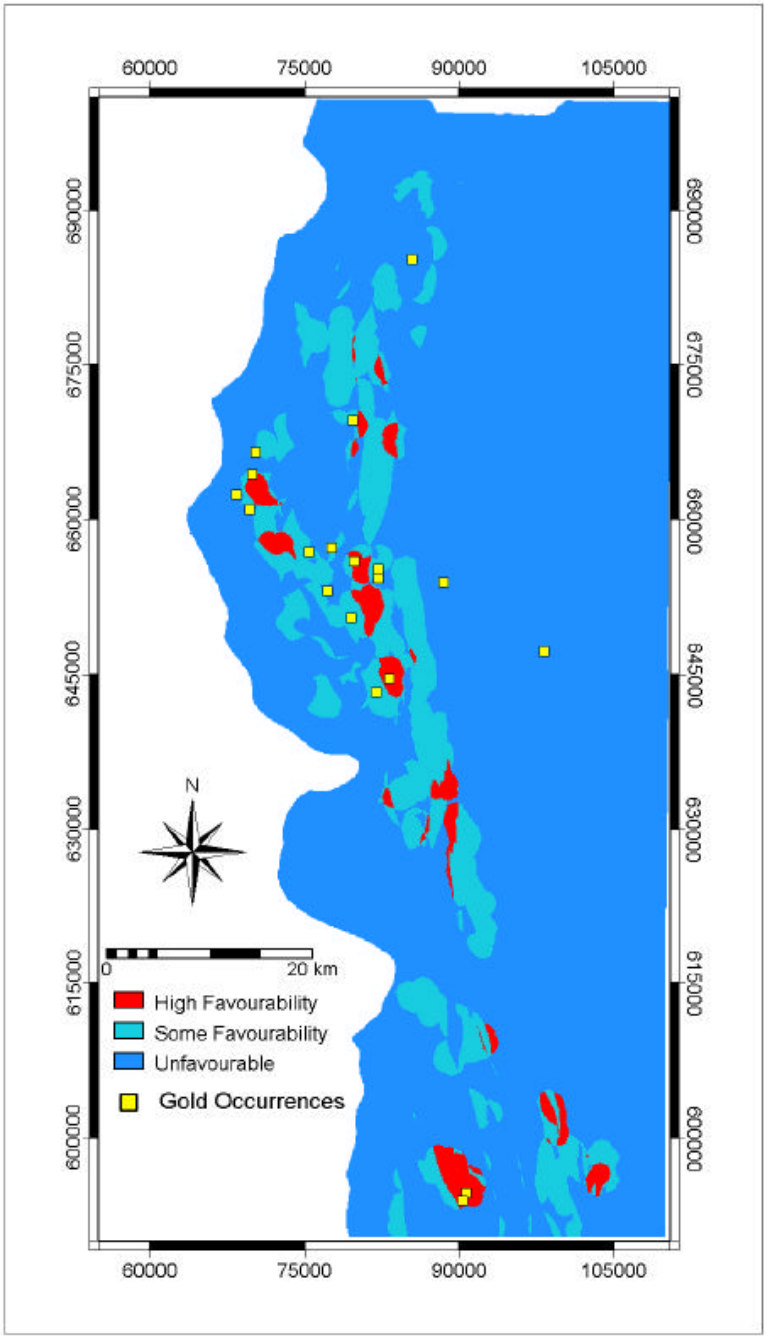

Figure 6.9: Best predictive map out of 19 analyses using all the evidence maps (WALT, WFHR, WSHEA, WFRAC)

The best predicted number of 35 is however 94% greater than the actual number of 18 mineral occurrences used for the modelling, indicating the presence of some conditional dependence, despite the apparent lack of CI problems in the pairwise tests. Therefore, to check the possible effects of this dependence, the fractures evidence map which was a suspect in the CI tests and also has a relatively low studentised C value was removed from the analysis and new predictive maps generated this time using the equation below.

$$\text{Pred. map} = exp(-10 + \text{WHR} + \text{WSZ} + \text{WALT}/(1 + exp(-10 + \text{WHR} + \text{WSZ} + \text{WALT})) \quad (6.17)$$

The generated maps were again validated using the above validation methods. The results are shown in table 6.7. From the table, the results are not significantly different from the previous results when all the four maps were integrated. The best predicted map value of the previous approach now has a prediction number of 37 which is even higher and still violates the overall conditional independence rule. The resulting predictive map of analysis 5 is shown in Fig 6.10

With the knowledge of the study area and the conceptual model of the lode gold in the Lawra belt described in chapter 3, the chemical sediments, which are the favourable host rocks, are genetically associated with the hydrothermal process. Therefore, notwithstanding the apparent lack of CI between the alteration zones and the favourable host rocks, they are in nature conditionally dependent according to the conceptual model. The binary predictor pattern of the alteration zones is therefore removed from the analysis and the predictor patterns of the shear zones, favourable host rocks and the structures are integrated using the equation below.

$$\text{Pred. map} = exp(-10 + \text{WHR} + \text{WSZ} + \text{WFr}/(1 + exp(-10 + \text{WHR} + \text{WSZ} + \text{WFr})) \quad (6.18)$$

The results of the analyses are shown in Table 6.8. From the table the best predicted number of mineral occurrences is reduced to 23, indicating that by removing the alteration zone predictor pattern map, the overall conditional independence in the predictive maps becomes acceptable. The optimum predictive map of the Lawra belt from this study is shown in Fig 6.11. Reclassification was done by considering values $<$0.000136 (i.e. 3 times prior probability) as unfavourable, 0.000136-0.000267 as some favourability and 0.000267-0.00053 as high favourability.

Table 6.8: A summary of validation of predictive maps generated by the removal of fractures predictor map from analysis

Sets of analysis	Predicted No. of mineral occu.	% area of favou. zones	predicts mineral occu.? (Y/N)	Value of post. prob.
1	35	22	Y	0.00075
2	37	22	Y	0.000089
3	37	22	N	<0.000045
4	39	24	Y	0.0002
5	**37**	**27**	**Y**	**0.0001**
6	39	22	Y	0.000089
7	40	21	N	<0.000045
8	39	27	Y	0.00006
9	39	27	Y	0.0002
10	40	27	N	<0.000045
11	36	27	N	<0.000045
12	40	26	Y	0.000052
13	36	25	N	<0.000045
14	37	20	N	<0.000045
15	39	27	Y	0.002
16	38	21	N	<0.000045
17	39	21	Y	0.000075
18	39	24	Y	0.001
19	39	24	Y	0.001

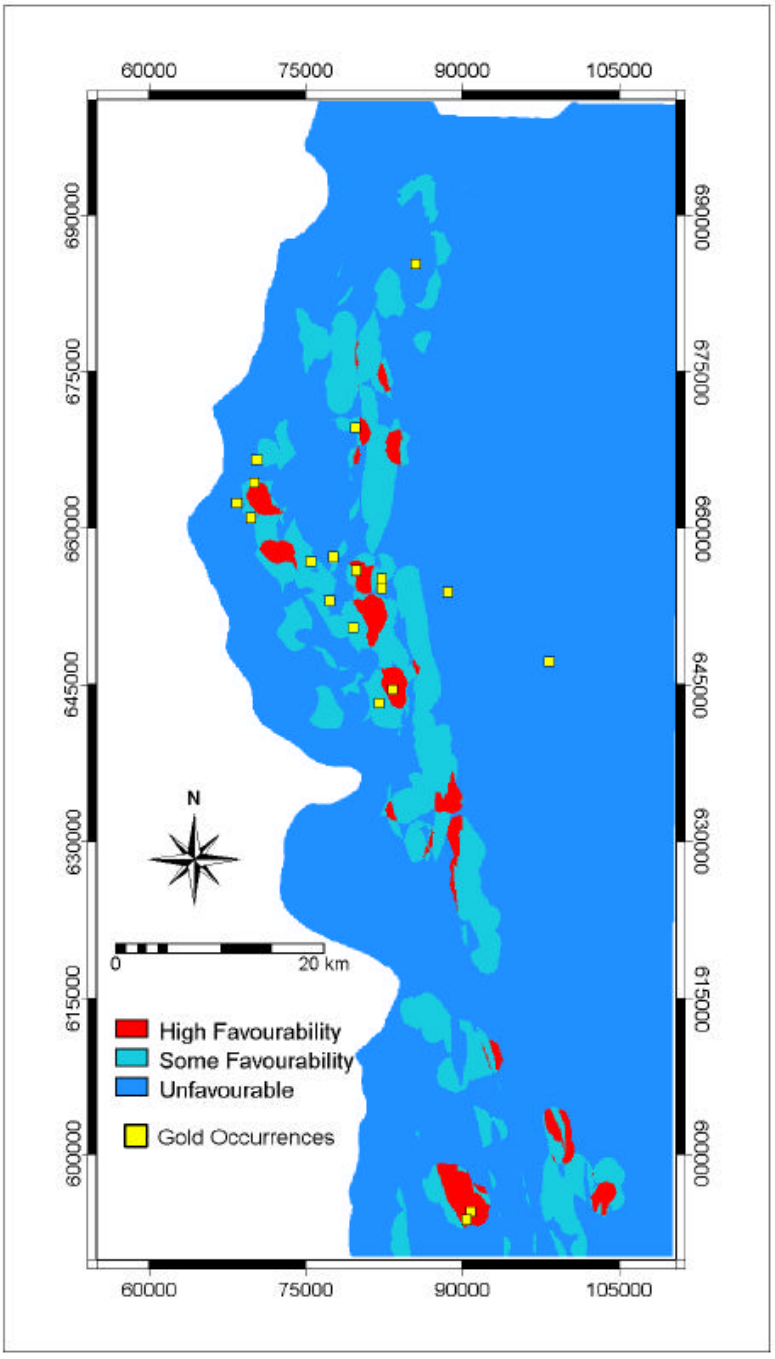

Figure 6.10: Analysis 5, predictive map using only WFHR, WALT and WSHE evidence maps

Table 6.9: A summary of validation of predictive maps generated by the removal of alteration binary map from analysis (supported by knowledge and conceptual model)

Sets of analysis	Predicted No. of mineral occu.	% area of favou. zones	Predicts min. occu.(Y/N)	Value of post. prob.
1	23	27	Y	0.00005
2	23	27	Y	0.000059
3	24	30	Y	0.00007
4	26	34	Y	0.00007
5	**23**	**27**	**Y**	**0.00007**
6	24	30	Y	0.00007
7	25	34	Y	0.00007
8	27	34	Y	0.00007
9	25	34	Y	0.00007
10	26	33	Y	0.00007
11	26	30	N	$<$0.000045
12	27	33	Y	0.00007
13	24	31	Y	0.00005
14	23	27	N	$<$0.000045
15	25	33	N	$<$0.000045
16	26	30	Y	0.00007
17	23	27	Y	0.00005
18	26	27	Y	0.00007
19	26	27	Y	0.00007

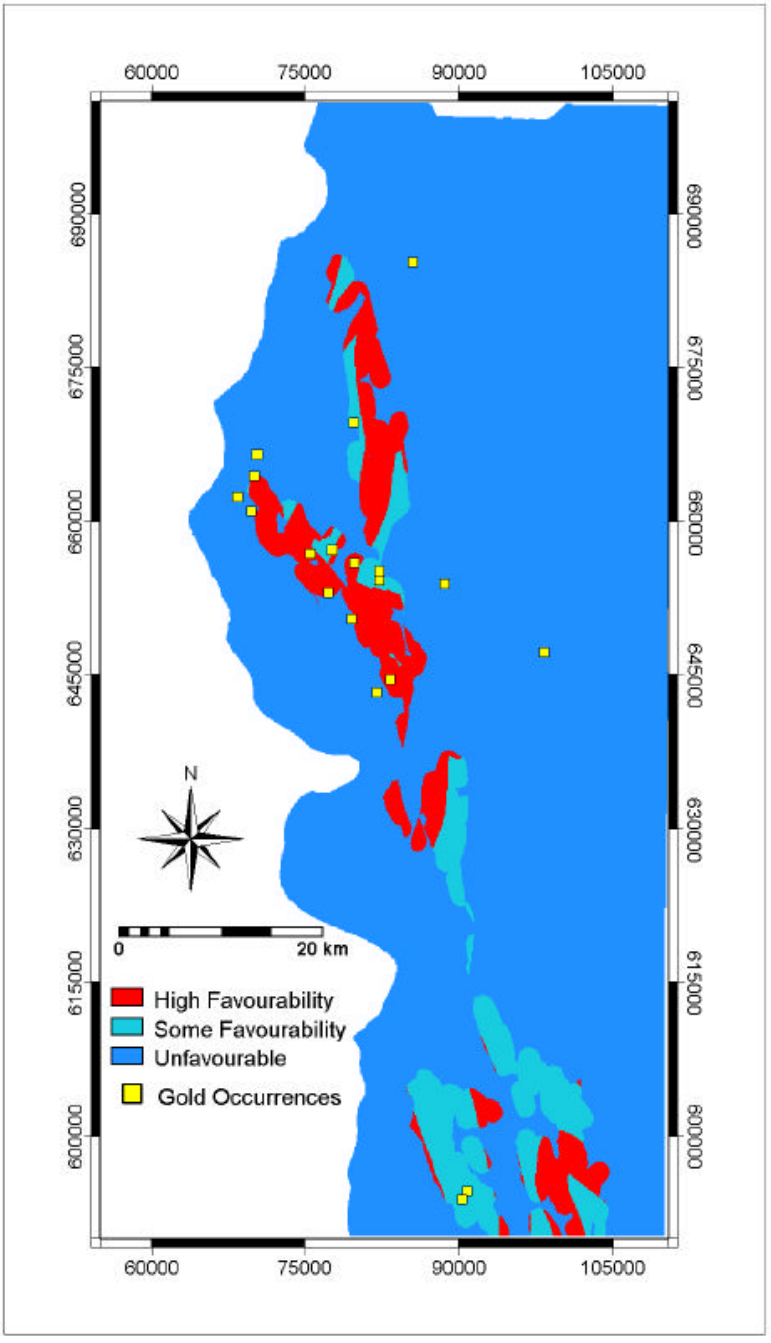

Figure 6.11: Best predictive map of gold in the Lawra belt using weights of evidence method

6.2 Analysis using fuzzy logic method

6.2.1 Fuzzy set

In the classical set theory, the membership of a set is defined as true or false, 1 or 0. Membership of a fuzzy set, however, is expressed on a continuous scale from 1 (full membership) to 0 (full non-membership) (Bonham-Carter, 1994). In fuzzy set theory, a fuzzy set is defined as a subset of objects whose membership in a set of objects is intermediate between complete and non-complete membership. Fuzzy membership values always lie in the range (0,1) and the values are chosen to reflect the degree of membership of a set, based on subjective judgement. The membership always relates to a certain proposition. In mineral exploration, the proposition is ”favourable location for mineral deposit” and therefore membership values must reflect the relative importance of each map, as well as the relative importance of each class of a single map to the proposition.

One example of set used in mineral exploration is the set of distances from a curvilinear geological features such as shear zones or folds. The subset is the distances, X, from the geologic feature. Hence, employing the theory of fuzzy sets introduced by Zadeh (1965), the class ”favourable distance”, d, translates into a series of measures (x) such that:

$$d = \{(x, \mu_d(x)) \,|x \in X\} \tag{6.19}$$

where $\mu_d(x)$ defines a grade of membership of distance x in the class ”favourable distance”.

A variety of operators can be used to combine the membership values of two or more maps with fuzzy membership functions. An et al.(1991) discuss five fuzzy operators that are useful for combining exploration datasets, namely the fuzzy AND, fuzzy OR, fuzzy algebraic product, fuzzy algebraic sum and Fuzzy gamma operator.

The **fuzzy AND** operation is equivalent to a Boolean AND (logical intersection) operation on classical set values of 1 and 0. It is defined as

$$\mu_combination = MIN(\mu_A, \mu_B, \mu_C, ...) \tag{6.20}$$

where μ_A is the membership value for map A at a particular location, μ_B is the fuzzy membership value for map B, and so on. The effect of this operation is that the output map is controlled by the smallest (minimum) fuzzy membership value occurring at each location. The AND operation is appropriate where two or more evidences for a

hypothesis must be present together for the hypothesis to be true.

The **fuzzy OR** is like the Boolean OR (logical union) in that the output membership values are controlled by the maximum values of any of the input maps for any particular location. The fuzzy OR is defined as

$$\mu_c ombination = MAX\left(\mu_A, \mu_B, \mu_C, ...\right) \tag{6.21}$$

This operator is reasonable in mineral potential mapping where favourable evidences for the occurrence of mineralisation are rare and the presence of any evidence may be sufficient to suggest favourability.

The **fuzzy algebraic product** is defined as

$$\mu_c ombination = \prod_{i=1}^{n} \mu_i \tag{6.22}$$

where μ_i are the fuzzy membership values for the i-th (i=1,2,...n) maps that are to be combined. The output map is always smaller than, or equal to, the smallest contributing fuzzy membership value and is therefore ”decreasive”.

The **fuzzy algebraic sum** operator is defined as

$$\mu_c ombination = \prod_{i=1}^{n} \left(1 - \mu_i\right) \tag{6.23}$$

The result of this operation is always larger than or equal to the largest contributing fuzzy membership value. Two or more pieces of evidence that both favour a hypothesis reinforce one another and the combined evidence is more supportive than either piece of evidence taken individually.

The **fuzzy gamma operation** is defined in terms of the fuzzy algebraic product and the fuzzy algebraic sum by

$$\mu_c ombination = \left(\prod_{i=1}^{n} \mu_i\right)^{1-\gamma} \left(\prod_{i=1}^{n} \left(1 - \mu_i\right)\right)^{\gamma} \tag{6.24}$$

where γ is a parameter chosen in the range zero to one. When γ is equal to 1, the combination is the same as the fuzzy algebraic sum; when γ is equal to 0, the combination becomes the fuzzy algebraic product.

6.2.2 Application of the fuzzy logic method to the Lawra belt

The fuzzy logic method is applied to the extracted spatial geologic features (host rocks, alteration zones, shear zones and fractures) indicative of lode gold occurrence in the Lawra belt. To generate fuzzy sets of favourable proximity distances to the shear zones, fractures and alteration zones, the results of the spatial association analyses by the weights of evidence method (section2) are used. However in the case of host rocks the various lithologic units in the area are used rather than proximity analyses. Fuzzy membership values are then assigned to these classes based on subjective judgement.

The distances to the geologic features having the optimum spatial associations with the known mineral occurrences by the weight of evidence method is summarised in Table 6.10 (i.e. in the case of the best predictive map).

Table 6.10: The optimum spatial association between proximity to geologic features and mineral occurrences.

Geologic Feature	Optimum distance(m)	Farthest distance(m)
Alteration zones	1000	27000
Favourable rocks	1000	28000
Fractures	1500	37000
Shear zones	1000	14000

The fuzzy membership values assigned to the various sets of spatial features indicative of gold are given in Table 6.10. In the table, fuzzy sets of increasing distances within the range of the optimum association of a geologic feature are assigned a fuzzy membership values of 0.9. The fuzzy sets of increasing distances beyond the range of optimum spatial association are assigned decreasing fuzzy membership values in the range of 0.4 to 0.1. The chemical sediments are considered to be genetically associated with the mineral occurrences and therefore assigned the highest membership value of 0.9 and the volcanogenic detrital sediments 0.7. The metavolcanics and the Dixcove granites are potential host rocks but are not known to host lode gold in the Lawra belt and therefore given a value of 0.4 and the Cape Coast granites 0.3. The dykes on the other hand are believed to postdate mineralisation in the area and are therefore assigned the lowest membership value of 0.1.

Table 6.11: The optimum spatial association between proximity to geologic features and mineral occurrences.

Hydrothermal alteration zones		**Favourable host rocks**		**Fractures**		**Shear zones**	
Distance class(m)	Fuzzy score	Lithologic units	Fuzzy score	Distance class(m)	Fuzzy score	Distance class(m)	Fuzzy score
<500	0.9	Chemical sed.	0.9	<500	0.9	<500	0.9
500-1000	0.9	Volcanic det. sed	0.7	500-1000	0.9	500-1000	0.9
1000-1500	0.4	Metavolcanics	0.4	1000-1500	0.9	1000-1500	0.4
1500-2000	0.35	Dixcove Gr.	0.4	1500-2000	0.4	1500-2000	0.35
2000-3000	0.3	Cape Coast Gr.	0.3	2000-3000	0.20	2000-3000	0.3
3000-4000	0.25	Dykes	0.1	>3000	0.1	3000-4000	0.25
4000-6000	0.2					4000-6000	0.2
6000-8000	0.15					6000-8000	0.15
>8000	0.1					>8000	0.1

Integration of fuzzy sets of evidences of lode gold occurrences

From the described conceptual model of the Lawra belt in chapter 3, hydrothermal metamorphogenic fluids remobilized gold from the chemical sediments, the gold was then transported and deposited in structurally favourable zones.

The fuzzy sets are therefore combined in three intermediate steps to generate a final predictive model. Three hypotheses are considered in the combination. The first step involves combining the shear zones and fractures using various fuzzy operators to provide evidence for favourable conduits and trap zones for the mineralised fluids. The second step involves combining the hydrothermal alteration and favourable host rocks using fuzzy operators to provide evidence for a hydrothermal system. The third step involves combining the above two intermediate evidence maps of favourable conduits and trap zones, and the hydrothermal system indicative of lode gold using fuzzy operators to generate a predictive map. Fig 6.12 shows the schematic inference network for predicting gold mineralisation potential in the Lawra belt using fuzzy logic as the 'inference engine'.

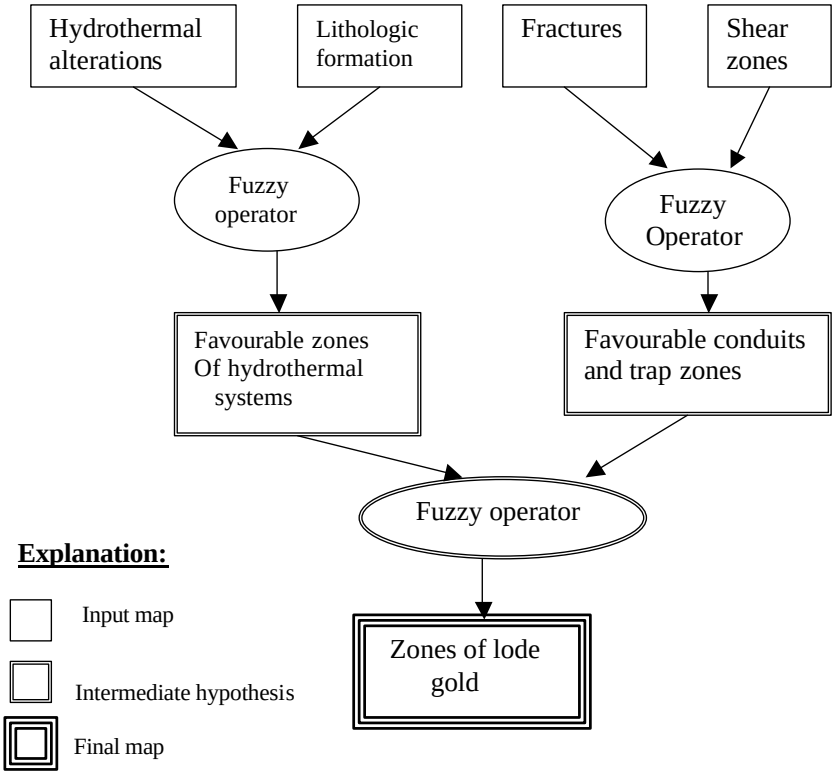

Figure 6.12: Schematic inference network for generating predictive map of lode gold in the Lawra belt

It is evident from Fig 6.12, that several combinations with fuzzy operators are possible to derive a final membership map of zones of lode gold potential in the Lawra belt. To obtain an optimum predictive map, i.e, a map with high predictive strength, a set of criteria were used to select the best maps for both 'intermediate hypothesis' maps and final predictive maps. This follows several experiments with various combinations of fuzzy operations to produce the predictive maps.

Three criteria are used to select both the best 'intermediate hypothesis' maps and final predictive maps. The first criterion is that the favourable zones depicted by these maps should have a fuzzy score of $\geq$0.7. This criterion is based on visual inspection of the fuzzy membership maps and based on fuzzy scores of 0.72 (i.e. 0.9×0.8). The second criterion is that the favourable zones depicted by both the 'intermediate hypothesis' maps and final predictive maps should contain or predict at least 65% of the known mineral occurrences in the Lawra belt. This is to give the final map a high predictive strength. The third criterion is that the favourable zones occupy at most 25% of the Lawra belt. This is because of the fact that potentially mineralised zones are quite rare in nature and that this percentage area is what is to be recommended

for further exploration work.

Of the several experimental combinations of fuzzy operations tested to produce a final predictive map, the predictive map resulting from the inference network of Fig 6.13, was judged the best predictive map based on the above criteria. It shows the fuzzy sets of proximity to alteration zones and favourable host rocks are best combined using fuzzy γ operator of 0.74 to produce an intermediate hypothesis of hydrothermal system. The fuzzy set of proximity to shear zones and fractures on the other hand are best combined by using γ value of 0.79 to produce an intermediate hypothesis of favourable zones for transport and deposition of the remobilised auriferous fluid. The predictive map (Fig 6.14), indicates that 15% of the area has potential for further exploration work for lode gold mineralisation.

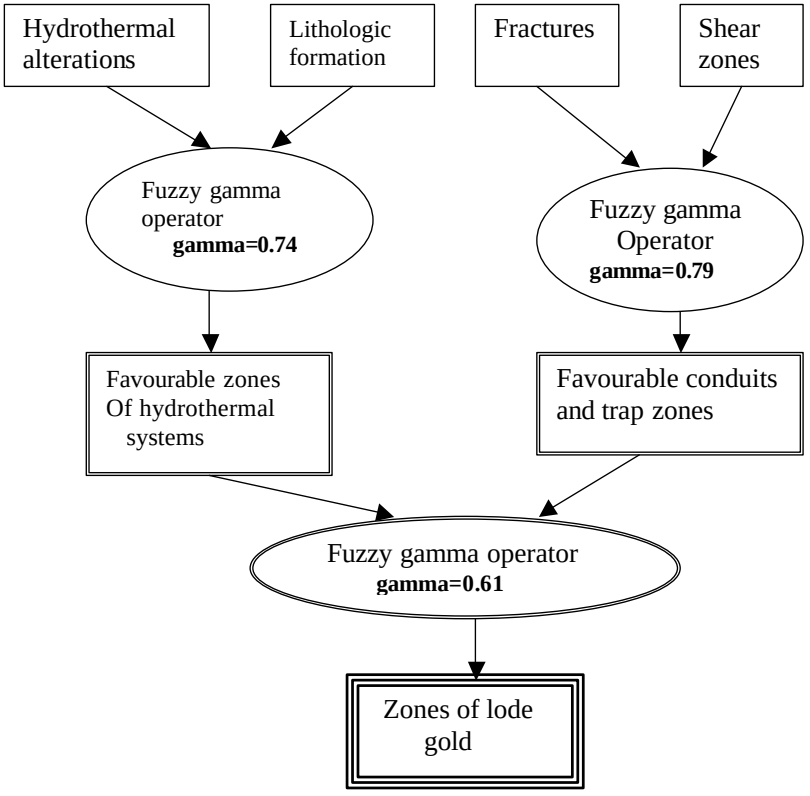

Figure 6.13: Inference network for generating the best predictive map of lode gold in the Lawra belt

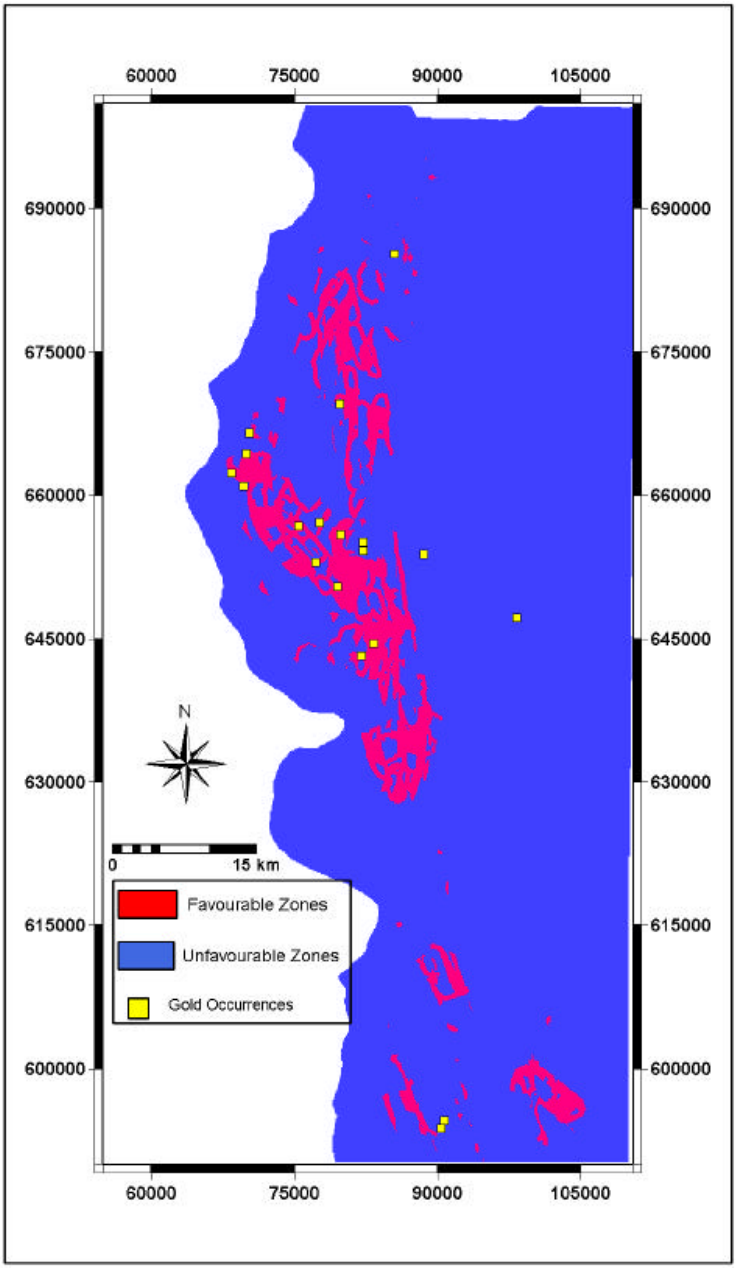

Figure 6.14: Fuzzy logic predictive map of gold in the Lawra belt

Validation of predictive map

To show whether the fuzzy logic predictive map has the capability to predict accurately unknown target areas, the 19 known mineral occurrences which were not used in this method were used to validate the predictive map. The predictive map predicts 13 out of the 19 known mineral occurrences of the Lawra belt, representing 68%. In the predictive map, the 5 unpredicted mineral occurrences are on average less than 800m from the delineated favourable zones.

6.3 Discussion

A variety of GIS-based integration techniques are available for generating predictive maps which have significant predictive strength of mineral deposits. The use of two such integration methods namely weights of evidence and fuzzy logic have been demonstrated to generate predictive maps of lode gold potential in the Lawra belt, NW Ghana.

Unlike other empirical methods which are spatially extrapolative i.e. a small controlled or trained area is used to represent a whole study area, the weight of evidence method adopts a spatially interpolative empirical approach in which the known mineral occurrences in the study area are used to quantify the spatial association of the geologic features with the mineral occurrences and also to statistically assign weights to the features. In the case of the Lawra belt where few mineral occurrences are known, by using a number of the mineral occurrences for the modelling and also repeating the analysis each time with a different set of mineral occurrences a predictive map is generated with 22% of the area been potential for mineralisation. Of this area, 3% is tagged highly favourable and contains 16% of the known mineral occurrences.

Notwithstanding the above results and the fact that the binary predictor patterns did not seriously violate the conditional independence hypothesis, the generated predictive maps in general are over predicting target areas (based on the overall conditional independence test, i.e. from Table 6.7). By removing the fractures binary predictor map, considered to be problematic, there was no significant change in the violation of the conditional dependence, from (Table 6.8) as such the above results should be interpreted with a low degree of confidence. This problem is attributed mainly to the fact that the geology of the Lawra belt is not thoroughly studied and as a result the true mineral deposit population of the area is under-represented. Consequently, the estimated weights are in error and therefore the weights have large variances.

The chemical sediments (the favourable host rocks) are genetically associated with the hydrothermal process (from the conceptual model) in the area, and therefore the two features are conditionally dependent notwithstanding the apparent lack of CI. On this basis, the hydrothermal alteration predictor map was removed which resulted in a better predictive map with acceptable overall conditional independence violation. Thus, the weights of evidence is applicable in areas with fairly well known mineral occurrences, however, in areas with few known occurrences one need to apply the appropriate knowledge and expertise to the method to generate a useful predictive model.

The fuzzy logic method, on the other hand, is knowledge driven and involves the application of field knowledge, expertise and conceptual models to the spatial geologic features to generate predictive maps. The two intermediate hypotheses used are based on the conceptual model described in chapter 3, where the gold in the Lawra belt was remobilised from the chemically precipitated sediments genetically associated with the hydrothermal process of the area and then transported and deposited in structurally favourable zones mainly in the sediments.

The subjective criteria applied to select the best 'intermediate hypotheses' and fuzzy predictive maps are guided by field knowledge. Since in nature, exploring for gold is just like searching for a needle in a haystack, and that favourable zones are quite rare, a small favourable area is much more appropriate than a large exploration area.

The inference network that produced the best fuzzy predictive map, Fig 6.13 shows the fuzzy sets of proximity to alteration zones and favourable host rocks are best combined using fuzzy γ operator of 0.74 to produce an intermediate hypothesis of a hydrothermal system. The high value of γ implies a dominant effect of the fuzzy algebraic sum operator over the algebraic product, which is appropriate for combining evidences that complement one another in support of a particular proposition. Thus, gold concentration in the Lawra belt is by volcanic related syngenetic processes, principally chemical precipitation in exhalative sediments. The fuzzy set of proximity to shear zones and fractures on the other hand are best combined by using γ value of 0.79 to produce an intermediate hypothesis of favourable zones for transport and deposition of the remobilised auriferous fluid. Again, the high value of gamma implies a dominant effect of the fuzzy algebraic operator. The intermediate hypothesis maps are best combined using a gamma value of 0.61.

In general, the pattern of the favourable areas in the generated predictive maps

using both weights of evidence and fuzzy logic methods are similar. However, the area defined or tagged as favourable zones (27%) by the weights of evidence method is higher than the favourable area defined by the fuzzy logic method (15%), and since gold mineralisation is rare, the predictive map by the fuzzy logic method gives better results. In addition, only one mineral occurrence was used to validate the predictive map by the weights of evidence method because of the fact that the rest were used in generating the predictive map. In the case of the fuzzy logic method all the 19 known mineral occurrences of the belt were used to validate the predictive map. Thus, there is a higher confidence in the validation method used in validating the fuzzy logic predictive map. Therefore, in the Lawra greenstone belt, the knowledge-driven method (Fuzzy logic) is more appropriate than the data-driven method (weights of evidence).

Chapter 7

Conclusions and Recommendations

7.1 Conclusions

1. The gold in the Lawra belt is concentrated by volcanic related syngenetic processes, principally chemical precipitation in exhalative sediments. The gold and associated minerals were remobilized from these chemical sediments by metamorphogenic processes with the auriferous fluid transported and deposited in structurally favourable sites.

2. The four most important spatial features or exploration guides to greenstone hosted lode gold mineralisation in the Lawra belt as seen in the genetic model are shear zones, fractures, host rocks and hydrothermal alterations.

3. The qualitative interpretation of the various airborne geophysical surveys has proved the old geological map to be of high quality since most of the geophysical responses could be attributed to the various rock units. The favourable host rocks, which are mainly the chemical sediments of the transition zones together with the detrital volcanogenic sediment components are reflected in the EM data as banded anomaly complexes with moderate and high conductivity.

4. The weights of evidence method adopts a spatially interpolative empirical approach in which the known mineral occurrences in the study area are used to quantify the spatial association, certain geologic features have with the mineral occurrences and also to statistically assign weights to these geologic features. The method reveals a close spatial association between gold-bearing quartz veins in the Lawra belt and

the following geologic features (in order of decreasing magnitude in the spatial association) hydrothermal alterations, shear zones, chemical sediments and fractures. The conceptual model of gold mineralisation in the study area indicates that the chemical sediments (favourable host rocks) are genetically associated with the hydrothermal process of the area and therefore these sediments and alteration zones are naturally conditionally dependent. Incorporating this model in the weights of evidence method led to a much better predictive map with acceptable violation of conditional independence, which also defines 6.2% of the Lawra greenstone belt as high favourable zones for lode gold mineralisation and a further 20.8% of the belt as having some favourability for lode gold mineralisation.

5. The application of the theory of fuzzy sets to mineral potential mapping provides a quantitative yet subjective technique for predicting mineral potential. The method requires the expert's knowledge of the spatial association between known mineral occurrence and geologic features in an area to make a subjective decision on the appropriate fuzzy membership scores. In the Lawra belt, the inference network that produced the best fuzzy predictive map and the use of intermediate hypotheses of hydrothermal systems, favourable conduits and trap zones is based on the conceptual model of the lode gold in the belt. The best predictive map generated by the fuzzy logic method defines 15% of the Lawra belt as favourable zone for gold mineralisation and predicts 13 out of the 19 known mineral occurrences in the area, representing 68%. In addition, 4 out of the 6 unpredicted mineral occurrences are on average less than 800m from the delineated favourable zones.

6. On the basis of the results of the analyses, the size of area defined as favourable zones in each method (i.e. 27% in the case of weights of evidence as against 15% with fuzzy logic method) and the strength of the validation method applied to each method, the fuzzy logic method of generating predictive map is considered more applicable or appropriate in the Lawra belt than the weights of evidence method.

7.2 Recommendations

1. Further prospecting work should be undertaken in the defined target areas to test the predictive capabilities of the generated predictive maps and thus the applicabilities of the described methods.

2. A much detail interpretation of the geophysical data especially the electromagnetics data should be carry out to enhance the extracted indicative geologic features.

3. A detailed structural study of the belt should be undertaken to determine the exact nature of fractures which are associated with the lode gold mineralisation to help distinguish them from fractures which are not related with the mineralisation. This will hugely improve spatial association analysis of the fractures with the known mineral occurrences.

Bibliography

Amedufo, S. (1995). Gold in Ghana. *PANGEA*, 23.

Amoako, Y., Johanson, R., Amedufo, S., Triumf, C., and Akamaluk, T. (1998). Processing and interpretation of data from airbourne. Final report, Geological Surveys Department Of Ghana And Sweden. 102pp.

An, P., Moon, W., and Rencz, A. (1991). Application of fuzzy set theory for integration of geological, geophysical and remote sensing data. *Canadian Journal of Exploration Geophysics*, 27:1–11.

Aryee, N. (June 2001). Ghana's mining sector: its contribution to the national economy. *RESOURCES POLICY The international journal of minerals policy and economics*, 27(2):61–75.

Asadi, H. and Hale, M. (1999). Integrated analysis of aeromagnetic, landsat tm and mineral occurrence data for epithermal gold exploration in northwest iran. In *13th International Conference on Applied Geologic Remote Sensing, Vancouver, British C*.

Ash, C. and Alldrick, D. (1996). Au-quartz veins. Technical report, British Columbia Ministry of Energy, Mines and Petroleum. http://www.em.gov.bc.ca/Mining/Geolsurv/EconomicGeology/MetallicMinerals.

Bates, L. B. and Jackson, A. J., editors (1985). *Glossary of Geology*. Mcgraw-Hill. 387pp.

Bonham-Carter, F. (1994). *Geographic Information System For Geoscientists*. Pergamon. 398pp.

Bonham-Carter, G., Wright, D., and Agterberg, D. (1989). Weights of evidence modelling with GIS:a new approach to mapping mineral deposits. *Geological Survey Canada Paper*, 89-9:171–183.

Boyle, R. (1979). *The Geochemistry Of Gold and its deposits*. Canadian Government Publishing centre, Hull,Quebec, Canada KIAOS9. 280pp.

Boyle, R. (1991). Auriferous archaean greenstone-sedimentary belts. In Hutchinson, R. and Graunch, I., editors, *Historical Perspectives Of Genetic Concepts And Case Histories Of Famous Discoveries*, pages 164–191pp. The Economic Geology Publishing Company.

Carranza, J. and Hale, M. (1999). Geologically-constrained probalistic mapping of gold potential, baguio district, philipines. Geocomputation.

Colvine, A. (1989). An empirical model for the formation of archaean gold deposits:products of final cratonization to the Superior province, Canada. *Econ. Geol*, 6:37–53.

Colvine, A., Heather, K., Fyon, J., Marmont, S., Smith, P., and Troop, D. (1988). Archaean Lode Gold Deposits in ontario. Misc. paper 139, Geological Survey of Canada. 136p.

DzigbodiAdjimah, K. (1993). Geology and geochemical patterns of the Birimian gold deposits, Ghana, West Africa. *Journal of geochemical exploration*, 47:305–320.

Eilu, P., Mikucki, J. E., and Groves, I. D. (1998). *Wallrock Alteration And Primary Geochemical Dispersion In Lode-Gold Exploration*, volume 1 of *SGA short course series*. Kem printing 16250 South Golden Road Golden,Colarado. 65pp.

Eisenlohr, B. and Hirdes, W. (1992). The structural development of the early Proterozoic Birimian and Tarkwaian rocks of southwest Ghana, West Africa. *Journal of African Earth Sciences*, 14(3):313–325.

Groves, D. and Foster, R. (1991). Archaean lode gold deposits. In Forster, R., editor, *Gold Metallogeny And Exploration*, pages 63–96pp. Blackie and Son Ltd.

Gunn, P., Minty, B., and Milligan, P. (1997). The airborne gamma-ray spectrometric response over arid Austrialia terranes. In Gubins, A. G., editor, *Geophysics and Geochemistry at the Millenium - Proceedings of the fourth Decennial International Conference on Mineral Exploration*, pages 733–740.

Hasting, D. (1982). On the tectonics and metallogenesis of West Africa: A model incorporating new geophysical data. *Geoexploration*, 20:295–327.

Ho, S. and Groves, D. (1987). Recent advances in understanding precambrian gold deposits. Publ.11.

Junner, N. (1935). Gold in gold coast. Memoir 4, Geological Survey Department, Ghana.

Kesse, G. (1985). *The mineral and rock resources of Ghana*. Rotterdam/Boston(Balkema). 610pp.

Kitson, A. (1928). Provisional geological map of the Gold Coast and Western Togoland, with brief notes thereon. Bull. 2, Gold Coast Geol. Surv.

Klein, T. and Day, W. (1994). Descriptive and grade-tonnage models of Archaean low-sulfide au-quartz veins and revised grade-tonnage model of homestake au. website.

Knox-Robinson, C. and Groves, D. I. (1997). Gold prospectivity mapping using GIS with examples from the Yilgarn Block of Western Australia. *Chronicle of Mineral Research*, 529:127–138.

Leube, A., Hirdes, W., Mauer, R., and Kesse, G. (1990). The early proterozoic Birimian supergroup of Ghana and some aspects of its associated gold mineralisation. *Precambrian Research*, 46:139–165.

Melcher, F. and Stumpfl, E. (1993). Chemical facies and gold mineralisation in northern Ghana. *Zeitschrift Feur Angewandte Geologie*, 39(859 A):43–46.

Melcher, F. and Stumpfl, E. (1994). Palaeoproterozoic exhalite Formation in Northern Ghana: Source of epigenetic gold-quartz vein mineralisation. *Geologisches Jahrbuch*, pages 201–246.

Ntiamoah-Agyakwa, Y. (1979). Relationship between gold and manganese mineralisations in the Birimian of Ghana, West Africa. *Geol. Mag.*, 116:345–352.

Oleary, D., Friedman, J., and Pohn, H. (1976). Lineament, linear, lineation:some proposed new standards for old terms. *Geological Society of American Bulletin*, 87:1463–1469.

Philips, G. and Groves, D. (1984). Fluid access and fluid-wall rock interaction in the genesis of the Archaean gold-quartz vein deposit at hunt mine, kambalda, western australia. In Foster, R., editor, *The Geology, Geochemistry and Genesis of Gold Deposits*, pages 389–416. R.P,Balkema,Rotterdam.

Phillips, G. and Groves, D. (1983). The nature of archaean bearing fluids as deduced from gold deposits of Western Australia. *Geol. Soc. Aust*, 30:25–39.

Phillips, G., Groves, D., and Brown, I. (1987). Sources requirement for the Golden Mile, Kalgoolie: Significance to the metamorphic replacement model for archaean gold deposits. *J. Earth Sci.*, 24:1643–1651.

Pobedash, I. (1965). Report on the geology and minerals of the southwestern part of the wa field sheet. Archive Report 51, Geological Survey Department,Ghana. 95pp.

Reeves, C. V. (1990). Mineral exploration geophysics. Course 1.48, Division of Exploration Geophysics, ITC, The Netherlands.

Reeves, C. V. (2000). Introduction to airborne geophysical mapping. Course 1.47, Division of Exploration Geophysics, ITC, The Netherlands;.

Richards, J. P. (2000). Lineaments revisited. *Society of Economic Geologists Newsletter*, 42:14–20.

Roudakov, V. (1965). Report on the geology and minerals of the wa field sheet. Mineral Commission and GTZ Publication Project Accra,Ghana. 95pp.

Roy, D. (2000). Using geostatistics to estimate the resources of a narrow vein gold deposit. Degree of master of applied science, DALHOUSIE UNIVERSITY DALTECH.

Roy, S. (1965). Comparative study of the metamorphosed manganese protores of the world-the problem of the nomenclature of the gondites and kodurites. *Econ. Geol.*, 60:1238–1260.

Westerhof, A. (1999). Area selection, terrain analysis and ore deposit modelling. ITC, Branch of Exploration and Engineering Geosciences Kanaalweg 3;2628EB Delft, The Netherlands.

Woods, V. (1987). Geophysics for exploration geologist. Short course number 8 201pp.

Wright, J., Hastings, D., Jones, W., and Williams, H. (1985). *Geology and Mineral Resources of West Africa*. George Allen and Unwin publishers Ltd. 187pp.

Zadeh, L. (1965). Fuzzy sets. *IEEE information and control*, 8:338–353.

APPENDIX

.1 Other results of 18 analyses using weights of evidence method

Table 1: ANALYSIS 2, using weights of evidence method

ALTERATION ANALYSIS2

dist (m)	npixbd	wp	stdwp	Wn	stdWn	C	stdC	sigC
500	5	1.0664	0.4472	-0.2249	0.2774	1.2914	0.526	2.4541
1000	**11**	**1.3538**	**0.3015**	**-0.7727**	**0.378**	**2.1265**	**0.484**	**4.3981**
1500	13	1.184	0.2774	-1.0311	0.4472	2.2151	0.526	4.2093
2000	14	1.0232	0.2673	-1.1762	0.5	2.1993	0.567	3.8792
3000	16	0.8535	0.25	-1.7214	0.7071	2.5749	0.75	3.4333
4000	17	0.7101	0.2425	-2.2662	1	2.9764	1.029	2.8926
6000	17	0.4658	0.2425	-1.992	1	2.4578	1.029	2.3886
8000	17	0.3344	0.2425	-1.7633	1	2.0976	1.029	2.0386
10000	17	0.2424	0.2425	-1.539	1	1.7815	1.029	1.7314
27000	18	0.2502	0.2357	?	?	?	?	?

HOST ROCKS ANALYSIS2

dist(m)	npixbd	wp	stdwp	Wn	stdWn	C	stdC	sigC
500	10	0.7129	0.3162	-0.493	0.3536	1.2059	0.474	2.5422
1000	13	0.7721	0.2774	-0.8749	0.4472	1.647	0.526	3.1297
1500	**15**	**0.767**	**0.2582**	**-1.3024**	**0.5774**	**2.0694**	**0.633**	**3.2718**
2000	16	0.7262	0.25	-1.6351	0.7071	2.3612	0.75	3.1483
4000	16	0.4865	0.25	-1.4065	0.7071	1.893	0.75	2.524
6000	17	0.424	0.2425	-1.9279	1	2.3519	1.029	2.2857
8000	17	0.3335	0.2425	-1.7615	1	2.095	1.029	2.036
12000	17	0.1978	0.2425	-1.3991	1	1.5969	1.029	1.5519
28000	18	0	0.2357	?	?	?	?	?

SHEAR ZONES ANALYSIS2

dist(m)	npixbd	Wp	stdWp	Wn	stdWn	C	stdC	sigC
500	7	1.2243	0.378	-0.3711	0.3015	1.5954	0.484	3.2996
1000	**11**	**1.2016**	**0.3015**	**-0.7414**	**0.378**	**1.943**	**0.484**	**4.0185**
1500	11	0.9748	0.3015	-0.6824	0.378	1.6572	0.484	3.4274
2000	13	0.989	0.2774	-0.9681	0.4472	1.9572	0.526	3.7191
3000	15	0.9133	0.2582	-1.3848	0.5774	2.2981	0.633	3.6334
4000	16	0.8065	0.25	-1.6917	0.7071	2.4982	0.75	3.331
6000	16	0.5662	0.25	-1.4949	0.7071	2.0611	0.75	2.7482
8000	17	0.4664	0.2425	-1.9929	1	2.4594	1.029	2.3901
10000	17	0.3563	0.2425	-1.8076	1	2.1639	1.029	2.1029
37000	18	0	0.2357	?	?	?	?	?

FRACTURES ANALYSIS2

dist(m)	npixbd	wp	stdwp	Wn	stdwn	C	stdC	sigC
500	6	0.6266	0.4083	-0.2093	0.2887	0.8359	0.5	1.6716
1000	9	0.4461	0.3333	-0.3074	0.3333	0.7535	0.471	1.5986
1500	**13**	**0.4894**	**0.2774**	**-0.6963**	**0.4472**	**1.1857**	**0.526**	**2.2531**
2000	14	0.3648	0.2673	-0.7274	0.5	1.0922	0.567	1.9264
2500	15	0.2984	0.2582	-0.8285	0.5774	1.1269	0.633	1.7817
14000	18	0	0.2357	?	?	?	?	?

Table 2: ANALYSIS 3, using weights of evidence method

ALTERATION ANALYSIS3

dist (m)	npixbd	wp	stdwp	Wn	stdWn	C	stdC	sigC
500	5	1.0664	0.4472	-0.2249	0.2774	1.2914	0.526	2.4541
1000	**11**	**1.3538**	**0.3015**	**-0.7727**	**0.378**	**2.1265**	**0.484**	**4.3981**
1500	13	1.184	0.2774	-1.0311	0.4472	2.2151	0.526	4.2093
2000	14	1.0232	0.2673	-1.1762	0.5	2.1993	0.567	3.8792
3000	16	0.8535	0.25	-1.7214	0.7071	2.5749	0.75	3.4333
4000	17	0.7101	0.2425	-2.2662	1	2.9764	1.029	2.8926
6000	17	0.4658	0.2425	-1.992	1	2.4578	1.029	2.3886
8000	17	0.3344	0.2425	-1.7633	1	2.0976	1.029	2.0386
10000	17	0.2424	0.2425	-1.539	1	1.7815	1.029	1.7314
27000	18	0.2502	0.2357	?	?	?	?	?

HOST ROCKS ANALYSIS3

dist(m)	npixbd	wp	stdwp	Wn	stdWn	C	stdC	sigC
500	10	0.7129	0.3162	-0.493	0.3536	1.2059	0.474	2.5422
1000	13	0.7721	0.2774	-0.8749	0.4472	1.647	0.526	3.1297
1500	**15**	**0.767**	**0.2582**	**-1.3024**	**0.5774**	**2.0694**	**0.633**	**3.2718**
2000	16	0.7262	0.25	-1.6351	0.7071	2.3612	0.75	3.1483
4000	16	0.4865	0.25	-1.4065	0.7071	1.893	0.75	2.524
6000	17	0.424	0.2425	-1.9279	1	2.3519	1.029	2.2857
8000	17	0.3335	0.2425	-1.7615	1	2.095	1.029	2.036
12000	17	0.1978	0.2425	-1.3991	1	1.5969	1.029	1.5519
28000	18	0	0.2357	?	?	?	?	?

SHEAR ZONES ANALYSIS3

dist(m)	npixbd	Wp	stdWp	Wn	stdWn	C	stdC	sigC
500	7	1.2243	0.378	-0.3711	0.3015	1.5954	0.484	3.2996
1000	**11**	**1.2016**	**0.3015**	**-0.7414**	**0.378**	**1.943**	**0.484**	**4.0185**
1500	12	1.0619	0.2887	-0.8365	0.4083	1.8984	0.5	3.7964
2000	14	1.0632	0.2673	-1.1913	0.5	2.2544	0.567	3.9763
3000	15	0.9133	0.2582	-1.3848	0.5774	2.2981	0.633	3.6334
4000	16	0.8065	0.25	-1.6917	0.7071	2.4982	0.75	3.331
6000	16	0.5662	0.25	-1.4949	0.7071	2.0611	0.75	2.7482
8000	17	0.4664	0.2425	-1.9929	1	2.4594	1.029	2.3901
10000	17	0.3563	0.2425	-1.8076	1	2.1639	1.029	2.1029
37000	18	0	0.2357	?	?	?	?	?

FRACTURES ANALYSIS3

dist(m)	npixbd	wp	stdwp	Wn	stdwn	C	stdC	sigC
500	6	0.6266	0.4083	-0.2093	0.2887	0.8359	0.5	1.6716
1000	9	0.4461	0.3333	-0.3074	0.3333	0.7535	0.471	1.5986
1500	**12**	**0.4094**	**0.2887**	**-0.514**	**0.4083**	**0.9233**	**0.5**	**1.8464**
2000	13	0.2906	0.2774	-0.5043	0.4472	0.7949	0.526	1.5105
2500	15	0.2984	0.2582	-0.8285	0.5774	1.1269	0.633	1.7817
14000	18	0	0.2357	?	?	?	?	?

Table 3: ANALYSIS 4, using weights of evidence method

ALTERATION ANALYSIS 4

dist(m)	npixbd	wp	stdwp	Wn	stdwn	C	stdc	SigC
500	5	1.0664	0.4472	-0.2249	0.2774	1.2914	0.526	2.454
1000	**11**	**1.3538**	**0.3015**	**-0.7727**	**0.378**	**2.1265**	**0.484**	**4.398**
1500	13	1.184	0.2774	-1.0311	0.4472	2.2151	0.526	4.2092
2000	14	1.0232	0.2673	-1.1762	0.5	2.1993	0.567	3.8791
3000	16	0.8535	0.25	-1.7214	0.7071	2.5749	0.75	3.4332
4000	17	0.7101	0.2425	-2.2662	1	2.9764	1.029	2.8926
6000	17	0.4658	0.2425	-1.992	1	2.4578	1.029	2.3886
8000	17	0.3344	0.2425	-1.7633	1	2.0976	1.029	2.0385
10000	17	0.2424	0.2425	-1.539	1	1.7815	1.029	1.7313
27000	18	0	0.2357	?	?	?	?	?

HOST ROCKS ANALYSIS 4

dist(m)	npixbd	wp	stdwp	Wn	stdWn	C	stdC	sigC
500	10	0.7129	0.3162	-0.493	0.3536	1.2059	0.474	2.5422
1000	13	0.7721	0.2774	-0.8749	0.4472	1.647	0.526	3.1297
1500	**15**	**0.767**	**0.2582**	**-1.3024**	**0.5774**	**2.0694**	**0.633**	**3.2718**
2000	16	0.7262	0.25	-1.6351	0.7071	2.3612	0.75	3.1483
4000	16	0.4865	0.25	-1.4065	0.7071	1.893	0.75	2.524
6000	17	0.424	0.2425	-1.9279	1	2.3519	1.029	2.2857
8000	17	0.3335	0.2425	-1.7615	1	2.095	1.029	2.036
12000	17	0.1978	0.2425	-1.3991	1	1.5969	1.029	1.5519
28000	**18**	0	0.2357	?	?	?	?	?

SHEAR ZONES ANALYSIS 4

dist(m)	npixbd	wp	stdwp	Wn	stdWn	C	stdC	sigC
500	7	1.2243	0.378	-0.3711	0.3015	1.5954	0.484	3.2996
1000	10	1.1062	0.3162	-0.6079	0.3536	1.7141	0.474	3.6135
1500	11	0.9748	0.3015	-0.6824	0.378	1.6572	0.484	3.4274
2000	**13**	**0.989**	**0.2774**	**-0.9681**	**0.4472**	**1.9572**	**0.526**	**3.7191**
3000	15	0.9133	0.2582	-1.3848	0.5774	2.2981	0.633	3.6334
4000	16	0.8065	0.25	-1.6917	0.7071	2.4982	0.75	3.331
6000	16	0.5662	0.25	-1.4949	0.7071	2.0611	0.75	2.7482
8000	17	0.4664	0.2425	-1.9929	1	2.4594	1.029	2.3901
10000	17	0.3563	0.2425	-1.8076	1	2.1639	1.029	2.1029
37000	18	0	0.2357	?	?	?	?	?

FRACTURES ANALYSIS 4

dist(m)	npixbd	wp	stdwp	Wn	stdwn	C	stdC	sigC
500	6	0.6266	0.4083	-0.2093	0.2887	0.8359	0.5	1.6716
1000	9	0.4461	0.3333	-0.3074	0.3333	0.7535	0.471	1.5986
1500	**12**	**0.4094**	**0.2887**	**-0.514**	**0.4083**	**0.9233**	**0.5**	**1.8464**
2000	13	0.2906	0.2774	-0.5043	0.4472	0.7949	0.526	1.5105
2500	15	0.2984	0.2582	-0.8285	0.5774	1.1269	0.633	1.7817
14000	18	0	0.2357	?	?	?	?	?

Table 4: ANALYSIS 5, using weights of evidence method

ALTERATION ANALYSIS 5

dist(m)	npixbd	wp	stdwp	Wn	stdWn	C	stdC	sigC
500	6	1.2488	0.4083	-0.305	0.2887	1.5538	0.5	3.1072
1000	**11**	**1.3538**	**0.3015**	**-0.7727**	**0.378**	**2.1265**	**0.484**	**4.398**
1500	13	1.184	0.2774	-1.0311	0.4472	2.2151	0.526	4.2092
2000	14	1.0232	0.2673	-1.1762	0.5	2.1993	0.567	3.8791
3000	16	0.8535	0.25	-1.7214	0.7071	2.5749	0.75	3.4332
4000	17	0.7101	0.2425	-2.2662	1	2.9764	1.029	2.8926
6000	17	0.4658	0.2425	-1.992	1	2.4578	1.029	2.3886
8000	17	0.3344	0.2425	-1.7633	1	2.0976	1.029	2.0385
10000	17	0.2424	0.2425	-1.539	1	1.7815	1.029	1.7313
27000	18	0	0.2357	?	?	?	?	?

HOST ROCKS ANALYSIS 5

dist(m)	npixbd	wp	stdwp	Wn	stdWn	C	stdC	sigC
500	10	0.7129	0.3162	-0.493	0.3536	1.2059	0.474	2.5422
1000	13	0.7721	0.2774	-0.8749	0.4472	1.647	0.526	3.1297
1500	**15**	**0.767**	**0.2582**	**-1.3024**	**0.5774**	**2.0694**	**0.633**	**3.2718**
2000	16	0.7262	0.25	-1.6351	0.7071	2.3612	0.75	3.1483
4000	16	0.4865	0.25	-1.4065	0.7071	1.893	0.75	2.524
6000	17	0.424	0.2425	-1.9279	1	2.3519	1.029	2.2857
8000	17	0.3335	0.2425	-1.7615	1	2.095	1.029	2.036
12000	17	0.1978	0.2425	-1.3991	1	1.5969	1.029	1.5519
28000	**18**	0	0.2357	?	?	?	?	?

SHEAR ZONES ANALYSIS 5

dist(m)	npixbd	wp	stdwp	Wn	stdWn	C	stdC	sigC
500	7	1.2243	0.378	-0.3711	0.3015	1.5954	0.484	3.2996
1000	**11**	**1.2016**	**0.3015**	**-0.7414**	**0.378**	**1.943**	**0.484**	**4.0185**
1500	12	1.0619	0.2887	-0.8365	0.4083	1.8984	0.5	3.7964
2000	14	1.0632	0.2673	-1.1913	0.5	2.2544	0.567	3.9763
3000	15	0.9133	0.2582	-1.3848	0.5774	2.2981	0.633	3.6334
4000	16	0.8065	0.25	-1.6917	0.7071	2.4982	0.75	3.331
6000	16	0.5662	0.25	-1.4949	0.7071	2.0611	0.75	2.7482
8000	17	0.4664	0.2425	-1.9929	1	2.4594	1.029	2.3901
10000	17	0.3563	0.2425	-1.8076	1	2.1639	1.029	2.1029
37000	18	0	0.2357	?	?	?	?	?

FRACTURES ANALYSIS 5

dist(m)	npixbd	wp	stdwp	Wn	stdwn	C	stdC	sigC
500	6	0.6266	0.4083	-0.2093	0.2887	0.8359	0.5	1.6716
1000	9	0.4461	0.3333	-0.3074	0.3333	0.7535	0.471	1.5986
1500	**12**	**0.4094**	**0.2887**	**-0.514**	**0.4083**	**0.9233**	**0.5**	**1.8464**
2000	13	0.2906	0.2774	-0.5043	0.4472	0.7949	0.526	1.5105
2500	15	0.2984	0.2582	-0.8285	0.5774	1.1269	0.633	1.7817
14000	18	0	0.2357	?	?	?	?	?

Table 5: ANALYSIS 6, using weights of evidence method

ALTERATION ANALYSIS 6

dist(m)	npixbd	wp	stdwp	Wn	stdWn	C	stdC	sigC
500	6	1.2488	0.4083	-0.305	0.2887	1.5538	0.5	3.1072
1000	**12**	**1.4408**	**0.2887**	**-0.9268**	**0.4083**	**2.3677**	**0.5**	**4.7349**
1500	13	1.184	0.2774	-1.0311	0.4472	2.2151	0.526	4.2092
2000	14	1.0232	0.2673	-1.1762	0.5	2.1993	0.567	3.8791
3000	16	0.8535	0.25	-1.7214	0.7071	2.5749	0.75	3.4332
4000	17	0.7101	0.2425	-2.2662	1	2.9764	1.029	2.8926
6000	17	0.4658	0.2425	-1.992	1	2.4578	1.029	2.3886
8000	17	0.3344	0.2425	-1.7633	1	2.0976	1.029	2.0385
10000	17	0.2424	0.2425	-1.539	1	1.7815	1.029	1.7313
27000	18	0	0.2357	?	?	?	?	?

HOST ROCKS ANALYSIS 6

dist(m)	npixbd	wp	stdwp	Wn	stdWn	C	stdC	sigC
500	10	0.7129	0.3162	-0.493	0.3536	1.2059	0.474	2.5422
1000	13	0.7721	0.2774	-0.8749	0.4472	1.647	0.526	3.1297
1500	**15**	**0.767**	**0.2582**	**-1.3024**	**0.5774**	**2.0694**	**0.633**	**3.2718**
2000	16	0.7262	0.25	-1.6351	0.7071	2.3612	0.75	3.1483
4000	16	0.4865	0.25	-1.4065	0.7071	1.893	0.75	2.524
6000	17	0.424	0.2425	-1.9279	1	2.3519	1.029	2.2857
8000	17	0.3335	0.2425	-1.7615	1	2.095	1.029	2.036
12000	17	0.1978	0.2425	-1.3991	1	1.5969	1.029	1.5519
28000	**18**	0	0.2357	?	?	?	?	?

SHEAR ZONES ANALYSIS 6

dist(m)	npixbd	wp	stdwp	Wn	stdWn	C	stdC	sigC
500	7	1.2243	0.378	-0.3711	0.3015	1.5954	0.484	3.2996
1000	**11**	**1.2016**	**0.3015**	**-0.7414**	**0.378**	**1.943**	**0.484**	**4.0185**
1500	12	1.0619	0.2887	-0.8365	0.4083	1.8984	0.5	3.7964
2000	14	1.0632	0.2673	-1.1913	0.5	2.2544	0.567	3.9763
3000	15	0.9133	0.2582	-1.3848	0.5774	2.2981	0.633	3.6334
4000	16	0.8065	0.25	-1.6917	0.7071	2.4982	0.75	3.331
6000	16	0.5662	0.25	-1.4949	0.7071	2.0611	0.75	2.7482
8000	17	0.4664	0.2425	-1.9929	1	2.4594	1.029	2.3901
10000	17	0.3563	0.2425	-1.8076	1	2.1639	1.029	2.1029
37000	18	0	0.2357	?	?	?	?	?

FRACTURES ANALYSIS 6

dist(m)	npixbd	wp	stdwp	Wn	stdwn	C	stdC	sigC
500	6	0.6266	0.4083	-0.2093	0.2887	0.8359	0.5	1.6716
1000	9	0.4461	0.3333	-0.3074	0.3333	0.7535	0.471	1.5986
1500	**12**	**0.4094**	**0.2887**	**-0.514**	**0.4083**	**0.9233**	**0.5**	**1.8464**
2000	13	0.2906	0.2774	-0.5043	0.4472	0.7949	0.526	1.5105
2500	15	0.2984	0.2582	-0.8285	0.5774	1.1269	0.633	1.7817
14000	18	0	0.2357	?	?	?	?	?

Table 6: ANALYSIS 7, using weights of evidence method

ALTERATION ANALYSIS 7

dist(m)	npixbd	wp	stdwp	Wn	stdWn	C	stdC	sigC
500	6	1.2488	0.4083	-0.305	0.2887	1.5538	0.5	3.1072
1000	**12**	**1.4408**	**0.2887**	**-0.9268**	**0.4083**	**2.3677**	**0.5**	**4.7349**
1500	14	1.2581	0.2673	-1.2543	0.5	2.5124	0.567	4.4313
2000	15	1.0922	0.2582	-1.4638	0.5774	2.556	0.633	4.0411
3000	16	0.8535	0.25	-1.7214	0.7071	2.5749	0.75	3.4332
4000	17	0.7101	0.2425	-2.2662	1	2.9764	1.029	2.8926
6000	17	0.4658	0.2425	-1.992	1	2.4578	1.029	2.3886
8000	17	0.3344	0.2425	-1.7633	1	2.0976	1.029	2.0385
10000	17	0.2424	0.2425	-1.539	1	1.7815	1.029	1.7313
27000	18	0	0.2357	?	?	?	?	?

HOST ROCKS ANALYSIS 7

dist(m)	npixbd	wp	stdwp	Wn	stdWn	C	stdC	sigC
500	10	0.7129	0.3162	-0.493	0.3536	1.2059	0.474	2.5422
1000	13	0.7721	0.2774	-0.8749	0.4472	1.647	0.526	3.1297
1500	**15**	**0.767**	**0.2582**	**-1.3024**	**0.5774**	**2.0694**	**0.633**	**3.2718**
2000	16	0.7262	0.25	-1.6351	0.7071	2.3612	0.75	3.1483
4000	16	0.4865	0.25	-1.4065	0.7071	1.893	0.75	2.524
6000	17	0.424	0.2425	-1.9279	1	2.3519	1.029	2.2857
8000	17	0.3335	0.2425	-1.7615	1	2.095	1.029	2.036
12000	17	0.1978	0.2425	-1.3991	1	1.5969	1.029	1.5519
28000	**18**	0	0.2357	?	?	?	?	?

SHEAR ZONES ANALYSIS 7

dist(m)	npixbd	wp	stdwp	Wn	stdWn	C	stdC	sigC
500	6	1.0701	0.4083	-0.2841	0.2887	1.3542	0.5	2.7081
1000	10	1.1062	0.3162	-0.6079	0.3536	1.7141	0.474	3.6135
1500	11	0.9748	0.3015	-0.6824	0.378	1.6572	0.484	3.4274
2000	**13**	**0.989**	**0.2774**	**-0.9681**	**0.4472**	**1.9572**	**0.526**	**3.7191**
3000	15	0.9133	0.2582	-1.3848	0.5774	2.2981	0.633	3.6334
4000	16	0.8065	0.25	-1.6917	0.7071	2.4982	0.75	3.331
6000	16	0.5662	0.25	-1.4949	0.7071	2.0611	0.75	2.7482
8000	17	0.4664	0.2425	-1.9929	1	2.4594	1.029	2.3901
10000	17	0.3563	0.2425	-1.8076	1	2.1639	1.029	2.1029
37000	18	0	0.2357	?	?	?	?	?

FRACTURES ANALYSIS 7

dist(m)	npixbd	wp	stdwp	Wn	stdwn	C	stdC	sigC
500	5	0.4442	0.4472	-0.1292	0.2774	0.5735	0.526	1.0898
1000	8	0.3283	0.3536	-0.202	0.3162	0.5303	0.474	1.1179
1500	**12**	**0.4094**	**0.2887**	**-0.514**	**0.4083**	**0.9233**	**0.5**	**1.8464**
2000	13	0.2906	0.2774	-0.5043	0.4472	0.7949	0.526	1.5105
2500	15	0.2984	0.2582	-0.8285	0.5774	1.1269	0.633	1.7817
14000	18	0	0.2357	?	?	?	?	?

Table 7: ANALYSIS 8 using weights of evidence method

ALTERATION ANALYSIS 8

dist(m)	npixbd	wp	stdwp	Wn	stdWn	C	stdC	sigC
500	6	1.2488	0.4083	-0.305	0.2887	1.5538	0.5	3.1072
1000	**12**	**1.4408**	**0.2887**	**-0.9268**	**0.4083**	**2.3677**	**0.5**	**4.7349**
1500	14	1.2581	0.2673	-1.2543	0.5	2.5124	0.567	4.4313
2000	15	1.0922	0.2582	-1.4638	0.5774	2.556	0.633	4.0411
3000	16	0.8535	0.25	-1.7214	0.7071	2.5749	0.75	3.4332
4000	17	0.7101	0.2425	-2.2662	1	2.9764	1.029	2.8926
6000	17	0.4658	0.2425	-1.992	1	2.4578	1.029	2.3886
8000	17	0.3344	0.2425	-1.7633	1	2.0976	1.029	2.0385
10000	17	0.2424	0.2425	-1.539	1	1.7815	1.029	1.7313
27000	18	0	0.2357	?	?	?	?	?

HOST ROCKS ANALYSIS 8

dist(m)	npixbd	wp	stdwp	Wn	stdWn	C	stdC	sigC
500	10	0.7129	0.3162	-0.493	0.3536	1.2059	0.474	2.5422
1000	13	0.7721	0.2774	-0.8749	0.4472	1.647	0.526	3.1297
1500	**15**	**0.767**	**0.2582**	**-1.3024**	**0.5774**	**2.0694**	**0.633**	**3.2718**
2000	16	0.7262	0.25	-1.6351	0.7071	2.3612	0.75	3.1483
4000	16	0.4865	0.25	-1.4065	0.7071	1.893	0.75	2.524
6000	17	0.424	0.2425	-1.9279	1	2.3519	1.029	2.2857
8000	17	0.3335	0.2425	-1.7615	1	2.095	1.029	2.036
12000	17	0.1978	0.2425	-1.3991	1	1.5969	1.029	1.5519
28000	**18**	0	0.2357	?	?	?	?	?

SHEAR ZONES ANALYSIS 8

dist(m)	npixbd	wp	stdwp	Wn	stdWn	C	stdC	sigC
500	6	1.0701	0.4083	-0.2841	0.2887	1.3542	0.5	2.7081
1000	10	1.1062	0.3162	-0.6079	0.3536	1.7141	0.474	3.6135
1500	11	0.9748	0.3015	-0.6824	0.378	1.6572	0.484	3.4274
2000	**13**	**0.989**	**0.2774**	**-0.9681**	**0.4472**	**1.9572**	**0.526**	**3.7191**
3000	15	0.9133	0.2582	-1.3848	0.5774	2.2981	0.633	3.6334
4000	16	0.8065	0.25	-1.6917	0.7071	2.4982	0.75	3.331
6000	16	0.5662	0.25	-1.4949	0.7071	2.0611	0.75	2.7482
8000	17	0.4664	0.2425	-1.9929	1	2.4594	1.029	2.3901
10000	17	0.3563	0.2425	-1.8076	1	2.1639	1.029	2.1029
37000	18	0	0.2357	?	?	?	?	?

FRACTURES ANALYSIS 8

dist(m)	npixbd	wp	stdwp	Wn	stdwn	C	stdC	sigC
500	6	0.6266	0.4083	-0.2093	0.2887	0.8359	0.5	1.6716
1000	9	0.4461	0.3333	-0.3074	0.3333	0.7535	0.471	1.5986
1500	**13**	**0.4894**	**0.2774**	**-0.6963**	**0.4472**	**1.1857**	**0.526**	**2.2531**
2000	14	0.3648	0.2673	-0.7274	0.5	1.0922	0.567	1.9264
2500	15	0.2984	0.2582	-0.8285	0.5774	1.1269	0.633	1.7817
14000	18	0	0.2357	?	?	?	?	?

Table 8: ANALYSIS 9, using weights of evidence method

ALTERATION ANALYSIS 9

dist(m)	npixbd	wp	stdwp	Wn	stdWn	C	stdC	sigC
500	5	1.0664	0.4472	-0.2249	0.2774	1.2914	0.526	2.454
1000	**11**	**1.3538**	**0.3015**	**-0.7727**	**0.378**	**2.1265**	**0.484**	**4.398**
1500	13	1.184	0.2774	-1.0311	0.4472	2.2151	0.526	4.2092
2000	14	1.0232	0.2673	-1.1762	0.5	2.1993	0.567	3.8791
3000	16	0.8535	0.25	-1.7214	0.7071	2.5749	0.75	3.4332
4000	17	0.7101	0.2425	-2.2662	1	2.9764	1.029	2.8926
6000	17	0.4658	0.2425	-1.992	1	2.4578	1.029	2.3886
8000	17	0.3344	0.2425	-1.7633	1	2.0976	1.029	2.0385
10000	17	0.2424	0.2425	-1.539	1	1.7815	1.029	1.7313
27000	18	0	0.2357	?	?	?	?	?

HOST ROCKS ANALYSIS 9

dist(m)	npixbd	wp	stdwp	Wn	stdWn	C	stdC	sigC
500	10	0.7129	0.3162	-0.493	0.3536	1.2059	0.474	2.5422
1000	13	0.7721	0.2774	-0.8749	0.4472	1.647	0.526	3.1297
1500	**15**	**0.767**	**0.2582**	**-1.3024**	**0.5774**	**2.0694**	**0.633**	**3.2718**
2000	16	0.7262	0.25	-1.6351	0.7071	2.3612	0.75	3.1483
4000	16	0.4865	0.25	-1.4065	0.7071	1.893	0.75	2.524
6000	17	0.424	0.2425	-1.9279	1	2.3519	1.029	2.2857
8000	17	0.3335	0.2425	-1.7615	1	2.095	1.029	2.036
12000	17	0.1978	0.2425	-1.3991	1	1.5969	1.029	1.5519
28000	**18**	0	0.2357	?	?	?	?	?

SHEAR ZONES ANALYSIS 9

dist(m)	npixbd	wp	stdwp	Wn	stdWn	C	stdC	sigC
500	6	1.0701	0.4083	-0.2841	0.2887	1.3542	0.5	2.7081
1000	10	1.1062	0.3162	-0.6079	0.3536	1.7141	0.474	3.6135
1500	11	0.9748	0.3015	-0.6824	0.378	1.6572	0.484	3.4274
2000	**13**	**0.989**	**0.2774**	**-0.9681**	**0.4472**	**1.9572**	**0.526**	**3.7191**
3000	15	0.9133	0.2582	-1.3848	0.5774	2.2981	0.633	3.6334
4000	16	0.8065	0.25	-1.6917	0.7071	2.4982	0.75	3.331
6000	16	0.5662	0.25	-1.4949	0.7071	2.0611	0.75	2.7482
8000	17	0.4664	0.2425	-1.9929	1	2.4594	1.029	2.3901
10000	17	0.3563	0.2425	-1.8076	1	2.1639	1.029	2.1029
37000	18	0	0.2357	?	?	?	?	?

FRACTURES ANALYSIS 9

dist(m)	npixbd	wp	stdwp	Wn	stdwn	C	stdC	sigC
500	5	0.4442	0.4472	-0.1292	0.2774	0.5735	0.526	1.0898
1000	8	0.3283	0.3536	-0.202	0.3162	0.5303	0.474	1.1179
1500	**12**	**0.4094**	**0.2887**	**-0.514**	**0.4083**	**0.9233**	**0.5**	**1.8464**
2000	13	0.2906	0.2774	-0.5043	0.4472	0.7949	0.526	1.5105
2500	15	0.2984	0.2582	-0.8285	0.5774	1.1269	0.633	1.7817
14000	18	0	0.2357	?	?	?	?	?

Table 9: ANALYSIS 10, using weights of evidence method

ALTERATION ANALYSIS 10

dist(m)	npixbd	wp	stdwp	Wn	stdwn	C	stdc	SigC
500	6	1.2488	0.4083	-0.305	0.2887	1.5538	0.5	3.1072
1000	**12**	**1.4408**	**0.2887**	**-0.9268**	**0.4083**	**2.3677**	**0.5**	**4.7349**
1500	13	1.184	0.2774	-1.0311	0.4472	2.2151	0.526	4.2092
2000	14	1.0232	0.2673	-1.1762	0.5	2.1993	0.567	3.8791
3000	16	0.8535	0.25	-1.7214	0.7071	2.5749	0.75	3.4332
4000	17	0.7101	0.2425	-2.2662	1	2.9764	1.029	2.8926
6000	17	0.4658	0.2425	-1.992	1	2.4578	1.029	2.3886
8000	17	0.3344	0.2425	-1.7633	1	2.0976	1.029	2.0385
10000	17	0.2424	0.2425	-1.539	1	1.7815	1.029	1.7313
27000	18	0	0.2357	?	?	?	?	?

HOST ROCKS ANALYSIS 10

dist(m)	npixbd	wp	stdwp	Wn	stdWn	C	stdC	sigC
500	10	0.7129	0.3162	-0.493	0.3536	1.2059	0.474	2.5422
1000	13	0.7721	0.2774	-0.8749	0.4472	1.647	0.526	3.1297
1500	**15**	**0.767**	**0.2582**	**-1.3024**	**0.5774**	**2.0694**	**0.633**	**3.2718**
2000	16	0.7262	0.25	-1.6351	0.7071	2.3612	0.75	3.1483
4000	16	0.4865	0.25	-1.4065	0.7071	1.893	0.75	2.524
6000	17	0.424	0.2425	-1.9279	1	2.3519	1.029	2.2857
8000	17	0.3335	0.2425	-1.7615	1	2.095	1.029	2.036
12000	17	0.1978	0.2425	-1.3991	1	1.5969	1.029	1.5519
28000	**18**	0	0.2357	?	?	?	?	?

SHEAR ZONES ANALYSIS 10

dist(m)	npixbd	wp	stdwp	Wn	stdWn	C	stdC	sigC
500	6	1.0701	0.4083	-0.2841	0.2887	1.3542	0.5	2.7081
1000	10	1.1062	0.3162	-0.6079	0.3536	1.7141	0.474	3.6135
1500	11	0.9748	0.3015	-0.6824	0.378	1.6572	0.484	3.4274
2000	**13**	**0.989**	**0.2774**	**-0.9681**	**0.4472**	**1.9572**	**0.526**	**3.7191**
3000	15	0.9133	0.2582	-1.3848	0.5774	2.2981	0.633	3.6334
4000	16	0.8065	0.25	-1.6917	0.7071	2.4982	0.75	3.331
6000	16	0.5662	0.25	-1.4949	0.7071	2.0611	0.75	2.7482
8000	17	0.4664	0.2425	-1.9929	1	2.4594	1.029	2.3901
10000	17	0.3563	0.2425	-1.8076	1	2.1639	1.029	2.1029
37000	18	0	0.2357	?	?	?	?	?

FRACTURES ANALYSIS 10

dist(m)	npixbd	wp	stdwp	Wn	stdwn	C	stdC	sigC
500	5	0.4442	0.4472	-0.1292	0.2774	0.5735	0.526	1.0898
1000	8	0.3283	0.3536	-0.202	0.3162	0.5303	0.474	1.1179
1500	**12**	**0.4094**	**0.2887**	**-0.514**	**0.4083**	**0.9233**	**0.5**	**1.8464**
2000	13	0.2906	0.2774	-0.5043	0.4472	0.7949	0.526	1.5105
2500	15	0.2984	0.2582	-0.8285	0.5774	1.1269	0.633	1.7817
14000	18	0	0.2357	?	?	?	?	?

Table 10: ANALYSIS 11, using weights of evidence method

ALTERATION ANALYSIS 11

dist(m)	npixbd	wp	stdwp	Wn	stdwn	C	stdc	SigC
500	6	1.2488	0.4083	-0.305	0.2887	1.5538	0.5	3.1072
1000	**12**	**1.4408**	**0.2887**	**-0.9268**	**0.4083**	**2.3677**	**0.5**	**4.7349**
1500	13	1.184	0.2774	-1.0311	0.4472	2.2151	0.526	4.2092
2000	14	1.0232	0.2673	-1.1762	0.5	2.1993	0.567	3.8791
3000	16	0.8535	0.25	-1.7214	0.7071	2.5749	0.75	3.4332
4000	17	0.7101	0.2425	-2.2662	1	2.9764	1.029	2.8926
6000	17	0.4658	0.2425	-1.992	1	2.4578	1.029	2.3886
8000	17	0.3344	0.2425	-1.7633	1	2.0976	1.029	2.0385
10000	17	0.2424	0.2425	-1.539	1	1.7815	1.029	1.7313
27000	18	0	0.2357	?	?	?	?	?

HOST ROCKS ANALYSIS 11

dist(m)	npixbd	wp	stdwp	Wn	stdWn	C	stdC	sigC
500	11	0.8082	0.3015	-0.6265	0.378	1.4347	0.484	2.9672
1000	**14**	**0.8462**	**0.2673**	**-1.098**	**0.5**	**1.9442**	**0.567**	**3.4291**
1500	15	0.767	0.2582	-1.3024	0.5774	2.0694	0.633	3.2718
2000	16	0.7262	0.25	-1.6351	0.7071	2.3612	0.75	3.1483
4000	16	0.4865	0.25	-1.4065	0.7071	1.893	0.75	2.524
6000	17	0.424	0.2425	-1.9279	1	2.3519	1.029	2.2857
8000	17	0.3335	0.2425	-1.7615	1	2.095	1.029	2.036
12000	17	0.1978	0.2425	-1.3991	1	1.5969	1.029	1.5519
28000	18	0	0.2357	?	?	?	?	?

SHEAR ZONES ANALYSIS 11

dist(m)	npixbd	wp	stdwp	Wn	stdWn	C	stdC	sigC
500	6	1.0701	0.4083	-0.2841	0.2887	1.3542	0.5	2.7081
1000	10	1.1062	0.3162	-0.6079	0.3536	1.7141	0.474	3.6135
1500	11	0.9748	0.3015	-0.6824	0.378	1.6572	0.484	3.4274
2000	**13**	**0.989**	**0.2774**	**-0.9681**	**0.4472**	**1.9572**	**0.526**	**3.7191**
3000	15	0.9133	0.2582	-1.3848	0.5774	2.2981	0.633	3.6334
4000	16	0.8065	0.25	-1.6917	0.7071	2.4982	0.75	3.331
6000	16	0.5662	0.25	-1.4949	0.7071	2.0611	0.75	2.7482
8000	17	0.4664	0.2425	-1.9929	1	2.4594	1.029	2.3901
10000	17	0.3563	0.2425	-1.8076	1	2.1639	1.029	2.1029
37000	18	0	0.2357	?	?	?	?	?

FRACTURES ANALYSIS 11

dist(m)	npixbd	wp	stdwp	Wn	stdwn	C	stdC	sigC
500	6	0.6266	0.4083	-0.2093	0.2887	0.8359	0.5	1.6716
1000	9	0.4461	0.3333	-0.3074	0.3333	0.7535	0.471	1.5986
1500	**13**	**0.4894**	**0.2774**	**-0.6963**	**0.4472**	**1.1857**	**0.526**	**2.2531**
2000	14	0.3648	0.2673	-0.7274	0.5	1.0922	0.567	1.9264
2500	15	0.2984	0.2582	-0.8285	0.5774	1.1269	0.633	1.7817
14000	18	0	0.2357	?	?	?	?	?

Table 11: ANALYSIS 12, using weights of evidence method

ALTERATION ANALYSIS 12

dist(m)	npixbd	wp	stdwp	Wn	stdWn	C	stdC	sigC
500	6	1.2488	0.4083	-0.305	0.2887	1.5538	0.5	3.1072
1000	**12**	**1.4408**	**0.2887**	**-0.9268**	**0.4083**	**2.3677**	**0.5**	**4.7349**
1500	14	1.2581	0.2673	-1.2543	0.5	2.5124	0.567	4.4313
2000	14	1.0232	0.2673	-1.1762	0.5	2.1993	0.567	3.8791
3000	16	0.8535	0.25	-1.7214	0.7071	2.5749	0.75	3.4332
4000	17	0.7101	0.2425	-2.2662	1	2.9764	1.029	2.8926
6000	17	0.4658	0.2425	-1.992	1	2.4578	1.029	2.3886
8000	17	0.3344	0.2425	-1.7633	1	2.0976	1.029	2.0385
10000	17	0.2424	0.2425	-1.539	1	1.7815	1.029	1.7313
27000	18	0	0.2357	?	?	?	?	?

HOST ROCKS ANALYSIS 12

dist(m)	npixbd	wp	stdwp	Wn	stdWn	C	stdC	sigC
500	11	0.8082	0.3015	-0.6265	0.378	1.4347	0.484	2.9672
1000	13	0.7721	0.2774	-0.8749	0.4472	1.647	0.526	3.1297
1500	**15**	**0.767**	**0.2582**	**-1.3024**	**0.5774**	**2.0694**	**0.633**	**3.2718**
2000	16	0.7262	0.25	-1.6351	0.7071	2.3612	0.75	3.1483
4000	16	0.4865	0.25	-1.4065	0.7071	1.893	0.75	2.524
6000	17	0.424	0.2425	-1.9279	1	2.3519	1.029	2.2857
8000	17	0.3335	0.2425	-1.7615	1	2.095	1.029	2.036
12000	17	0.1978	0.2425	-1.3991	1	1.5969	1.029	1.5519
28000	18	0	0.2357	?	?	?	?	?

SHEAR ZONES ANALYSIS 12

dist(m)	npixbd	wp	stdwp	Wn	stdWn	C	stdC	sigC
500	6	1.0701	0.4083	-0.2841	0.2887	1.3542	0.5	2.7081
1000	10	1.1062	0.3162	-0.6079	0.3536	1.7141	0.474	3.6135
1500	11	0.9748	0.3015	-0.6824	0.378	1.6572	0.484	3.4274
2000	**13**	**0.989**	**0.2774**	**-0.9681**	**0.4472**	**1.9572**	**0.526**	**3.7191**
3000	15	0.9133	0.2582	-1.3848	0.5774	2.2981	0.633	3.6334
4000	16	0.8065	0.25	-1.6917	0.7071	2.4982	0.75	3.331
6000	16	0.5662	0.25	-1.4949	0.7071	2.0611	0.75	2.7482
8000	17	0.4664	0.2425	-1.9929	1	2.4594	1.029	2.3901
10000	17	0.3563	0.2425	-1.8076	1	2.1639	1.029	2.1029
37000	18	0	0.2357	?	?	?	?	?

FRACTURES ANALYSIS 12

dist(m)	npixbd	wp	stdwp	Wn	stdwn	C	stdC	sigC
500	6	0.6266	0.4083	-0.2093	0.2887	0.8359	0.5	1.6716
1000	9	0.4461	0.3333	-0.3074	0.3333	0.7535	0.471	1.5986
1500	**13**	**0.4894**	**0.2774**	**-0.6963**	**0.4472**	**1.1857**	**0.526**	**2.2531**
2000	14	0.3648	0.2673	-0.7274	0.5	1.0922	0.567	1.9264
2500	15	0.2984	0.2582	-0.8285	0.5774	1.1269	0.633	1.7817
14000	18	0	0.2357	?	?	?	?	?

Table 12: ANALYSIS 13, using weights of evidence method

ALTERATION ANALYSIS 13

dist(m)	npixbd	wp	stdwp	Wn	stdWn	C	stdC	sigC
500	6	1.2488	0.4083	-0.305	0.2887	1.5538	0.5	3.1072
1000	**11**	**1.3538**	**0.3015**	**-0.7727**	**0.378**	**2.1265**	**0.484**	**4.398**
1500	13	1.184	0.2774	-1.0311	0.4472	2.2151	0.526	4.2092
2000	14	1.0232	0.2673	-1.1762	0.5	2.1993	0.567	3.8791
3000	16	0.8535	0.25	-1.7214	0.7071	2.5749	0.75	3.4332
4000	17	0.7101	0.2425	-2.2662	1	2.9764	1.029	2.8926
6000	17	0.4658	0.2425	-1.992	1	2.4578	1.029	2.3886
8000	17	0.3344	0.2425	-1.7633	1	2.0976	1.029	2.0385
10000	17	0.2424	0.2425	-1.539	1	1.7815	1.029	1.7313
27000	18	0	0.2357	?	?	?	?	?

HOST ROCKS ANALYSIS 13

dist(m)	npixbd	wp	stdwp	Wn	stdWn	C	stdC	sigC
500	11	0.8082	0.3015	-0.6265	0.378	1.4347	0.484	2.9672
1000	14	0.8462	0.2673	-1.098	0.5	1.9442	0.567	3.4291
1500	15	0.767	0.2582	-1.3024	0.5774	2.0694	0.633	3.2718
2000	16	0.7262	0.25	-1.6351	0.7071	2.3612	0.75	3.1483
4000	16	0.4865	0.25	-1.4065	0.7071	1.893	0.75	2.524
6000	17	0.424	0.2425	-1.9279	1	2.3519	1.029	2.2857
8000	17	0.3335	0.2425	-1.7615	1	2.095	1.029	2.036
12000	17	0.1978	0.2425	-1.3991	1	1.5969	1.029	1.5519
28000	18	0	0.2357	?	?	?	?	?

SHEAR ZONES ANALYSIS 13

dist(m)	npixbd	wp	stdwp	Wn	stdWn	C	stdC	sigC
500	6	1.0701	0.4083	-0.2841	0.2887	1.3542	0.5	2.7081
1000	10	1.1062	0.3162	-0.6079	0.3536	1.7141	0.474	3.6135
1500	11	0.9748	0.3015	-0.6824	0.378	1.6572	0.484	3.4274
2000	**13**	**0.989**	**0.2774**	**-0.9681**	**0.4472**	**1.9572**	**0.526**	**3.7191**
3000	15	0.9133	0.2582	-1.3848	0.5774	2.2981	0.633	3.6334
4000	16	0.8065	0.25	-1.6917	0.7071	2.4982	0.75	3.331
6000	16	0.5662	0.25	-1.4949	0.7071	2.0611	0.75	2.7482
8000	17	0.4664	0.2425	-1.9929	1	2.4594	1.029	2.3901
10000	17	0.3563	0.2425	-1.8076	1	2.1639	1.029	2.1029
37000	18	0	0.2357	?	?	?	?	?

FRACTURES ANALYSIS 13

dist(m)	npixbd	wp	stdwp	Wn	stdwn	C	stdC	sigC
500	5	0.4442	0.4472	-0.1292	0.2774	0.5735	0.526	1.0898
1000	8	0.3283	0.3536	-0.202	0.3162	0.5303	0.474	1.1179
1500	**12**	**0.4094**	**0.2887**	-0.514	0.4083	0.9233	0.5	1.8464
2000	13	0.2906	0.2774	-0.5043	0.4472	0.7949	0.526	1.5105
2500	15	0.2984	0.2582	-0.8285	0.5774	1.1269	0.633	1.7817
14000	18	0	0.2357	?	?	?	?	?

Table 13: ANALYSIS 14, using weights of evidence method

ALTERATION ANALYSIS 14

dist(m)	npixbd	wp	stdwp	Wn	stdWn	C	stdC	sigC
500	6	1.2488	0.4083	-0.305	0.2887	1.5538	0.5	3.1072
1000	**12**	**1.4408**	**0.2887**	**-0.9268**	**0.4083**	**2.3677**	**0.5**	**4.7349**
1500	14	1.2581	0.2673	-1.2543	0.5	2.5124	0.567	4.4313
2000	15	1.0922	0.2582	-1.4638	0.5774	2.556	0.633	4.0411
3000	17	0.9141	0.2425	-2.4146	1	3.3287	1.029	3.2349
4000	17	0.7101	0.2425	-2.2662	1	2.9764	1.029	2.8926
6000	17	0.4658	0.2425	-1.992	1	2.4578	1.029	2.3886
8000	17	0.3344	0.2425	-1.7633	1	2.0976	1.029	2.0385
10000	17	0.2424	0.2425	-1.539	1	1.7815	1.029	1.7313
27000	18	0	0.2357	?	?	?	?	?

HOST ROCKS ANALYSIS 14

dist(m)	npixbd	wp	stdwp	Wn	stdWn	C	stdC	sigC
500	11	0.8082	0.3015	-0.6265	0.378	1.4347	0.484	2.9672
1000	**14**	**0.8462**	**0.2673**	**-1.098**	**0.5**	**1.9442**	**0.567**	**3.4291**
1500	15	0.767	0.2582	-1.3024	0.5774	2.0694	0.633	3.2718
2000	16	0.7262	0.25	-1.6351	0.7071	2.3612	0.75	3.1483
4000	16	0.4865	0.25	-1.4065	0.7071	1.893	0.75	2.524
6000	17	0.424	0.2425	-1.9279	1	2.3519	1.029	2.2857
8000	17	0.3335	0.2425	-1.7615	1	2.095	1.029	2.036
12000	17	0.1978	0.2425	-1.3991	1	1.5969	1.029	1.5519
28000	18	0	0.2357	?	?	?	?	?

SHEAR ZONES ANALYSIS 14

dist(m)	npixbd	wp	stdwp	Wn	stdWn	C	stdC	sigC
500	7	1.2243	0.378	-0.3711	0.3015	1.5954	0.484	3.2996
1000	**11**	**1.2016**	**0.3015**	**-0.7414**	**0.378**	**1.943**	**0.484**	**4.0185**
1500	12	1.0619	0.2887	-0.8365	0.4083	1.8984	0.5	3.7964
2000	14	1.0632	0.2673	-1.1913	0.5	2.2544	0.567	3.9763
3000	16	0.9778	0.25	-1.7903	0.7071	2.7681	0.75	3.6908
4000	16	0.8065	0.25	-1.6917	0.7071	2.4982	0.75	3.331
6000	16	0.5662	0.25	-1.4949	0.7071	2.0611	0.75	2.7482
8000	17	0.4664	0.2425	-1.9929	1	2.4594	1.029	2.3901
10000	17	0.3563	0.2425	-1.8076	1	2.1639	1.029	2.1029
37000	18	0	0.2357	?	?	?	?	?

FRACTURES ANALYSIS 14

dist(m)	npixbd	wp	stdwp	Wn	stdwn	C	stdC	sigC
500	5	0.4442	0.4472	-0.1292	0.2774	0.5735	0.526	1.0898
1000	8	0.3283	0.3536	-0.202	0.3162	0.5303	0.474	1.1179
1500	**12**	**0.4094**	**0.2887**	-0.514	0.4083	0.9233	0.5	1.8464
2000	13	0.2906	0.2774	-0.5043	0.4472	0.7949	0.526	1.5105
2500	15	0.2984	0.2582	-0.8285	0.5774	1.1269	0.633	1.7817
14000	18	0	0.2357	?	?	?	?	?

Table 14: ANALYSIS 15, using weights of evidence method

ALTERATION ANALYSIS 15

dist(m)	npixbd	wp	stdwp	Wn	stdWn	C	stdC	sigC
500	5	1.0664	0.4472	-0.2249	0.2774	1.2914	0.526	2.454
1000	**11**	**1.3538**	**0.3015**	**-0.7727**	**0.378**	**2.1265**	**0.484**	**4.398**
1500	13	1.184	0.2774	-1.0311	0.4472	2.2151	0.526	4.2092
2000	14	1.0232	0.2673	-1.1762	0.5	2.1993	0.567	3.8791
3000	16	0.8535	0.25	-1.7214	0.7071	2.5749	0.75	3.4332
4000	17	0.7101	0.2425	-2.2662	1	2.9764	1.029	2.8926
6000	17	0.4658	0.2425	-1.992	1	2.4578	1.029	2.3886
8000	17	0.3344	0.2425	-1.7633	1	2.0976	1.029	2.0385
10000	17	0.2424	0.2425	-1.539	1	1.7815	1.029	1.7313
27000	18	0	0.2357	?	?	?	?	?

HOST ROCKS ANALYSIS 15

dist(m)	npixbd	wp	stdwp	Wn	stdWn	C	stdC	sigC
500	10	0.7129	0.3162	-0.493	0.3536	1.2059	0.474	2.5422
1000	13	0.7721	0.2774	-0.8749	0.4472	1.647	0.526	3.1297
1500	**15**	**0.767**	**0.2582**	**-1.3024**	**0.5774**	**2.0694**	**0.633**	**3.2718**
2000	16	0.7262	0.25	-1.6351	0.7071	2.3612	0.75	3.1483
4000	16	0.4865	0.25	-1.4065	0.7071	1.893	0.75	2.524
6000	17	0.424	0.2425	-1.9279	1	2.3519	1.029	2.2857
8000	17	0.3335	0.2425	-1.7615	1	2.095	1.029	2.036
12000	17	0.1978	0.2425	-1.3991	1	1.5969	1.029	1.5519
28000	18	0	0.2357	?	?	?	?	?

SHEAR ZONES ANALYSIS 15

dist(m)	npixbd	wp	stdwp	Wn	stdWn	C	stdC	sigC
500	6	1.0701	0.4083	-0.2841	0.2887	1.3542	0.5	2.7081
1000	**10**	**1.1062**	**0.3162**	**-0.6079**	0.3536	1.7141	0.474	3.6135
1500	11	0.9748	0.3015	-0.6824	0.378	1.6572	0.484	3.4274
2000	**13**	**0.989**	**0.2774**	**-0.9681**	**0.4472**	**1.9572**	**0.526**	**3.7191**
3000	15	0.9133	0.2582	-1.3848	0.5774	2.2981	0.633	3.6334
4000	16	0.8065	0.25	-1.6917	0.7071	2.4982	0.75	3.331
6000	16	0.5662	0.25	-1.4949	0.7071	2.0611	0.75	2.7482
8000	17	0.4664	0.2425	-1.9929	1	2.4594	1.029	2.3901
10000	17	0.3563	0.2425	-1.8076	1	2.1639	1.029	2.1029
37000	18	0	0.2357	?	?	?	?	?

FRACTURES ANALYSIS 15

dist(m)	npixbd	wp	stdwp	Wn	stdwn	C	stdC	sigC
500	5	0.4442	0.4472	-0.1292	0.2774	0.5735	0.526	1.0898
1000	8	0.3283	0.3536	-0.202	0.3162	0.5303	0.474	1.1179
1500	**12**	**0.4094**	**0.2887**	-0.514	0.4083	0.9233	0.5	1.8464
2000	13	0.2906	0.2774	-0.5043	0.4472	0.7949	0.526	1.5105
2500	15	0.2984	0.2582	-0.8285	0.5774	1.1269	0.633	1.7817
14000	18	0	0.2357	?	?	?	?	?

Table 15: ANALYSIS 16, using weights of evidence method

ALTERATION ANALYSIS 16

dist(m)	npixbd	wp	stdwp	Wn	stdWn	C	stdC	sigC
500	5	1.0664	0.4472	-0.2249	0.2774	1.2914	0.526	2.454
1000	**11**	**1.3538**	**0.3015**	**-0.7727**	**0.378**	**2.1265**	**0.484**	**4.398**
1500	13	1.184	0.2774	-1.0311	0.4472	2.2151	0.526	4.2092
2000	14	1.0232	0.2673	-1.1762	0.5	2.1993	0.567	3.8791
3000	16	0.8535	0.25	-1.7214	0.7071	2.5749	0.75	3.4332
4000	17	0.7101	0.2425	-2.2662	1	2.9764	1.029	2.8926
6000	17	0.4658	0.2425	-1.992	1	2.4578	1.029	2.3886
8000	17	0.3344	0.2425	-1.7633	1	2.0976	1.029	2.0385
10000	17	0.2424	0.2425	-1.539	1	1.7815	1.029	1.7313
27000	18	0	0.2357	?	?	?	?	?

HOST ROCKS ANALYSIS 16

dist(m)	npixbd	wp	stdwp	Wn	stdWn	C	stdC	sigC
500	10	0.7129	0.3162	-0.493	0.3536	1.2059	0.474	2.5422
1000	13	0.7721	0.2774	-0.8749	0.4472	1.647	0.526	3.1297
1500	**15**	**0.767**	**0.2582**	**-1.3024**	**0.5774**	**2.0694**	**0.633**	**3.2718**
2000	16	0.7262	0.25	-1.6351	0.7071	2.3612	0.75	3.1483
4000	16	0.4865	0.25	-1.4065	0.7071	1.893	0.75	2.524
6000	17	0.424	0.2425	-1.9279	1	2.3519	1.029	2.2857
8000	17	0.3335	0.2425	-1.7615	1	2.095	1.029	2.036
12000	17	0.1978	0.2425	-1.3991	1	1.5969	1.029	1.5519
28000	18	0	0.2357	?	?	?	?	?

SHEAR ZONES ANALYSIS 16

dist(m)	npixbd	wp	stdwp	Wn	stdWn	C	stdC	sigC
500	7	1.2243	0.378	-0.3711	0.3015	1.5954	0.484	3.2996
1000	**11**	**1.2016**	**0.3015**	**-0.7414**	**0.378**	**1.943**	**0.484**	**4.0185**
1500	12	1.0619	0.2887	-0.8365	0.4083	1.8984	0.5	3.7964
2000	13	0.989	0.2774	-0.9681	0.4472	1.9572	0.526	3.7191
3000	15	0.9133	0.2582	-1.3848	0.5774	2.2981	0.633	3.6334
4000	16	0.8065	0.25	-1.6917	0.7071	2.4982	0.75	3.331
6000	16	0.5662	0.25	-1.4949	0.7071	2.0611	0.75	2.7482
8000	17	0.4664	0.2425	-1.9929	1	2.4594	1.029	2.3901
10000	17	0.3563	0.2425	-1.8076	1	2.1639	1.029	2.1029
37000	18	0	0.2357	?	?	?	?	?

FRACTURES ANALYSIS 16

dist(m)	npixbd	wp	stdwp	Wn	stdwn	C	stdC	sigC
500	5	0.4442	0.4472	-0.1292	0.2774	0.5735	0.526	1.0898
1000	8	0.3283	0.3536	-0.202	0.3162	0.5303	0.474	1.1179
1500	**12**	**0.4094**	**0.2887**	-0.514	0.4083	0.9233	0.5	1.8464
2000	13	0.2906	0.2774	-0.5043	0.4472	0.7949	0.526	1.5105
2500	15	0.2984	0.2582	-0.8285	0.5774	1.1269	0.633	1.7817
14000	18	0	0.2357	?	?	?	?	?

Table 16: ANALYSIS 17, using weights of evidence method

ALTERATION ANALYSIS 17

dist(m)	npixbd	wp	stdwp	Wn	stdwn	C	stdc	sigC
500	6	1.2488	0.4083	-0.305	0.2887	1.5538	0.5	3.1072
1000	**12**	**1.4408**	**0.2887**	**-0.9268**	**0.4083**	**2.3677**	**0.5**	**4.7349**
1500	14	1.2581	0.2673	-1.2543	0.5	2.5124	0.567	4.4313
2000	15	1.0922	0.2582	-1.4638	0.5774	2.556	0.633	4.0411
3000	17	0.9141	0.2425	-2.4146	1	3.3287	1.029	3.2349
4000	18	0.7673	0.2357	?	?	?	?	?
6000	18	0.523	0.2357	?	?	?	?	?
8000	18	0.3915	0.2357	?	?	?	?	?
10000	18	0.2996	0.2357	?	?	?	?	?
27000	18	0	0.2357	?	?	?	?	?

HOST ROCKS ANALYSIS 17

dist(m)	npixbd	wp	stdwp	Wn	stdWn	C	stdC	sigC
500	11	0.8082	0.3015	-0.6265	0.378	1.4347	0.484	2.9672
1000	**14**	**0.8462**	**0.2673**	**-1.098**	**0.5**	**1.9442**	**0.567**	**3.4291**
1500	16	0.8316	0.25	-1.7078	0.7071	2.5394	0.75	3.3859
2000	17	0.7868	0.2425	-2.3282	1	3.115	1.029	3.0273
4000	17	0.5471	0.2425	-2.0997	1	2.6468	1.029	2.5722
6000	18	0.4812	0.2357	?	?	?	?	?
8000	18	0.3907	0.2357	?	?	?	?	?
12000	18	0.255	0.2357	?	?	?	?	?
28000	18	0	0.2357	?	?	?	?	?

SHEAR ZONES ANALYSIS 17

dist(m)	npixbd	wp	stdwp	Wn	stdWn	C	stdC	sigC
500	7	1.2243	0.378	-0.3711	0.3015	1.5954	0.484	3.2997
1000	**11**	**1.2016**	**0.3015**	**-0.7414**	**0.378**	**1.943**	**0.484**	**4.0186**
1500	12	1.0619	0.2887	-0.8365	0.4083	1.8984	0.5	3.7965
2000	14	1.0632	0.2673	-1.1913	0.5	2.2544	0.567	3.9763
3000	16	0.9778	0.25	-1.7903	0.7071	2.7681	0.75	3.6909
4000	17	0.8671	0.2425	-2.3848	1	3.252	1.029	3.1605
6000	17	0.6269	0.2425	-2.188	1	2.8149	1.029	2.7357
8000	18	0.5236	0.2357	?	?	?	?	?
10000	18	0.4135	0.2357	?	?	?	?	?
37000	18	0	0.2357	?	?	?	?	?

FRACTURES ANALYSIS 17

dist(m)	npixbd	wp	stdwp	Wn	stdwn	C	stdC	sigC
500	5	0.4442	0.4472	-0.1292	0.2774	0.5735	0.526	1.0898
1000	8	0.3283	0.3536	-0.202	0.3162	0.5303	0.474	1.1179
1500	**12**	**0.4094**	**0.2887**	**-0.514**	**0.4083**	**0.9233**	**0.5**	**1.8464**
2000	13	0.2906	0.2774	-0.5043	0.4472	0.7949	0.526	1.5105
2500	15	0.2984	0.2582	-0.8285	0.5774	1.1269	0.633	1.7817
14000	18	0	0.2357	?	?	?	?	?

Table 17: ANALYSIS 18, using weights of evidence method

ALTERATION ANALYSIS 18

dist(m)	npixbd	wp	stdwp	Wn	stdWn	C	stdC	sigC
500	5	1.0664	0.4472	-0.2249	0.2774	1.2914	0.526	2.454
1000	**11**	**1.3538**	**0.3015**	**-0.7727**	**0.378**	**2.1265**	**0.484**	**4.398**
1500	13	1.184	0.2774	-1.0311	0.4472	2.2151	0.526	4.2092
2000	14	1.0232	0.2673	-1.1762	0.5	2.1993	0.567	3.8791
3000	16	0.8535	0.25	-1.7214	0.7071	2.5749	0.75	3.4332
4000	17	0.7101	0.2425	-2.2662	1	2.9764	1.029	2.8926
6000	17	0.4658	0.2425	-1.992	1	2.4578	1.029	2.3886
8000	17	0.3344	0.2425	-1.7633	1	2.0976	1.029	2.0385
10000	17	0.2424	0.2425	-1.539	1	1.7815	1.029	1.7313
27000	18	0	0.2357	?	?	?	?	?

HOST ROCKS ANALYSIS 18

dist(m)	npixbd	wp	stdwp	Wn	stdWn	C	stdC	sigC
500	10	0.7129	0.3162	-0.493	0.3536	1.2059	0.474	2.5422
1000	13	0.7721	0.2774	-0.8749	0.4472	1.647	0.526	3.1297
1500	**15**	**0.767**	**0.2582**	**-1.3024**	**0.5774**	**2.0694**	**0.633**	**3.2718**
2000	16	0.7262	0.25	-1.6351	0.7071	2.3612	0.75	3.1483
4000	16	0.4865	0.25	-1.4065	0.7071	1.893	0.75	2.524
6000	17	0.424	0.2425	-1.9279	1	2.3519	1.029	2.2857
8000	17	0.3335	0.2425	-1.7615	1	2.095	1.029	2.036
12000	17	0.1978	0.2425	-1.3991	1	1.5969	1.029	1.5519
28000	18	0	0.2357	?	?	?	?	?

SHEAR ZONES ANALYSIS 18

dist(m)	npixbd	wp	stdwp	Wn	stdWn	C	stdC	sigC
500	6	1.0701	0.4083	-0.2841	0.2887	1.3542	0.5	2.7081
1000	10	1.1062	0.3162	-0.6079	0.3536	1.7141	0.474	3.6135
1500	11	0.9748	0.3015	-0.6824	0.378	1.6572	0.484	3.4274
2000	**13**	**0.989**	**0.2774**	**-0.9681**	**0.4472**	**1.9572**	**0.526**	**3.7191**
3000	15	0.9133	0.2582	-1.3848	0.5774	2.2981	0.633	3.6334
4000	16	0.8065	0.25	-1.6917	0.7071	2.4982	0.75	3.331
6000	16	0.5662	0.25	-1.4949	0.7071	2.0611	0.75	2.7482
8000	17	0.4664	0.2425	-1.9929	1	2.4594	1.029	2.3901
10000	17	0.3563	0.2425	-1.8076	1	2.1639	1.029	2.1029
37000	18	0	0.2357	?	?	?	?	?

FRACTURES ANALYSIS 18

dist(m)	npixbd	wp	stdwp	Wn	stdwn	C	stdC	sigC
500	6	0.6266	0.4083	-0.2093	0.2887	0.8359	0.5	1.6716
1000	9	0.4461	0.3333	-0.3074	0.3333	0.7535	0.471	1.5986
1500	**13**	**0.4894**	**0.2774**	**-0.6963**	**0.4472**	**1.1857**	**0.526**	**2.2531**
2000	14	0.3648	0.2673	-0.7274	0.5	1.0922	0.567	1.9264
2500	15	0.2984	0.2582	-0.8285	0.5774	1.1269	0.633	1.7817
14000	18	0	0.2357	?	?	?	?	?

Table 18: ANALYSIS 19, using weights of evidence method

ALTERATION ANALYSIS 19

Dist(m)	npixbd	wp	stdwp	Wn	stdWn	C	stdC	sigC
500	6	1.2488	0.4083	-0.305	0.2887	1.5538	0.5	3.1072
1000	**11**	**1.3538**	**0.3015**	**-0.7727**	**0.378**	**2.1265**	**0.484**	**4.398**
1500	13	1.184	0.2774	-1.0311	0.4472	2.2151	0.526	4.2092
2000	14	1.0232	0.2673	-1.1762	0.5	2.1993	0.567	3.8791
3000	16	0.8535	0.25	-1.7214	0.7071	2.5749	0.75	3.4332
4000	17	0.7101	0.2425	-2.2662	1	2.9764	1.029	2.8926
6000	17	0.4658	0.2425	-1.992	1	2.4578	1.029	2.3886
8000	17	0.3344	0.2425	-1.7633	1	2.0976	1.029	2.0385
10000	17	0.2424	0.2425	-1.539	1	1.7815	1.029	1.7313
27000	18	0	0.2357	?	?	?	?	?

HOST ROCKS ANALYSIS 19

Dist(m)	npixbd	wp	stdwp	Wn	stdWn	C	stdC	sigC
500	10	0.7129	0.3162	-0.493	0.3536	1.2059	0.474	2.5422
1000	13	0.7721	0.2774	-0.8749	0.4472	1.647	0.526	3.1297
1500	**15**	**0.767**	**0.2582**	**-1.3024**	**0.5774**	**2.0694**	**0.633**	**3.2718**
2000	16	0.7262	0.25	-1.6351	0.7071	2.3612	0.75	3.1483
4000	16	0.4865	0.25	-1.4065	0.7071	1.893	0.75	2.524
6000	17	0.424	0.2425	-1.9279	1	2.3519	1.029	2.2857
8000	17	0.3335	0.2425	-1.7615	1	2.095	1.029	2.036
12000	17	0.1978	0.2425	-1.3991	1	1.5969	1.029	1.5519
28000	18	0	0.2357	?	?	?	?	?

SHEAR ZONES ANALYSIS 19

Dist(m)	npixbd	wp	stdwp	Wn	stdWn	C	stdC	sigC
500	6	1.0701	0.4083	-0.2841	0.2887	1.3542	0.5	2.7081
1000	10	1.1062	0.3162	-0.6079	0.3536	1.7141	0.474	3.6135
1500	11	0.9748	0.3015	-0.6824	0.378	1.6572	0.484	3.4274
2000	**13**	**0.989**	**0.2774**	**-0.9681**	**0.4472**	**1.9572**	**0.526**	**3.7191**
3000	15	0.9133	0.2582	-1.3848	0.5774	2.2981	0.633	3.6334
4000	16	0.8065	0.25	-1.6917	0.7071	2.4982	0.75	3.331
6000	16	0.5662	0.25	-1.4949	0.7071	2.0611	0.75	2.7482
8000	17	0.4664	0.2425	-1.9929	1	2.4594	1.029	2.3901
10000	17	0.3563	0.2425	-1.8076	1	2.1639	1.029	2.1029
37000	18	0	0.2357	?	?	?	?	?

FRACTURES ANALYSIS 19

Dist(m)	npixbd	wp	stdwp	Wn	stdwn	C	stdC	sigC
500	6	0.6266	0.4083	-0.2093	0.2887	0.8359	0.5	1.6716
1000	9	0.4461	0.3333	-0.3074	0.3333	0.7535	0.471	1.5986
1500	**13**	**0.4894**	**0.2774**	**-0.6963**	**0.4472**	**1.1857**	**0.526**	**2.2531**
2000	14	0.3648	0.2673	-0.7274	0.5	1.0922	0.567	1.9264
2500	15	0.2984	0.2582	-0.8285	0.5774	1.1269	0.633	1.7817
14000	18	0	0.2357	?	?	?	?	?